HAW
HAMBURG

BACHELORTHESIS
Alexander Maximilian Busch

Power Consumption Models for Sustainability in Wireless Communication Systems

FAKULTÄT TECHNIK UND INFORMATIK
Department Informations- und Elektrotechnik

Faculty of Computer Science and Engineering
Department of Information and Electrical Engineering

HAMBURG UNIVERSITY
OF APPLIED SCIENCES
Hochschule für Angewandte
Wissenschaften Hamburg

Alexander Maximilian Busch

Power Consumption Models for Sustainability in Wireless Communication Systems

Bachelor Thesis based on the examination and study regulations
for the Bachelor of Science degree programme
Bachelor of Science Elektro- und Informationstechnik
at the Department of Information and Electrical Engineering
of the Faculty of Engineering and Computer Science
of the University of Applied Sciences Hamburg
Supervising examiner: Prof. Dr. Kolja Eger
Second examiner: Prof. Dr. Heike Neumann

Day of delivery: 23 June 2023

Alexander Maximilian Busch

Title of Thesis

Power Consumption Models for Sustainability in Wireless Communication Systems

Keywords

wireless communication, LTE, 5G, 6G, cellular networks, base station, user equipment, power consumption model, power model, energy model, system model, energy efficiency

Abstract

This thesis examines analytic power consumption models for the base station, radio access network, user equipment, and system level relevant for 5th generation (5G) cellular networks. A literature survey is conducted to identify relevant models. Selected models are implemented and compared quantitatively and qualitatively. Focus of this work is on base station power models.

Alexander Maximilian Busch

Thema der Arbeit

Energiemodelle für Nachhaltigkeit in drahtlosen Kommunikationssystemen

Stichworte

Drahtlose Kommunikation, LTE, 5G, 6G, Mobilfunknetze, Basisstation, User Equipment, Leistungsaufnahme, Energiemodell, Systemmodell, Energieeffizienz

Kurzzusammenfassung

Diese Arbeit betrachtet analytische Modelle der Leistungsaufnahme von Basisstationen, Funkzugangsnetz, User Equipment sowie Modelle der Systemebene für Mobilfunknetze der fünften Generation (5G). Es wird ein Literaturüberblick erstellt, der relevante Modelle identifiziert. Ausgewählte Modelle werden implementiert sowie quantitativ und qualitativ verglichen. Der Fokus dieser Arbeit liegt auf Energiemodellen für Basisstationen.

Contents

List of Figures

List of Tables

Abbreviations

3GPP 3rd Generation Partnership Project.

BBU baseband unit.

DRX Discontinous Reception.

eMBB Enhanced Mobile Broadband.

ETSI European Telecommunications Standards Institute.

GSM Global System for Mobile Communications.

HSPA High Speed Packet Access.

LTE Long Term Evolution.

MIMO multiple-input (and) multiple-output.

mMIMO massive multiple-input (and) multiple-output.

mMTC massive Machine Type Communication.

PA power amplifier.

RAN radio access network.

RF radio frequency.

RRC Radio Resource Control.

RRH remote radio head.

RRM Radio Resource Management.

RRU remote radio unit.

UE user equipment.

UMTS Universal Mobile Telecommunications System.

URLLC Ultra Reliable and Low Latency Communication.

1 Motivation and Introduction

The design of wireless communication systems is traditionally focused on optimization of performance indicators, for example maximizing the spectral efficiency and the data throughput while minimizing the communication latency. However, sustainability of the communication system itself has become an important aspect in recent years.

Several studies concluded that the information and communication technology sector is responsible for a considerable share of the global greenhouse gas emissions. Recent publications [1] estimate it at more than 2% of the global emissions, which is comparable to the emissions of the aviation sector.

The requirements on mobile networks in terms of capacity and coverage are increasing as the number of users and data traffic are predicted to grow further. According to the *Ericsson Mobility Report* [2], the global mobile network data traffic has almost doubled from 2020 to 2022. It is projected to grow further due to an increase both in total smartphone subscriptions and the average data volume per subscription. Total monthly global mobile network traffic is estimated at 108 Exabytes (1 Exabyte = 10^{18} bytes) in the third quarter of 2022. Video streaming constitutes the largest share of this traffic, with around 70% of the global data traffic in 2022.

Additionally, new use cases are identified for current and next generation mobile networks. The European research project Hexa-X has presented use cases for 6th generation mobile networks (6G) in [3]. The defined use case families include sustainable development (autonomous supply chains, "E-Health" etc.), massive twinning (smart cities and digital twins) and "telepresence" (cyber-physical worlds, mixed/merged reality etc.). In light of this, the total number of cellular IoT connections is projected at over 5 billion globally in 2028, up from about 3 billion in 2023 [2]. Another aspect is the expanding importance of cloud computing, due to which the communication aspect becomes more important when assessing energy consumption of applications and services. As users are accessing cloud-based services, the increase in required data rate and total data transferred over

(mobile) networks leads to resource demand and energy consumption at the network hardware. Other emerging and growing technologies such as machine learning and virtual reality also amplify this trend.

This poses the challenge of developing energy efficient but also high-performing cellular networks. Considerable effort has been made towards energy-efficient 5th generation (5G) networks, but there is room for improvement: Hexa-X set the objective of "reducing energy consumption per bit in networks by >90%" for 6G [3]. From a network operator perspective [4], energy consumption is also relevant as a contributor to operating expenditures. This creates a financial incentive to optimize energy efficiency in wireless networks.

Models of power and energy consumption are required to offer a thorough understanding of the energy consumption in current and future cellular networks. The energy consumption may vary considerably depending on the architecture or deployment type of the network. Theoretical models would aid in understanding and quantifying these differences. Therefore, power consumption models are an important building block towards achieving better comparability in terms of the energy efficiency of different network configurations. In light of this, the following relevant major research projects have analyzed the energy consumption and energy efficiency of mobile networks, based on power consumption models developed as part of the project:

- EARTH (Energy Aware Radio and neTwork tecHnologies)[1] (results published until 2012): International consortium of experts from industry and academia.

- GreenTouch[2] (results published until 2015): International consortium of experts from industry, academia, and governments.

- UTAMO[3] (results published in February 2023): Fraunhofer IZM by order of the German Umweltbundesamt.

When comparing energy efficiency of network deployments, standardized metrics can help in the task of optimizing and quantifying the performance of a network in terms of energy consumption. Especially for the evaluation of new use cases of mobile networks, novel energy efficiency metrics are required as the key performance indicators evolve.

---

[1]Project website: cordis.europa.eu/project/id/247733 (visited on 16/06/2023)
[2]Project website: www.bell-labs.com/greentouch/ (visited on 16/06/2023)
[3]Project website: www.izm.fraunhofer.de/de/abteilungen/environmental_reliabilityengineering/projekte/utamo.html (visited on 16/06/2023)

This thesis is structured as follows: The next Chapter 2 provides an overview on the fundamental aspects of cellular networks in general and 5G specifically, the relevant aspects for power consumption modeling and energy efficiency are prioritized. Based on this, the following Chapter 3 defines the contributions, scope, and methodology of this thesis. Chapter 4 describes the power consumption models for the different system components of a cellular network. The comparison of the models is done in Chapter 5, which is based on the implementation of selected power consumption models. Energy efficiency metrics are discussed in Chapter 6. Final conclusions are given in Chapter 7.

2 Background

This chapter introduces fundamental aspects of cellular networks in general (Section 2.1) and 5G in particular (Section 2.2), which are required to understand the power consumption models described in Chapter 4. The main power saving techniques of 5G are summarized in Section 2.3. Additionally, energy consumption and energy efficiency of 5G systems is explained to provide context for the models and the energy efficiency metrics (Chapter 6). Beyond energy consumption and efficiency itself, using renewable energy sources to power network components such as base stations is a relevant aspect of sustainability in wireless communication systems. Consequently, a brief summary of research on renewable energy sources for wireless access networks is given in Section 2.5.

2.1 Cellular Networks and Wireless Communication Systems

This section presents the fundamentals of cellular networks and wireless communication system technology in order to introduce the more specific 5G mobile network specifications in Section 2.2.

2.1.1 Fundamentals of Cellular Networks

The fundamental architecture of cellular networks and relevant terminology is outlined in this section. The basic terminology and fundamental procedures are well-described in [5] and the important aspects are summarized hereafter.

The main purpose of a cellular network is to serve multiple users over a (large) geographical area. A cellular network utilizes multiple fixed antenna sites, called base stations. Users connect to and communicate with the base stations that provide the best radio signal for

the current location of the user. Smartphones, routers with SIM cards or similar user hardware is generically referred to as user equipment (UE).

The available frequency range in a network is finite and therefore needs to be shared in a way that avoids interference of adjacent base stations. To minimize interference, traditionally the following network layouts are preferred: A hexagonal grid of base stations using omnidirectional antennas or alternatively base stations with three sectors, each covered by a 120-degree antenna - this is illustrated in Figure 2.1. The area covered by one base station is defined as a cell [6]. Each cell is then usually further divided into a number of sectors, each covered by one antenna or an antenna array.

3-sector base station   omnidirectional base stations
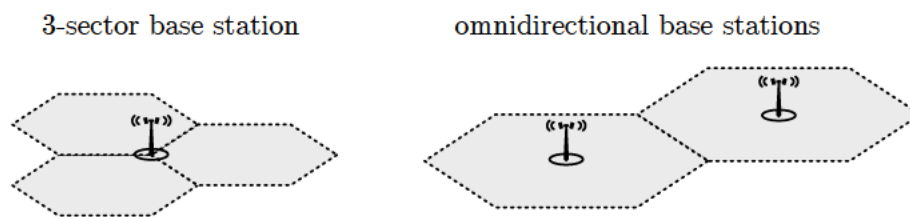
Figure 2.1: Three sector base station sites (left) and omnidirectional base station sites (right). Adapted from [5] Fig. 2.1

The base station transmits and receives data from the UE and if required, forwards the data to the core network over the backhaul connection. The communication link between base station and UE is referred to as the air interface. The communication direction from base station to UE is referred to as downlink and the opposite direction from UE to the base station is the uplink. The base stations (or other comparable components) within a network and the backhaul networks are known as the radio access network (RAN), which connects the UE to the core network. This is illustrated in Figure 2.2.
Although the backhaul (and other transport networks) are often represented by single connecting lines in schematic diagrams, in practice they are not usually point-to-point connections but may consist of complex (wired) network structures. When referring to the base stations in the context of the RAN, they are also known as nodes.

Data transfers between UE and base station can be initiated by either of them. The base station can reach any compatible UE within its coverage area by initiating a procedure referred to as paging. This indicates to the UE that a radio connection with the base station can be established. The UE triggers a connection to the base station through a procedure known as random access. To enable a UE to detect a network, each of the base stations within the network transmits a set of base station specific signals,
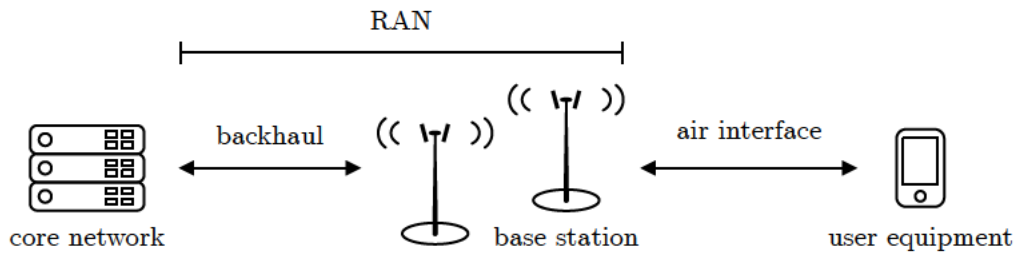
Figure 2.2: Basic system structure of a cellular network. Adapted from [5] Fig. 2.2

starting with a synchronization signal or correlation sequence known to the UE. The UE performs a correlation process to search for the synchronization signals. Depending on the configuration of the UE, this could be carried out using several frequency ranges supported by the UE. After the synchronization sequence is detected and confirmed, the UE utilizes the information that the base station transmits over its broadcast channel to complete the synchronization.

Another important functionality of a mobile wireless network is the seamless mobility of users between base stations. The process referred to as handover allows a UE to continue the connection to a network when crossing several cells. To enable this, the UE conducts measurements of the current signal strength of reference signals and synchronization signals that are reported to the base station. Based on this, the association to a base station is determined by the network.

The key task of a base station in a cellular network is to enable user multiplexing and divide the available network resources among the connected UEs. The resources are usually represented by a time-frequency grid. For systems based on orthogonal frequency division multiplexing (OFDM) such as Long Term Evolution (LTE) and 5G, time is divided into OFDM symbols and frequency is divided into subcarriers. The term scheduling refers to the task of deciding which resources are allocated to a UE. The currently allocated resources are indicated to the UE over a control channel by the base station.

2.1.2 Wireless Transceiver

The wireless transceiver is the hardware unit that transmits and receives radio waves over the air interface. A wireless transceiver consists of a transmitting path or transmitter (TX), shown in Figure 2.3, and a receiving path or receiver (RX), shown in figure 2.4. An explanation of wireless transceivers is provided in [7], which is summarized below.
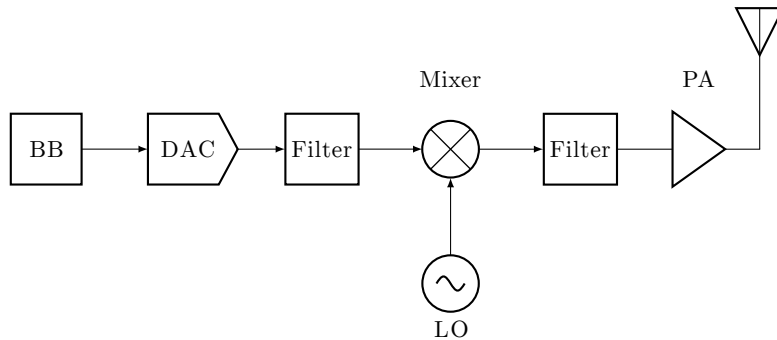
Figure 2.3: Block diagram of a wireless transmitter (TX). Adapted from [7] Fig 2.3

The transmitter (Figure 2.3) is built up as follows: The baseband processing unit (BB) generates the signal to be transmitted. The digital baseband signal is converted to an analog signal using a digital-to-analog converter (DAC) and filtered. The local oscillator (LO) in conjunction with a mixer modulates the filtered signal. The modulated signal is filtered again, and the power amplifier (PA) drives the transmitting antenna.
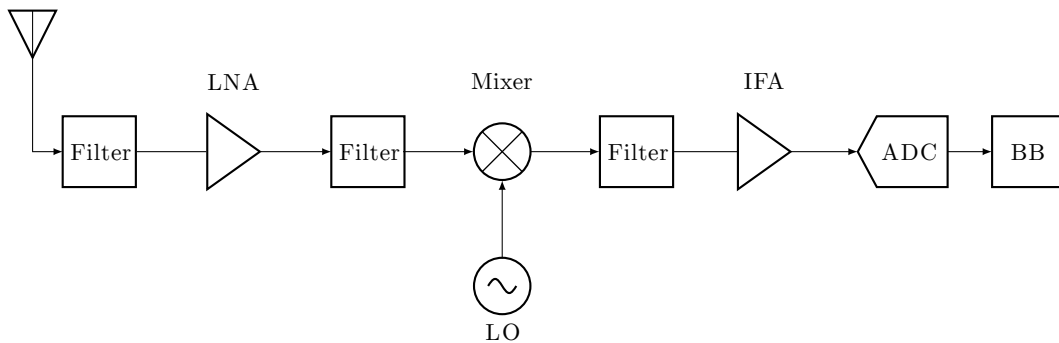
Figure 2.4: Block diagram of a wireless receiver (RX). Adapted from [7] Fig 2.3

The signal received by the antenna of the receiving path (Figure 2.4) is filtered and amplified by a low noise amplifier (LNA) before passing through another filter. The filtered and amplified signal is down converted by the mixer and local oscillator and

the intermediate frequency amplifier (IFA). The digital signal converted by the analog-to-digital converter (ADC) is fed into the baseband processing (BB). The filters in the transmitter and receiver are utilized to restrict the signal to the desired frequency bands defined in the employed communication standard.

Wireless transceivers are employed in the base station and the user equipment. It should be noted that the exact structure differs and unique transceiver architectures exist to complement the various requirements of wireless communication standards and the requirements to the functionality of the hardware, such as different types of user equipment and different types of base stations. For example, low-IF (intermediate frequency) and super-heterodyne architectures are employed in larger base stations and simpler zero-IF architectures in smaller base stations [8]. Nonetheless, the general structure shown in figures 2.3 and 2.4 is representative of the functional structure of a wireless transceiver.

Terminology

The wireless transceiver can be separated conceptually into the analog frontend part that encompasses everything between the antenna port and the baseband unit port, and the digital baseband processing part. Power consumption models usually also model the power amplifier of the transmitter separately (refer to Chapter 4 for description of the models). As shown, the receiver and transmitter components differ (most importantly, the receiver does not have a power amplifier). Though in the context of power consumption models they are often referred to as one component: The RF transceiver or analog frontend. The power amplifier is then described as a separate component. This conceptual split was introduced in models as early as 2011 such as [9] and [8].

The actual hardware implementation of wireless transceivers for base stations is usually split into two distinct units: The remote radio unit (RRU) which includes the analog frontend and power amplifier, and the baseband unit (BBU) which includes the baseband processing part. Several alternative terms exist to describe the RRU: Remote radio head (RRH), radio equipment (RE), or radio unit (RU). RRH and RRU are more commonly used when referring to the hardware device, while RE and RU are more often used in the context of specification of logical network nodes. The term radio unit (RU) is especially ambiguous, as it includes the analog frontend and, depending on the functional split option of the RAN, may contain digital signal processing functions (see Section 2.2.7).

Baseband Processing Unit

The digital signal passed to the RF transmitter or received from the RF receiver is generated or processed by the baseband unit (BBU). The baseband processing unit of a base station or user equipment performs digital up- and down-conversion, which includes digital filtering, modulation and demodulation, digital-pre-distortion, signal detection (including synchronization, channel estimation, equalization, and compensation of radio frequency nonidealities), channel coding and decoding, and FFT/IFFT computation [8]. Traditionally, the BBU is a system-on-chip based on a Field-Programmable Gate Array (FPGA) [10]. For 5G, the possibility of virtualizing the BBU functions and deploying them on commercial off-the-shelf hardware is increasingly important (see also Section 2.2.7).

Power Amplifier

The power amplifier (PA) amplifies the analog signal to be transmitted by the antenna. Orthogonal frequency division multiplex (OFDM) and orthogonal frequency division multiple access (OFDMA) are utilized in current wireless communication systems such as LTE and 5G. OFDM modulated signals show significant nonlinearity effects, as they have a high peak-to-average power ratio (PAPR) [11]. Power amplifiers generally exhibit lower efficiencies at low transmission powers - the decrease in efficiency is assumed to be non-linear, as shown in [10]. Due to the high fluctuations in transmission power of OFDM signals (high PAPR), power amplifiers in OFDM-based systems rarely operate at their maximum efficiency. An energy efficiency evaluation of power amplifiers in LTE systems is provided in [12].

2.2 Introduction to 5th Generation Mobile Networks (5G)

This section provides an introduction to the fifth-generation standard for broadband cellular networks (5G). The focus of this section is on aspects of 5G relevant to the power consumption models discussed in Chapter 4. The specification and standardization process and use cases are briefly explained. The system architecture and physical access specifications, as well as the access stratum protocol, are introduced. Then, radio access network architectures and base station types are exemplified. Important aspects of user

equipment for 5G are explained and massive MIMO, as a key technology for 5G systems with impact on power consumption, summarized.

The 5G standard is the successor to LTE, which is also referred to as the fourth generation (4G). The third generation (3G) comprises the Universal Mobile Telecommunications System (UMTS) standard and the improved High Speed Packet Access (HSPA), also referred to as 3.5G. The Global System for Mobile Communications (GSM) standard launched the second generation (2G), the first digital mobile telecommunication generation which replaced the analog 1G standards.

2.2.1 Specification and Standardization

As the practical realization of mobile networks is based on several standards and specifications, they are briefly introduced hereafter. The 3rd Generation Partnership Project (3GPP) began working on 5G concepts in 2015 and published the first version of the specifications in 3GPP Release 15 in 2018 [13]. Technical Specification (TS) documents are authored and discussed by the 3GPP working groups and subsequently published by the European Telecommunications Standards Institute (ETSI), as part of the releases. Release 15 primarily covers the Enhanced Mobile Broadband (eMBB) use cases - also referred to as "Phase 1" [14]. "Phase 2" (Release 16) is focused on requirements of low latency applications and reliable communications (Ultra Reliable and Low Latency Communication (URLLC)), as required by mainly the automotive industry and Industry 4.0 proponents. Specifications for Release 16 were finished in July 2020 and for Release 17 in June 2022 while the upcoming Release 18 is scheduled for June 2024 [15]. A list of important projects covered in Release 17 can be found in [16]. From Release 18 onwards, the 3GPP will refer to the 5G specifications with the new term "5G-Advanced", a summary of important work for the release is given in [17]. The release timeline for the 3GPP Releases 15 to 18 is shown in Figure 2.5. It illustrates the system of parallel releases, with the work of the next release starting before the previous is finalized.

It is expected that 6G systems are launched commercially by 2030, following the roughly 10-year interval between cellular standard generations according to [18]. The first concrete work on 6G specifications will presumably be started from 2026 onwards as part of 3GPP Release 20.
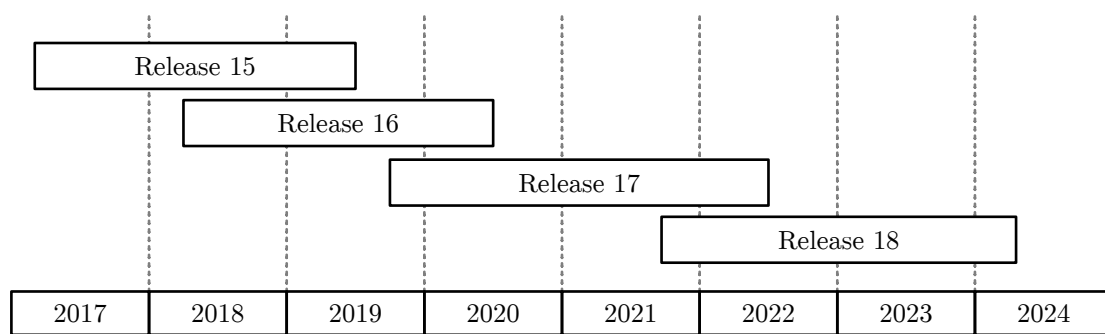
Figure 2.5: 3GPP release timeline. Based on [15] [13]

2.2.2 Use Cases

Use cases of cellular networks have evolved - 5G is designed with additional use cases in mind that previous generation systems have not targeted. This has implications on the design of the networks as well as the usage, both of which impact the energy consumption of the network. Voice services were central to the first generation mobile communication systems. For first- and second-generation cellular networks, they were integrated in all layers of the network [19]. 3G systems first enabled mobile broadband (MBB) services, though voice services were still handled through separate services and did not rely on packet data transport [20]. For 4G, the architecture was built around packet data transport, with mobile broadband as the central use case. Voice services in LTE and 5G are utilizing the Internet Protocol and do not require a separate proprietary protocol stack [20].

In the work towards 5G, additional use cases beyond mobile broadband (MBB) were identified. The following three usage scenarios are supported by 5G and are continuously enhanced with further 3GPP releases, also illustrated in Figure 2.6:

- enhanced mobile broadband (eMBB)

- massive Machine Type Communication (mMTC)

- ultra-reliable low-latency communication (URLLC)
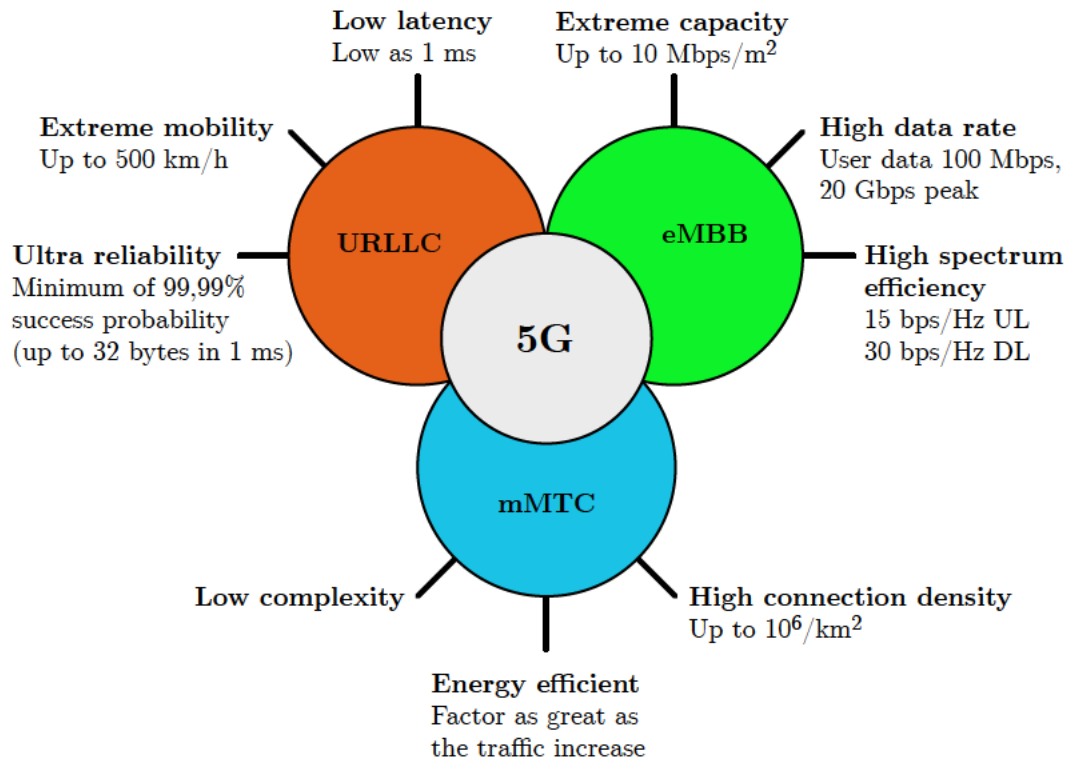
Figure 2.6: Main use cases for 5G. Adapted from [14]

Due to the new use cases introduced in 5G that require novel services, the 5G core network is designed in a way that can provide different logical networks while sharing the available hardware. This concept is known as network slicing, and each logical network is called a network slice [14].

According to [21], the attributes of URLLC support Industrial IoT (IIoT) applications, while mMTC supports the 4G LPWAN technologies (Low Power Wide Area Access Network) Narrowband IoT (NB-IoT) and LTE-M. In addition to this, the 3GPP introduced a new tier of reduced capability (RedCap) UE devices, also referred to as NR-Light in Release 17 [16]. The work in [21] outlines the most important aspects of RedCap: IoT use cases are targeted with RedCap, for example industrial wireless sensors and video surveillance cameras, but also wearable consumer electronics such as smartwatches, fitness trackers, and medical devices. Cost-effective, reduced complexity and energy efficient modules are to achieved, but the requirement for backwards compatibility to LTE (and previous generations) is dropped.

2.2.3 System Architecture

In this section, an overview of the 5G system architecture as specified by the 3GPP is provided. It is based on the general system structure of a cellular network (see Figure 2.2). The 5G system consists of the 5G core network (5GC) and the 5G access network (NG-RAN) - a good description of the overall architecture is given in [14] and summarized hereafter.

The core network for 5G is designed to be compatible with different access technologies. Besides NG-RAN, the access network could also be built from wireless LAN (WLAN) or wired broadband access. Within the NG-RAN, a new cellular access technology, called New Radio (NR) or 5G NR, is established. It is further differentiated between 5G NR standalone and non-standalone deployment. For standalone, the UE only utilizes the air interface of 5G NR as supplied by the NG-RAN and the connection to the 5GC. The non-standalone deployment allows deployment of 5G NR while reusing the LTE core. Due to this backwards compatibility, the non-standalone option also enables the UE to fall back on the connectivity provided by the LTE RAN, in case there is no NR coverage. The standalone deployment of 5G is the target of most network operators, but the non-standalone option enables the introduction of 5G NR without the need to implement a new 5G core network first.

An overview of the 5G architecture is shown in Figure 2.7 - compared to the generic overview in Figure 2.2, only the specific terminology of the network elements and interfaces is changed.
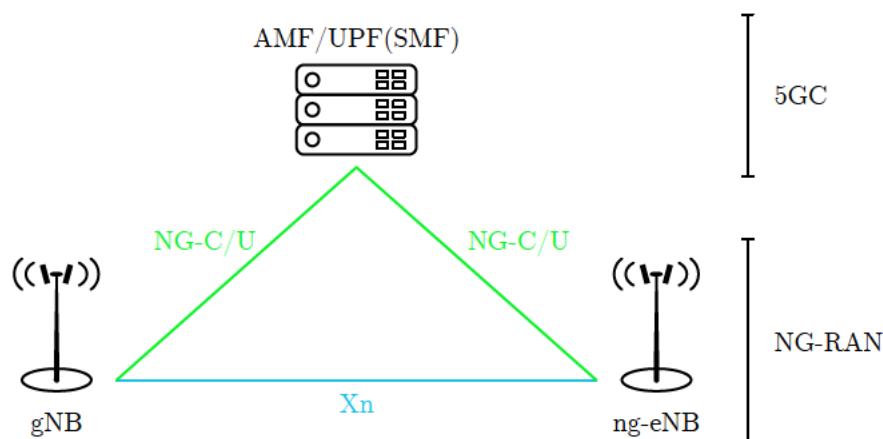
Figure 2.7: Overview of the 5G architecture. Adapted from [19]

The 5G core network comprises the functional components for authentication and mobility functions (AMF), user plane functions (UPF) and session management functions (SMF). A node in the NG-RAN can be a "next generation nodeB" (gNB) or a "next generation evolved nodeB" (ng-eNB), which is an LTE node that is connected to the 5GC instead of the LTE core (Evolved Packet Core, EPC). The term "nodeB" or "Node B" refers to the main telecommunication node in UMTS (3G) [13]. In LTE this is designated as "eNB" (evolved nodeB). The terms NodeB, eNB, gNB and ng-eNB represent a protocol anchor, while the term base station refers to the hardware. The base station and its specifics within 5G are further explained in Section 2.2.8. The gNB and ng-eNBs are connected through the logical Xn interface. The gNB and ng-eNB are connected to the 5G core network using a backhaul connection that is defined as the NG interface. This NG interface is further split into two separate interfaces: Connection to the AMF is realized via the NG-C, responsible for control messages. The NG-U interface connects to the UPF and transports the user data.

2.2.4 Physical Access Specification

The specification of the physical access parameters and procedures for the air interface have fundamental impact on the power consumption of mobile networks - both for the RAN and the UEs. Generally, the complexity and demands on hardware are increasing the larger the bandwidth and the higher the carrier frequency - thus the total energy consumption of the hardware may increase. The radio resource allocation is relevant for power consumption modeling to understand how transmission power as well as other time and frequency resources in 5G systems are allotted. An introduction to the specifications for 5G regarding the frequency and bandwidth, carrier aggregation and the allocation of radio resources is given hereafter.

Bandwidth, Frequency Bands, and Duplex Modes

5G NR allows for a much higher bandwidth (up to 400 MHz per carrier) compared to LTE with 20 MHz per carrier, as stated in [14] [13]. For comparison, UMTS utilized 5 MHz bandwidth [13]. High bandwidth is only available at higher frequencies, as the lower frequency spectrum is already allocated to a variety of wireless services. Therefore, 5G NR is designed for two main frequency ranges: FR1 contains the spectrum from 450 MHz to 7.125 GHz and FR2 from 24.25 GHz to 52.6 GHz [14]. The FR2 range includes part of

the extremely high frequency (EHF) or mmWave spectrum which comprises the spectrum from 30 to 300 GHz. Lower frequency bands are usually used in FDD (Frequency Division Duplex) mode. While TDD (Time Division Duplex) mode is often employed for cellular bandwidth above 2.5 GHz, the FR2 frequency range only supports TDD [22].

The 3GPP defined a target spectral efficiency of 30 bit/s/Hz for downlink and 15 bit/s/Hz for uplink. However, peak data rate should not be directly derived from peak spectral efficiency and bandwidth multiplication, as the spectral efficiency might vary depending on the used frequency band according to [23].

Carrier Aggregation

The capacity demands per base station have increased over time, and the increasing bandwidth in LTE and 5G alone are not sufficient to compensate for this [13]. Therefore, the 3GPP added the Carrier Aggregation (CA) procedure to the LTE standard. Based on [22], the important aspects are outlined. Carrier Aggregation is typically employed only in the downlink as need for higher bandwidth is usually larger than in the uplink. Effectively, it increases the bandwidth by combining several carriers (radio channels). An aggregated carrier is known as a component carrier (CC). The UE connects to one carrier in uplink and downlink, the primary carrier (or primary cell, referred to as PCell) and can subsequently add further carriers (secondary cells, SCells). There are three types in which radio channels can be combined in 5G NR and up to 16 component carriers are supported. The three types of carrier aggregation are: Intra-band contiguous, intra-band non-contiguous and inter-band non-contiguous. The types differentiate the combination of carriers within one frequency band (intra-band) and beyond the frequency band (inter-band).

Radio Resource Allocation

5G NR offers great flexibility in the allocation of time and frequency resources depending on the requirements. The frame structure is differentiated into five different numerologies each with different sub-carrier spacing, symbol lengths, number of slots in a frame, and the required bandwidth [24].

Terminology   Based on [19], the terminology of 5G frequency resource allocation is outlined in the following. A radio frame in 5G consists of 10 sub-frames. Each sub-frame consists of 2^μ slots, where μ indicates the numerology (0 to 4). Each numerology represents a different sub-carrier spacing. Each slot consists of 14 OFDM symbols.

Based on this, the following terms are defined for 5G:

- Resource Element (RE): One sub-carrier (frequency-domain) and one OFDM symbol (time-domain).

- Resource Block (RB): Twelve consecutive sub-carriers in frequency domain. The time-domain length of a resource block is variable in 5G, though the minimum is one OFDM symbol length. The number of resource blocks per carrier depends on the carrier bandwidth, numerology, and the frequency band.

- Resource Grid: Each antenna port, numerology, and transmission direction has one resource grid that consists of the available resource blocks.

There are two types of resource blocks: Common resource block (CRB) and physical resource block (PRB). The CRB is defined within the channel bandwidth. The network can configure a part of contiguous spectrum (equal to or smaller than the channel bandwidth) as a bandwidth part (BWP). The PRB is defined within one BWP.

Downlink Power Allocation   Relevant for the modeling of base station power consumption is the allocation of downlink transmit power. The work in [25] analyzes the power allocation for LTE under simplified assumptions, the results are summarized hereafter. The allocated downlink transmit power for each sub-frame is based on the calculation of the scheduler. For LTE, the power of the different carriers is calculated as different ratios to a reference value: The RS EPRE (Reference Signal Energy Per Resource Element). It is assumed that the transmit power (P_{TX}) depends linearly on the number of scheduled PRBs ($N_{\text{PRB,allocated}}$):

$$P_{\text{TX}} = m \cdot N_{\text{PRB,allocated}} + n \tag{2.1}$$

The fixed part of the transmit power (n) depends on channels and signals independent of the allocated PRBs such as broadcast channels, control channels, reference signals, and synchronization signals. The slope (m) depends on the reference signal power (RS EPRE)

and power allocation options. It is important to note that due to the variable slope, the maximum transmit power (for the maximum allocated PRBs) also depends on the value of the RS EPRE. Furthermore, the employed scheduling algorithm and power amplifier influence the transmit power - though this is negligible under the assumption that the power amplifier does not support adaption to lower bandwidth or sleep periods during empty OFDM symbols.

In conclusion, the transmit power is assumed to be a linear function of the allocated PRBs, though this is only valid under simplifying conditions. The slope and offset of the linear function depend on the specific physical layer setup. The downlink power allocation for 5G NR is similar to the LTE specification, the 5G procedures are described in TS 138 214 [26].

2.2.5 Access Stratum Protocol

The access stratum is the functional layer between RAN and UE. To further introduce the different RAN architectures and the communication and data transfer of radio access network and user equipment, the relevant aspects of the 5G access stratum protocol are summarized in this section. An extensive explanation is given in [14], which is outlined subsequently.

The 5G NR access stratum protocol uses a similar interface protocol and functions as in LTE. The two protocol stacks, user plane (UP) and control plane (CP) contain several protocols and adhere to the OSI (Open System Interconnection) reference model. The OSI reference model defines seven communication layers and the interaction between these via service access points (SAP). Additional information, for example the packet header, is added with each lower layer of the model. Packet and header information is referred to as the protocol data unit (PDU). If a PDU is received by a lower layer service, it is missing the protocol header for the corresponding higher layer and is therefore referred to as a service data unit (SDU). The lower layer transports the SDU to a higher layer service and adds the protocol and packet header - it provides a transport service. Communication between protocol layers on the same OSI layer level is referred to as peer-to-peer communication.

Channels

Channels are utilized to exchange data between different protocol layers, each of them associated with a service access point. The Figure 2.8 illustrates the channels and corresponding protocol layers in the 5G NR access stratum protocol.

```
                    ┌─────────────────────────┐
                    │           5GC           │
                    └─────────────────────────┘
                              │ QoS flow
                              ▼
                    ┌─────────────────────────┐
                    │          SDAP           │
                    └─────────────────────────┘
                              │ Radio bearer
                              ▼
                    ┌─────────────────────────┐
                    │          PDCP           │
                    └─────────────────────────┘
                              │ RLC channel
                              ▼
                    ┌─────────────────────────┐
                    │           RLC           │
                    └─────────────────────────┘
                              │ Logical channel
                              ▼
                    ┌─────────────────────────┐
                    │           MAC           │
                    └─────────────────────────┘
                              │ Transport channel
                              ▼
                    ┌─────────────────────────┐
                    │           PHY           │
                    └─────────────────────────┘
                              │ Physical channel
                              ▼
```
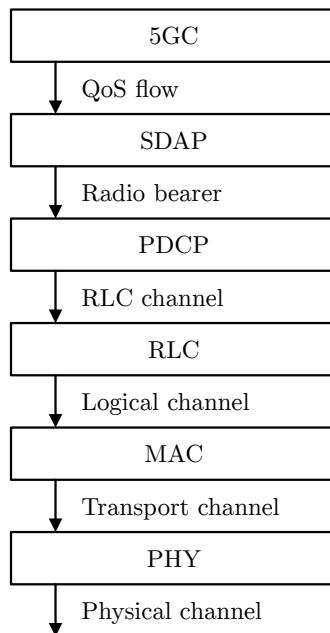
Figure 2.8: Overview of the 5G channel mapping. Adapted from [14]

Channel types for the higher layers are generally not particularly relevant in the context of power consumption modeling for base station and user equipment, thus these are not described here. In addition, the following channel types for the lower layers are defined for 5G:

- Logical channel: "What will be transferred?" Separates type of information (e.g., paging or broadcasting). Two types: Control channels and traffic channels.

- Transport channel: Multiplexing of logical channels to be transferred into physical channels.

- Physical channel: "How will the transfer be performed?" Determines the specifics of the transmission over the radio interface. Channels with specific characteristics (e.g., modulation or transmit power) are defined.

In Figure 2.8, the 5G core (5GC) is shown as the topmost layer, the functionality of the remaining protocol layers is explained briefly hereafter, based on [14].

- Service data adaptation protocol (SDAP): The SDAP is responsible for the transmission of service data, as it performs the mapping of the QoS flow to a radio bearer. It introduces a label that ensures transmission of the data packet with an assigned QoS profile in the lower layers.

- Packet data convergence protocol (PDCP): The PDCP is responsible for avoiding packet losses due to handovers. It also performs header compression and decompression of higher layer headers such as TCP/IP headers.

- Radio link control (RLC): The RLC layer provides RLC channels to the PDCP. RLC channel can be configured with three different transmission modes that ensure different levels of reliability and latency.

- Medium access protocol (MAC): The RLC layer provides RLC channels to the PDCP. RLC channel can be configured with three different transmission modes that ensure different levels of reliability and latency.

- Physical layer (PHY): Data transfer services are provided by the physical layer to the higher layers. It maps the characteristics of the transport channel to the radio interface, using techniques such as channel coding and modulation.

2.2.6 Core Network

The core network in 5G follows a few unique paradigms and introduces new functionalities, which are summarized in this section following the explanations in [13] and [27].

In 2G and 3G, every network function was typically described and implemented in physical, dedicated hardware. Often, proprietary hardware was developed for each network component. This changed with the introduction of LTE, when standard x86 servers and standard network hardware were replacing the specialized and costly single-purpose hardware. Furthermore, software for the core network was increasingly deployed in virtual machines. This enables the separate development and acquisition of software and hardware. For 5G, the 3GPP specification allows for a cloud-native implementation of the core network, which is based on containers. To enable this, the functionality of the core network is split into microservices. Each microservice is typically deployed in a

container. This concept is also referred to as network function virtualization (NFV). The tasks of the 5GC include: Performing mutual authentication between the UE and the network, registering UEs, tracking the location of the UE, establishing data sessions to different networks and forwarding traffic.

One of the novel paradigms introduced for the 5GC is the option to set up private networks. Various industries are interested in replacing and augmenting other communication systems with 5G, as it promises to offer new use cases - supporting low latency and high reliability communication (Section 2.2.2). Traditional deployments of cellular networks do not meet the privacy and reliability required in industry settings. To fill this gap, 5G enables private network deployments - where a network is partially or completely deployed on site, including the 5GC.

2.2.7 Radio Access Network Architectures

This section introduces the possible architectures for the radio access network in 5G. The choice of architecture can influence the energy consumption of the RAN as it mainly determines where the resource demanding digital signal processing is carried out (centralized or distributed).

Distributed or Centralized

The major differentiation of different RAN architectures is the traditional option of a distributed RAN (D-RAN) or the relatively new option of centralized RAN (C-RAN). Centralized RAN In a distributed RAN, the base station sites include the BBU and remote radio unit (RRU) - the connection to the core network is realized over a backhaul network (see Figure 2.9). The computing is completely carried out on distributed base station hardware.

The disadvantage of a distributed management of computation resources is the waste of computational resources due to highly dynamic traffic loads. The BBUs in a distributed RAN only process the traffic for one base station, which may be lightly loaded for most of the time, according to [28]. Centralized radio access networks (C-RAN) consolidate the baseband processing units of several base stations into a BBU pool that is shared among multiple base stations - and only the RRU remains at the base station site (illustrated in Figure 2.9). The computation resources of the centralized baseband units are dynamically
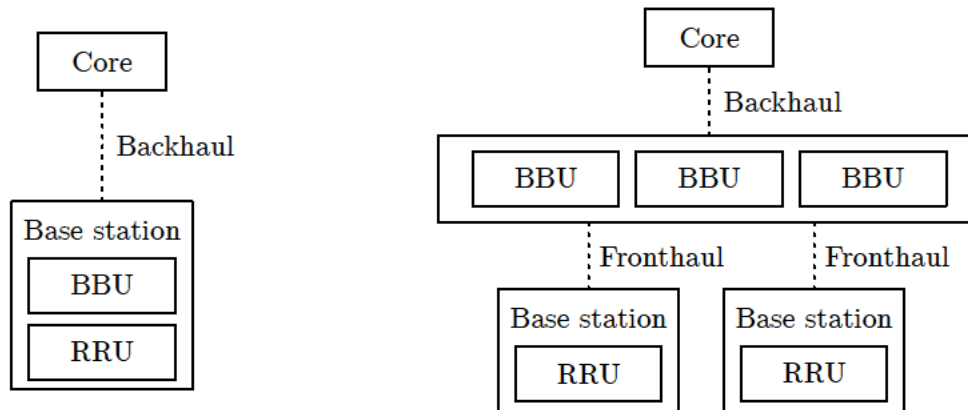
Figure 2.9: Comparison of distributed (left) and centralized radio access networks (right). Based on [22]

allocated. According to [28], this approach can lead to significant improvements in energy consumption compared to the conventional distributed architecture. It is assumed in [27] that baseband pooling as well as centralized radio resource coordination and scheduling are the most important advantages of a centralized RAN. As the processing capability of general-purpose processors improved, it became feasible to use it for baseband compute including MAC, RLC and (in part) the PHY layer protocol stack. This also enables the virtualization of the BBU pool.

The split between RRU and BBU in Figure 2.9 is simplified - the 5G specification defines several so-called functional split options that define which specific functionalities are centralized or remain distributed. These will be discussed in the following section.

Functional Split Options

The 3GPP defined eight functional split options for 5G, as illustrated in Figure 2.10. The functional splits are well-described in [27] and outlined hereafter.

The lower the split (lower in terms of the communication layer, but confusingly denoted by higher split numbers), the more functions are centralized - this results in higher potential performance gains and resource utilization gains due to centralized scheduling and resource sharing. On the other hand, lower splits also increase the required fronthaul bandwidth and latency requirements, and the complexity of the radio unit (RU). Thus,
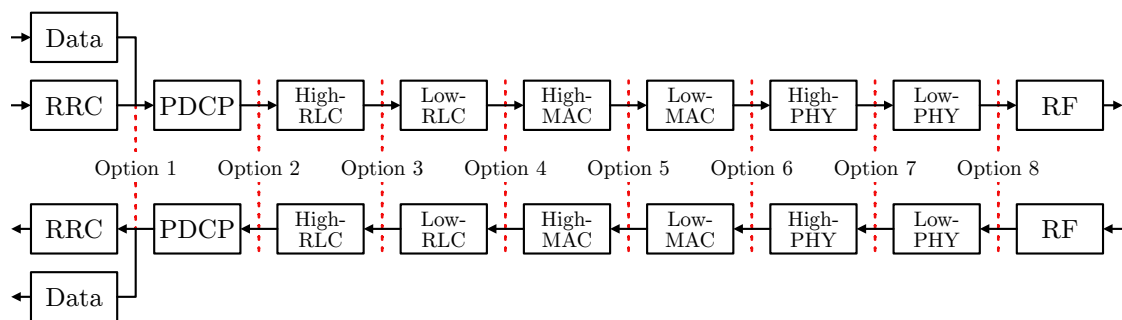
Figure 2.10: Split options defined for the 5G RAN. Adapted from [27] Fig. 7.1

these conflicting aspects need to be balanced when designing the RAN and deciding on the functional split option.

Based on the split option, a node in the NG-RAN is split into a CU (central unit) and a DU (distributed unit). The implemented functionality in each depends on the split option. The RU (radio unit) can optionally be split from the DU using a lower layer split option. When referring to Figure 2.10, the CU encompasses every function left of the split and the DU every function to the right of the split - and the RU optionally everything to the right of the DU. This means that the RU may contain solely the analog frontend (RF hardware) or additionally (parts) of the digital baseband processing, depending on the split option.

The transport network between DU and RU is known as fronthaul. The midhaul connects DU and CU, and the backhaul is the transport network between CU and the aggregation backbone/core. However, the transport networks each can have a complex network topology using different technologies - details on transport networks can be found in Chapter 6.6 of [27]. The three logical units and the respective transport networks are illustrated in Figure 2.11. The following three configurations can be distinguished: a) with a combined DU/CU if a lower layer split is implemented, b) in case of a high layer split (split option 2) or c) for a double split - combined high and low layer splits.

The 3GPP has standardized the split option 2 - the split between PDCP and RLC, in the CU/DU split architecture with a fronthaul interface called F1. In case a lower layer split is used, the DU/RU combination is split and the DU is separated from the RU (logically and spatially). The 3GPP could not agree on the concrete specification of a particular lower layer split, thus several split options are defined by other organizations such as O-RAN and CPRI. Notably, the split option 7 is further divided into three main split
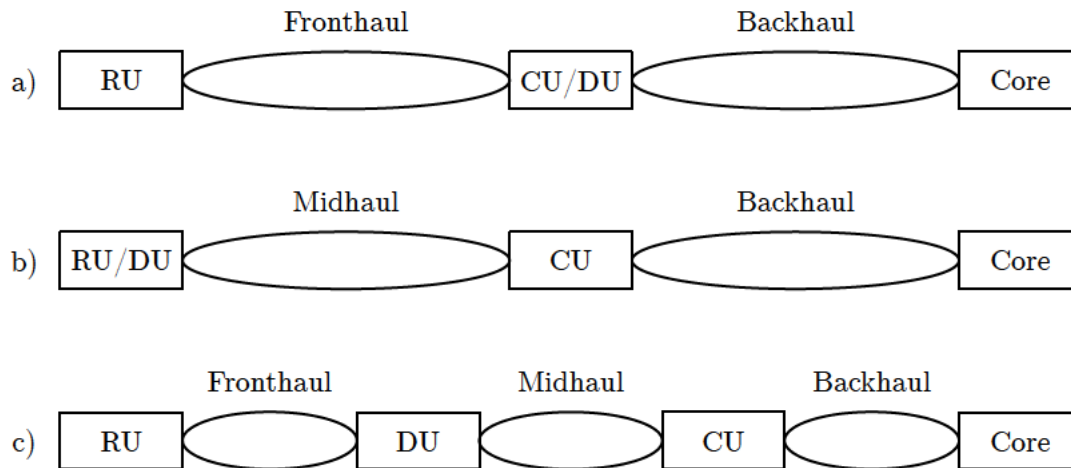
Figure 2.11: Transport networks for different RAN splits.

options (and further variants of these). A description of the split options[1] and details on the lower layer splits can be found in [27] and [22].

2.2.8 Base Stations and Cells

Base stations are the central components of the RAN and enable users to connect to the network over the air interface. In order to discuss the power consumption models in Chapter 4, the different types of base stations and how they are employed in a network to provide coverage is introduced in this section. Additionally, the hardware configuration of base stations is outlined.

Base Station Classes and Cell Types

Base station classes defined by the ETSI in [29] and [30] are the wide area base station, medium range base station, local area base station and home base station. The characteristics of these classes are derived from macro, micro, pico, and femto cell scenarios respectively. The different cell types represent different coverage areas. The macro cell covers the largest area (e.g., coverage in rural areas) down to the femto cell, which provides coverage to a single office or home.

---

[1]A good illustration of the concept is the poster by HUBER+SUHNER, available at: hubersuhner.com/en/documents-repository/technologies/pdf/fiber-optics-documents/5g-fundamentals-functional-split-overview (visited on 23/05/2023)

Limits for certain parameters are defined for the different base station classes in [30], from which relevant parameters are listed in Table 2.1.

Table 2.1: Base station classes parameters as defined in [30]

Base station class	Min. coupling loss	Base station to UE min. distance	Output power limit
Wide Area	70 dB	35 m	No limit
Medium Range	53 dB	5 m	$\leq$ 38 dBm
Local Area	45 dB	2 m	$\leq$ 24 dBm
Home	Not specified	Not specified	Not specified

The parameters define the classes or cell types only vaguely - as such, the exact coverage area or base station configuration can not be concluded from the cell type. Additionally, the terms large cell and small cell are often used - the base station power consumption model in [31] defines the large cell as equivalent to macro and micro cells, the small cell encompasses the micro and femto cells. The base station class names defined by the 3GPP/ETSI are seemingly not used in most of the literature.

Heterogeneous Networks

Heterogeneous networks (often abbreviated as HetNets) combine large cell base stations for area coverage with small cell base stations to meet capacity demand at certain hotspots [27]. The two tiers of base stations are also referred to as coverage tier and hotspot tier [32]. Thus, the coverage tier base station create large cells and the hotspot tier base stations create small cells. In practice, it is common to use different frequency bands for coverage tier and hotspot tier to avoid inter-tier coordination [32].

HetNets may be combined with a distributed or centralized RAN. A heterogeneous C-RAN is referred to as heterogeneous C-RAN (H-CRAN), it is meant to combine the advantages of both C-RAN and heterogeneous networks. A higher energy efficiency than with C-RAN can be achieved with H-CRAN according to [28].

Evolution of Base Station Hardware Configurations

The architecture of base stations has evolved through the mobile network generations, the major developments are summarized based on [5], [13] and [33]. In earlier base station configurations for 3G, the remote radio unit (RRU) is located away from the antennas and connected through long coaxial feeder cables (left configuration in Figure 2.12).

By moving the analog signal processing closer to the antennas, the losses induced by the coaxial feeder cables can be reduced. This configuration, typical for 4G base stations, is shown in the center of Figure 2.12, where the radio processing unit is typically referred to as Remote Radio Head (RRH). The RRH is connected to the baseband unit with fiber optic cables via the Common Public Radio Interface (CPRI) protocol.

For 5G, the Active Antenna Unit (AAU) is a new type of base station equipment. It integrates the antenna array of an active antenna system (for mMIMO, refer to Section 2.2.10) and the functionality of the RRH. The base station configuration using an AAU is illustrated on the right of Figure 2.12. Depending on the RAN functional split, the baseband unit and the RRH/AAU may encompass different functionality (see Section 2.2.7).
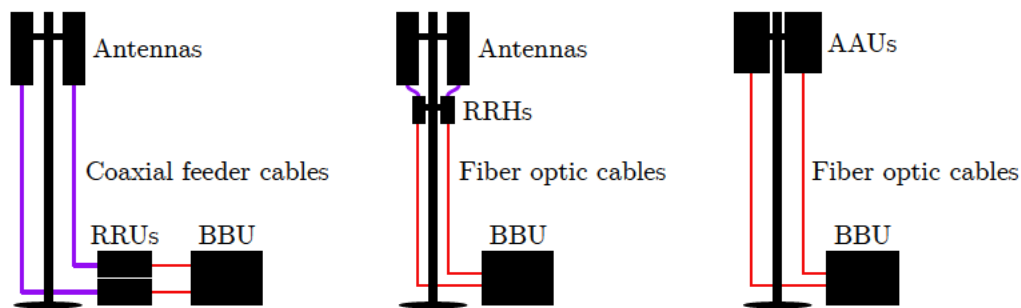
Figure 2.12: Evolution of base station configurations. Left: Traditional setup with long coaxial feeder cables (purple) from radio unit to antennas. Center: RRHs placed closer to antennas, shorter coaxial feeder cables. Right: Active antenna units connected directly via fiber optic cables (red) to the baseband processing unit. Based on [13] [5] [33]

2.2.9 User Equipment and Radio Resource Control

User equipment refers to the variety of different devices (phones, tablets, industrial routers etc.) that can establish a radio connection to the RAN. The specifications of LTE and 5G define different categories of UEs that are distinguished by their respective capabilities, such as peak data rate and modulation type.

Uplink Transmission Power Control

The transmission power of the user equipment is controlled by a procedure referred to as uplink power control. The uplink power control for 5G is described in TS 138 213 [34] and related specifications. Brief explanations and summaries of the specifications can be found in Chapter 3 and 4 of [19].

Radio Resource Control

The radio resource control is well-described in [13] and [14] and outlined hereafter. The radio resource control protocol manages the exchange of control messages over the radio interface between the UE and the gNB. It includes functions related to the establishment, maintenance, and release of an RRC connection between the UE and NG-RAN, controlling carrier aggregation and dual connectivity. Security functions such as key management, ciphering, and authorization as well as the task of handling radio bearers are part of the RRC. Supplemented by mobility functions, quality of service management functions, and UE measurement reporting.

There are three states defined for 5G NR RRC. The corresponding state machine is shown in Figure 2.13.
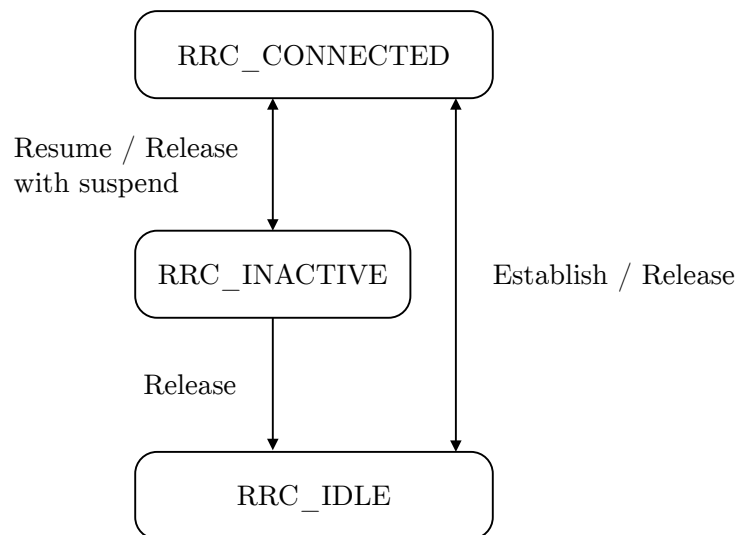
Figure 2.13: UE RRC state machine in 5G NR. Adapted from (ETSI TS 138 331 V15.3.0)

In the RRC_IDLE state, no RRC connection is established. The UE selects which cell to connect based on its configuration and periodically acquires system information and paging. When triggered, the UE uses the random access procedure to establish a connection and transition into the RRC_CONNECTED state.

If an RRC connection is established, the UE is in the RRC_CONNECTED state. In this state, transfer of user data is possible and the mobility procedure is controlled by the network. In the connected state, the UE is required to perform periodic signal measurements, leading to a higher power consumption. To save power, the UE can request the transition into idle or inactive mode, the gNB then may transmit a release message. The maximum rate of release requests is controlled by the network.

The RRC_INACTIVE state indicates that an RRC connection is established, but no user data can be transferred. The connection can be resumed using random access or paging, this triggers a transition into the RRC_CONNECTED state . If the connection is released, the UE switches to the RRC_IDLE state.

LTE only has two RRC states, and the state RRC_INACTIVE was added for 5G. The reason for this was to reduce the number and frequency of connections between the gNB and the core network, as the sporadic transfer of packets leads to frequent transitions between the idle and connected state in LTE.

2.2.10 Massive MIMO

The concept of massive multiple-input (and) multiple-output (mMIMO) is a key technology that enables high data rates for 5G [32]. It is also relevant for the power consumption of 5G systems as it employs different antenna structures, and requires different radio frequency (RF) and digital signal processing hardware. The energy efficiency of mMIMO depends on the exact configuration and deployment scenario - theoretical assessment is provided in the works by Emil Björnson et al. [32] [35] [36] [37] [38]. Evaluations regarding the effect on total network energy consumption are presented in [33].

Multiple-input (and) multiple-output (MIMO) antenna technology increases the capacity of a wireless radio link by employing multiple transmit antennas and multiple receive antennas. Multiple data streams can use the same radio channel, which increases the peak data rate or the overall capacity of the cellular network. MIMO is utilized in other wireless communication standards, for example WLAN and LTE. According to [14], LTE

MIMO is specified for a maximum of eight spatial layers in downlink and four spatial layers in uplink direction. Fore example, a typical LTE configuration of 4×2 MIMO requires four transmit antennas at the base station and two receive antennas at the user equipment [14]. A MIMO configuration with four transmit and receive antennas at the base station is specified in the format 4T4R [33].

For mMIMO, the number of antennas is further increased. In this context the terminology of antenna arrays and antenna elements is used, antenna arrays for mMIMO usually consist of 32, 64, 128 or even more antenna elements [33]. A typical configuration for 5G is 64 transmit and receive antennas (64T64R). This increase of antenna elements does not increase the number of spatial layers. The maximum number of spatial layers is not changed in 5G compared to 4G as the purpose of employing more antenna elements is the combination of spatial multiplexing with beamforming [14].

Beamforming is also used in radar technology to identify objects - similarly, by focusing the signal energy onto smaller areas, the user throughput, capacity, and energy efficiency can be improved for radio communication links [14]. mMIMO beamforming utilizes multiple antennas for reception and transmission for multiple parallel data streams to several users, while sharing the same time-frequency resources, and without the need for additional bandwidth or transmit power [24]. The work in [14] argues that beamforming compensates the higher path loss at higher carrier frequencies, which enables the deployment of 5G in higher frequency bands. Beam direction can be steered dynamically by controlling phase and optionally the amplitude of the signal at each antenna element, which is also beneficial in blockage scenarios due to user mobility [14].

A more formal definition and explanation of mMIMO and extensive information on mMIMO in the context of spectral efficiency and energy efficiency is provided in [32].

2.3 Power Saving Techniques in 5G

This section summarizes power saving techniques implemented or proposed for 5G. Most of the power saving schemes are specified for the user equipment, as profound improvements can be achieved here through the optimization of protocols. User equipment power saving schemes are described in Section 2.3.1. In the following, base station sleep modes (also referred to as discontinuous transmission - DTX) are outlined (Section 2.3.2).

Further base station and RAN power saving potential also results out of more general specifications, such as the RAN architectures.

2.3.1 User Equipment

In the following, power saving techniques for user equipment are summarized based on the extensive explanations in [14].

Discontinuous Reception and Transmission

Common power saving techniques for user equipment are Discontinuous Reception (DRX) and Discontinuous Transmission (DTX). In DRX, the UE can stop monitoring certain channels, while DTX pauses the transmission in certain channels.

The enhanced extended idle mode DRX was defined for the 5G core in Release 16, it was first introduced in Release 12 for IoT devices. When using the extended idle mode DRX, the delay tolerance of the services needs to be considered, as the UE is only available within a certain delay that is set by the DRX cycle value. A longer cycle length could negatively affect the applications and services of the UE. The extended idle mode DRX is requested by the UE and negotiated with the core network, the parameters may be set by the authentication and mobility functions of the 5G core. DRX requires the UE to wake up periodically according to the DRX cycle value for a certain period, during which the control channel is monitored. The UE must wake up - no matter whether data is expected or not.

Mobile Initiated Connection Only

Mobile Initiated Connection Only mode was introduced for 5G. In this mode, the UE is completely suspending the periodic reception of paging. Typically, devices intended for this mode are special purpose devices. For example, IoT devices which do not require reception of data and mostly send infrequent status updates.

Further Power Saving Enhancements in 3GPP Release 16

The 3GPP study on user equipment power saving for Release 16 identified two aspects that improve the energy efficiency of user equipment: Efficient data transmission in active connected mode and low energy consumption in sleep mode. Subsequently, several new power saving mechanisms targeting UE were conceived for the 3GPP Release 16. In Release 16, additional power saving parameters were introduced that enable the UE to configure power saving methods such as DRX. These changes initiate a transition from network-centric configuration towards UE-centric configuration of power saving methods.

A large share of the UE power consumption is due to the frequent monitoring of the downlink control channel and performing signal quality measurements and reporting. A new mechanism allows reduced control channel reception for specific secondary cells in a carrier aggregation configuration. Control channel monitoring is responsible for a large share of the typical 5G eMBB device energy consumption. Release 16 therefore further improves the DRX procedure with a wake-up signal. The UE can skip receiving the complete control channel data, if the wake-up signalling is enabled and the network provides a certain indicator to the UE. The periodic measurement of the cells conducted by the UE to determine its position and initiate the cell handover require relatively high power consumption. The UE may reduce the RRM measurement under certain conditions. For example, the mobility of the UE is low, therefore the cell measurement changes only slightly or the UE is not near the cell edges.

Since Release 15 the UE can dynamically switch from a larger bandwidth to a narrower bandwidth. This is further optimized in Release 16 by also adapting the number of MIMO layers in addition to the bandwidth adaption.

2.3.2 Base Station Sleep Modes

To reduce the energy consumption of a base station, some hardware components may be turned off during periods where no reception or transmission is required. There are no standardized procedures for base station sleep modes in 5G. However, a significant number of publications have covered sleep modes theoretically. The general approach is to gradually deactivate more hardware components depending on the available sleep time,

the current traffic demand and the activation or deactivation time of the component as indicated in [24]. Typically, up to four sleep modes are proposed for 5G base stations.

One of the main functionality that prevents a base station from entering a sleep mode are periodic signals such as reference signals. In 5G NR, the synchronization signals are combined into a Synchronization Signal Block (SSB) that is transmitted with a periodicity between 5 ms and 160 ms [24]. Due to this periodicity, potential sleep modes that require longer activation or deactivation times than the maximum of 160 ms, can not be entered.

Tractable measurement-based evaluations of sleep modes in 5G base station hardware are only limitedly available. Evaluations by the telecommunications company Ericsson [39] indicate that shutting-off power amplifiers during "micro-sleep" during low and medium traffic can reduce power consumption by 70% in 5G NR in a base station transmitting 40 W using 4 antennas. The reduction achieved with LTE for the same setup is lower, at about 45%.

2.4 Energy Consumption and Energy Efficiency of 5G

In this section, general findings on the energy consumption and energy efficiency of 5G systems are outlined.

2.4.1 Power Consumption and Energy Efficiency in Wireless Communication Systems

The approximate total power consumption of different wireless communication devices spans several orders of magnitude, as illustrated in Figure 2.14.
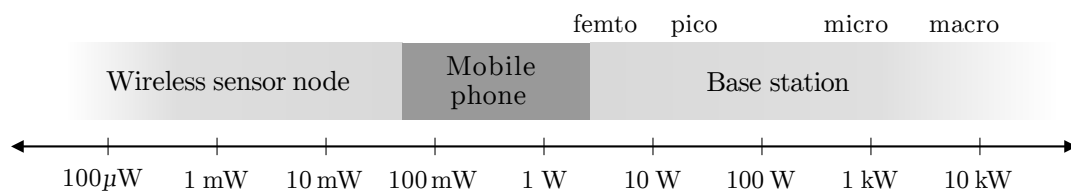
Figure 2.14: Magnitude of the power consumption of wireless communication equipment. Based on [27] [7]

This wide range of power consumption across the whole spectrum of different devices and within a single device category, as well as the complex architecture and deployment of current wireless communication systems, complicates the evaluation of energy consumption.

In [40] the authors theoretically assess the upper limit to energy efficiency of a wireless communication system. They conclude that the limit depends on which parameter values can be selected in practice and for the energy consumption modeling. The ultimate physical upper limit of the energy efficiency is placed at around 1 Pbit/Joule. Due to practical constraints such as the number of antennas and channel gains, a maximum energy efficiency in the order of a few Tbit/Joule is expected for practical systems. According to [32], values in the order of kbit/Joule or Mbit/Joule are to be expected for current wireless communication systems.

A general introduction to energy efficiency and principal measures to improve it in cellular networks are discussed in [32]. Chapter 6 of this thesis outlines energy efficiency for URLLC and mMTC network slices.

2.4.2 Total Mobile Network Energy Consumption

There are several studies available on the total energy consumption of cellular networks. However, in practice cellular technology generations are usually deployed in parallel and several networks, operated by different operators, coexist in the same area. This complicates the evaluation of energy consumption of one specific radio access technology such as 5G. For example, in Germany the 3G networks were phased out in 2021 but 2G is still operated until 2030 to provide basic coverage - 4G and 5G are operated and expanded on top of this infrastructure [33]. The three German mobile network operators Telekom, Vodafone and Telefónica each deploy their own network infrastructure - the networks also differ in total energy consumption due to the diverse network planning and setup of the operators [33].

Private 5G deployments ("campus networks") are still relatively rare: The website [41] lists 73 networks deployed in Europe (June 2023). Thus, it is not surprising that there is no publicly available and tractable data on energy consumption for these networks yet (to the best knowledge of the author). Due to the relatively recent introduction of 5G in general, potential effects of the new technology are probably not fully captured in any study that is based on current deployment data.

Furthermore, the energy consumption of cellular networks and especially individual network components is rarely disclosed fully. Neither network operators nor device manufacturers publicize any detailed information in datasheets or reports. If data is published, it usually lacks context as no exact configuration, operating conditions of network devices or deployment architecture of networks are disclosed. Therefore, studies conducted on energy consumption of cellular networks largely rely on estimations and/or aggregated data from operators that do not allow conclusions on individual networks.

Generally, the studies on mobile network energy consumption only include RAN and core network energy consumption and exclude the UE energy consumption. It is reasonable to evaluate the UE energy consumption separately as the energy consumed by one device can not be attributed to any single network (e.g., a smartphone supports multiple wireless communication standards and switches seamlessly between networks) and includes energy consumption completely unrelated to the network/radio part (such as the device screen and other peripheral devices). The results of some relevant network energy consumption studies are summarized in the following paragraphs.
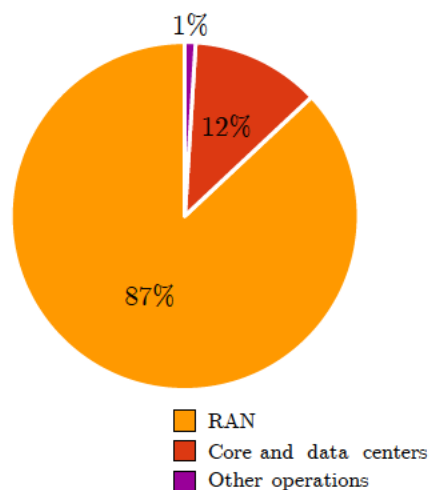
Figure 2.15: Relative energy consumption of 5G networks (excluding user equipment). Data from [42]

Studies conducted by Vodafone, as cited by [43] in 2011, give the following figures: The base stations account for about 60% of the total network power consumption. Mobile switching consumes 20%, core transmission 15%, and data centers less than 5%. Retail accounts for the rest. However, the study is from the pre-LTE generation.

A study on 5G network power consumption was conducted in 56 countries with ten operator groups and 58 networks in 2021. It reports the following values: "87% of the energy of the participating operators is consumed in the RAN. The network core and owned data centers (12%) and other operations (1%) account for the rest" [42]. This is illustrated in Figure 2.15. No figures are given for base stations specifically. But the study confirms that the majority of power is consumed in the RAN.

Generally, it is assumed that base stations consume about 60 - 80% of the energy in a network [24]. Deploying additional base stations on top of the existing network infrastructure to improve coverage likely further increases the total energy consumption. According to a report cited by [24], a significant increase in the number of base stations for 5G would be required to achieve a similar coverage compared to 4G networks. This is confirmed in [44], where an increase in deployment density of 2 to 3 times compared to 4G is assumed.

Therefore, research has mainly focused on quantifying and optimizing base station energy efficiency, as it promises the biggest reduction in overall network power consumption when energy saving is implemented. A literature review on whole network studies of energy consumption is conducted in [45]. It is concluded that there is a lack of whole network studies that include clear quantitative findings for 5G.

A very extensive evaluation of energy consumption and environmental lifecycle assessment of cellular networks and network equipment in Germany was recently published by the Umweltbundesamt within the "UTAMO project" - the results can be found in the report in [33]. The total baseline energy consumption of the mobile communications networks in Germany is calculated for 2019 at 2.31 TWh [33]. The figure includes RAN and transport core network energy consumption. Depending on the scenario, different predictions are given for the future energy consumption up to the year 2030. The baseline scenario assumes an increase of 325% to 7.51 TWh in 2030 [33].

The increase in energy consumption is accompanied by a disproportionately higher upper bound of the theoretically achievable data rate provided by macro cells, which is projected to reach 8133 Tbit/s in 2030 (45 times or 4400% higher than the 179 Tbit/s in 2019) [33].

The observed and projected increase in total network energy consumption is a strong indicator of a rebound effect, due to the increase in energy efficiency (bit/Joule) that results from the disproportionately higher data rate. William Stanley Jevons first described the

rebound effect in his 1865 book *The Coal Question* [46] after he observed an increase in the total coal demand after the invention of a more efficient steam engine. The reason for this was the economical viability of coal for new use cases due to the higher efficiency of the engine.

In the context of 5G or mobile networks in general, the rebound effect has not been extensively studied. According to [45], there is a lack of user-centric studies that focus on the interplay of mobile network energy consumption and user behavior. Whereas the energy consumption, energy efficiency, and the user activity metrics (traffic, number of users) have been studied on their own, comprehensive research on the relationship of these has not been conducted. Whether demand for higher data rates is driven by the efficiency improvements of new mobile network generations, or this demand exists independently of the improvements, can not be concluded unambiguously. The literature survey in [45] points towards the former, as the performance benefits of 5G are actively marketed towards consumers and industry.

Beyond the evaluation of operational energy consumption, further important aspects are the enablement effects (reduction or increase of energy consumption in other sectors due to 5G usage) as well as embodied energy (energy consumed during production and installation of network hardware). The literature survey in [45] considers these aspects. The evaluation of the UTAMO project [33] includes the embodied energy. Furthermore, Hexa-X [3] has set an objective of enabling a reduction of emissions of more than 30% CO2 equivalents through utilization of 6G in related sectors.

The work in [47] calculates the country-wide RAN energy consumption in Belgium based on power consumption models - the results show that concurrently operating 4G and 5G RANs consumes more energy than using only one generation. This supports the main findings in [33] for Germany. According to [47] this issue requires sufficiency policies for future network deployments. Another solution suggested in [33] is the already partially used concept of dynamic spectrum sharing, that allows the flexible use of carrier frequencies in 4G or 5G RAN depending on the current traffic demands.

2.4.3 Energy Consumption of the Radio Access Network

Detailed information on the power consumption or energy consumption of RAN infrastructure is only sparsely available, as the data sheets of radio units and baseband units usually only include maximum power consumption and a value for typical operating conditions - though the exact definition of "typical" is not further elaborated. This is also indicated in the UTAMO project report [33] - the report also includes an overview of several power consumption values from datasheets for various radio and baseband units.

Three examples of unspecific power consumption figures for base stations that are relatively vague and inconclusive are described in the following paragraphs:

A white paper by Huawei [48] indicates that the typical maximum power consumption of a 5G base station site increases significantly compared to 3G or 4G sites. However, this increase is due to the parallel deployment of hardware for the different cellular generations. In the example from Huawei, the 5G base station features an additional AAU and BBU, on top of the hardware deployed for previous generation base stations. The same is true for the 4G base station, which includes an additional RRU, that increases the maximum total power consumption of the site compared to the 3G base station. The typical maximum power consumption increases from about 4.9 kW (2G-3G base station) to about 6.9 kW (2G-4G base station) up to 11.6 kW (2G-5G base station) [48].

According to [44] the power consumption of a typical 5G macro cell base station is about 4.3 kW and the average power consumption of a 4G base station is 1.1 kW.

"The average power consumption for 2G-4G base station site is around 6 kW, which may raise to 10 kW at peak loads" [27].

The aforementioned examples show that the reported power consumption of base stations has a large variation. This is likely due to the aspects not reported: Different configurations (such as base station class/cell type, bandwidth, frequency band, MIMO setup, number of antenna ports etc.) and the operating parameters (such as maximum and average traffic load).

The share of the RAN energy consumption within the total network consumption calculated within the UTAMO project [33] for Germany is 83.3% in 2019 and 90.5% in 2030 for the baseline scenario. The radio units of the base stations are responsible for 60% of the total network energy consumption. The associated total increase in energy consumption is attributed to the increased requirements on computation for baseband processing and

analog-digital-conversion due to the higher data rates enabled by larger bandwidths, mMIMO, and new modulation schemes. Furthermore, the power amplifiers that usually only exhibit optimized efficiencies at fixed operating points and are not adaptive to the load are contributing significantly to the energy consumption - increased operating frequency due to the inclusion of higher frequency bands is likely to further increase the energy consumption.

The EARTH project results in [12] and [49] show that the relative share of power consumption per base station component differs depending on the base station class/cell type. Whereas more than half of the power consumption of a macro base station at peak load is attributed to the power amplifier, it is only about one third of the total for pico base stations. In contrast, the share of power required for the baseband processing is larger in smaller base stations.

The evaluations of the EARTH project in [12] and the UTAMO project in [33] show that base stations spend a considerable amount of time in a light traffic load state. This motivates the use of base station sleep modes that further reduce the power consumption by shutting off components not required in the idle or low-load time periods.

2.4.4 Energy Consumption of the Core Network

To the best knowledge of the author, there are no extensive evaluations of the power consumption or energy consumption specifically for 5G core networks publicly available.

The evaluation of the UTAMO project in [33] includes the core network (transport core network), calculating not only the server energy consumption but also the energy consumption of the metro and aggregation network (switches, routers, gateways) of mobile networks (including 5G). The evaluation provides a country-wide energy consumption for Germany as part of the total network energy consumption projections. In the baseline scenario, the transport and core network amounts to a total energy consumption of 0.39 TWh in 2019 and a projected increase to 0.71 TWh in 2030 [33]. The almost doubling of the energy consumption is mainly due to the increase in traffic which increases the demand on optical network unit, radio network controller, routers, and servers - only the increase in energy efficiency of the switches is projected to completely offset their increased computational demand, leading to an assumed decrease in energy consumption of the switches in 2030.

The 5G core is heavily based on the paradigm of virtualization and implementation in the cloud, as described in Section 2.2.6. Network function virtualization (NFV) or virtual network functions (VNF) are the relevant keywords in this regard. A few publications analyzing the energy consumption effects of virtualizing the LTE core are outlined in the following.

A breakdown of the power and performance behavior when employing a virtualization of the Evolved Packet Core (vEPC), the LTE core network, is explored in [50]. The conducted estimation from 2017 is based on real performance levels and datasheet values of existing commercial products for legacy and NFV network architectures for different deployment scenarios. The results show that a deployment of NFV in the EPC may lead to a minimum increase of 106% in energy consumption compared to the non-virtualized network solutions [50]. In case the hardware and software combination is not optimized, this figure increases further. The authors note that the results are limited to one specific, popular processor category.

In [51] the effects of virtualization on energy consumption are quantified using the online tool "GWATT" (developed by Nokia Bell Labs/GreenTouch[2]). According to this paper, virtualizing the EPC leads to a reduction in network energy consumption of 22%.

A mixed integer linear programming optimization model is developed in [52] with the objective of minimizing the total network power consumption by optimizing the location and server utilization of virtual machines used to implement the EPC. The model results indicate that virtualization leads to an energy saving of up to 38% compared to the scenario without virtualization. The authors claim that the results are applicable to 5G networks, even though the LTE core network is analyzed.

---

[2]Initially published, though not available online anymore at the time of writing this thesis, at: bell-labs.com/greentouch/index-page=gwatt-visualizing-the-greentouch-results.html

2.4.5 Energy Efficiency and Energy Saving of 5G Radio Access Network

An issue that arises from the increased virtualization, both in the 5G core and the RAN, is the reduced power efficiency of commercial off-the-shelf hardware compared to dedicated hardware and ASICs (application-specific integrated circuits) [27]. Power saving options in operating system and BIOS (basic input/output system) can not be enabled, if it results in the violation of timing requirements - which is often the case for time-sensitive services such as scheduling [27].

The evaluation of the virtualization of the RAN based on LTE deployment datasets in [53] compares the energy consumption of conventional BBU devices and a RAN deployment based on virtualized network functions. The virtualized BBU pool provides power consumption proportional to the load and improved power consumption at lower loads. On average, the energy consumption is about 250% higher for the virtualized BBU pool compared to the conventional BBU devices [54]. However, the deployment of virtualized BBUs alongside the optimized BBU hardware solutions showed energy savings up to 20% compared to the non-virtualized baseline deployment [54]. According to [54] the scalability of virtualized software solutions improves the RAN power consumption at lower traffic loads and the higher performance of specialized BBU hardware is advantageous at higher loads.

Potential energy savings of base stations due to architecture optimization and technology advancements are assessed in [1]. It is concluded that the largest relative savings are possible for baseband processing (saving of 40%) and cooling (50%), when employing centralized RAN. The largest relative saving due to technology advancement is expected for the RF hardware. The EARTH project results [25] and the UTAMO project report [33] also discuss potential areas of improvement extensively.

2.5 Renewable Energy Sources in Wireless Access Networks

When analyzing the sustainability of information and communication technology in terms of energy consumption or energy efficiency, the source of the energy and the corresponding emissions of greenhouse gases are also important aspects.

Several mobile network operators disclose their total energy consumption. Even though the share of energy consumption of the network infrastructure is usually not given. Additionally, the greenhouse gas emissions associated with the energy consumption are indicated as CO2 equivalents, however the method used to obtain these figures is often not documented. Therefore, such statements are not comparable and should be viewed with caution.

Furthermore, the share of renewable energy in the total consumption is often publicized. Almost all the operators considered in [33] report a figure of 100% energy from renewable sources. However, the Deutsche Telekom and Telefónica Deutschland state in their footnotes that this is based on the purchase of CO2 certificates. The percentage of own generation by the operators or even purchase of renewable energy is currently very low, according to [33]. Additionally, the UTAMO project evaluation provides figures on the carbon footprint associated with mobile network operation and manufacturing of the required hardware - this includes estimations of the current and future total renewable energy usage in German mobile networks.

Several papers theoretically examine the potential of renewable energy sources to power wireless access networks. A few relevant publications are summarized in the following: Powering wireless access networks with renewable energy sources only proves to be challenging due to the intermittent nature and variability of generation of wind power and solar power [55]. According to [56], air cooled and light-weight base stations can remove the need for power consuming air conditioning and provide coverage in rural areas using renewable energy sources. A stochastic model of the daily solar energy production is proposed in [57]. The model is utilized to evaluate the possible self-sufficiency of base stations on solar power generation. In [58] the general challenges that arise from introducing renewable energy sources to power radio access networks are discussed. General energy saving approaches and renewable energy source deployment for cellular communication systems are discussed in [59].

Furthermore, the recommendations of the ITU-T (International Telecommunication Union - Telecommunication Standardization Sector) published in L.1380: "Smart energy solution

for telecom sites" [60] describes photovoltaic powered base station sites and considerations for energy management. However, the document is not very detailed and far-off from a detailed specification that enables the practical introduction of renewable energy sources in wireless access networks.

In conclusion, practical use of renewable energy generation to supply base station power demand is still in its infancy, even though considerable research on the topic has been published. In this light, Vodafone announced a pilot project that includes the deployment of wind turbines to directly power base station sites, according to [33].

Based on the background on cellular networks and 5G presented in this chapter, the contributions, scope, and methodology of the thesis are discussed in the following chapter.

3 Contributions, Scope, and Methodology

3.1 Contributions and Scope

3.1.1 Contributions

In light of the background discussed in the previous chapter and the initial motivation, several research questions arise: How is the power consumption of 5G systems modeled? How do the models relate, and how can they be compared to each other? The first step in order to identify existing power consumption models is to review the models described in scientific publications. These models should then be examined to identify the differences and similarities. This furthermore enables and motivates the improvement and adaption of the models to suit the intended use case. To enable the comparison, selected models are to be implemented. Additionally, the implementation is a step towards a unified evaluation framework that is suitable to calculate the power and energy consumption of 5G network deployments based on paremeterized configurations.

Consequently, the two major contributions of this thesis are as follows:

1. Conduct a literature survey of power consumption models relevant for 5G.

2. Implement selected models to enable comparison of the models.

Based on the system structure of mobile networks (see Figure 2.2), the power consumption models can be categorized by the system components that are modeled. Therefore, power consumption models are described and discussed in the following categories:

- Base station models (Section 4.1)

- Radio access network models (Section 4.2)

- User equipment models (Section 4.3)

- System level models (Section 4.4)

The base station models and, of secondary importance, the additional aspects covered in the RAN models, are the focus of this thesis. This is justified, as the base stations are the major contributor to the energy consumption of mobile networks (refer to Section 2.4 in the background and the following Section 3.1.2). User equipment power consumption models are generally only suited for exploration of different configurations and energy efficiency targeted optimization of functionalities such as discontinuous reception and transmission, not for network level quantification of energy consumption. Analytic system level models are additionally discussed in this thesis.

In Chapter 5 the implementation of the power consumption models is described. The purpose of the implementation is to plot model results and, where possible, facilitate a quantitative comparison of the models in addition to the qualitative comparison.

An additional contribution is a survey of energy efficiency metrics specific to the new 5G use cases URLLC and mMTC. The traditional metric "energy per bit" does not sufficiently capture the unique requirements and performance indicators of these use cases, such as low latency and high reliability. An overview of alternative energy efficiency metrics is provided in Chapter 6.

3.1.2 Scope of the Thesis

The core network is excluded, as it requires the specific analysis of the energy consumption in cloud computing and data centers. Furthermore, the existing research on energy consumption in cellular networks in general and 5G in particular focuses on the RAN (particularly base stations) as it consumes the largest share of energy within the network architecture. To the best knowledge of the author, no power or energy consumption models specific to the 5G core network have been published. A few relevant publications on related topics such as the energy efficiency of network function virtualization are introduced in Section 2.4.4.

Lower level models, such as component level models (e.g., models of the power amplifier or ADC) are only included as part of the higher level base station or UE models. Detailed analysis of component level power consumption modeling is beyond the scope of this thesis. It is more feasible to focus on the modeling approaches within higher-level models specific to wireless communication systems, as the hardware components such

as the power amplifier are usually not standard components or are operated outside the typical operating range. Thus, when applying power consumption models for hardware components to models for wireless communication systems, aspects such as the parameter values may require additional attention.

Discussion of traffic models, load profiles, and similar aspects is excluded from this thesis as well. The modeling of network traffic depends on aspects which are not related to the modeling of power consumption, such as deployment location, user behavior, and utilization of the network. Therefore, this exclusion enables a more detailed focus on the power consumption models.

Important to note in this regard is the difference between power consumption and energy consumption modeling: Power is defined as the rate at which energy is transferred, therefore the modeling of energy consumption requires assumptions on the time period for which a device or component is drawing power. In case of load- or traffic-dependent power consumption, which should be expected in wireless communication systems, it requires the aforementioned traffic models or load models. Therefore, the focus of this thesis is on power consumption models only.

3.2 Methodology

3.2.1 Selection of the Power Consumption Models

Relevant literature on power consumption models for wireless communication systems was primarily found using the IEEE Xplore (ieeexplore.ieee.org) and Google Scholar (scholar.google.com) platforms. The search strings and keywords used for the research are listed in the Table A.9 in the appendix. The search for publications using the functionality "cited by" on Google Scholar or the "Citations" tab in IEEE Xplore revealed further relevant literature when starting from a previously identified publication. The identified models were subsequently grouped and selected for inclusion to this thesis on the basis of the following criteria:

- Relevance to 5G, 5G-Advanced or 6G based on recency, parameters, covered aspects

- Methodology and approach

It is not the objective of this thesis to offer the most complete survey on power consumption models, but rather an overview on the most influential and well-developed methods, relevant parameters and parameter values.

Analytic models with a main component or subcomponent approach are prioritized as they offer the most insight into power consumption under varying parameters and flexible in their application (optimization problems, quantification, and exploration using different parameter values). Machine learning, stochastic, and other regression-based models are excluded because they usually do not enable such applications. Furthermore, these models can not be readily compared to the analytic models and only offer limited insight into the power consumption for different configurations. Detailed analytic power consumption models for mobile networks have been developed since about 2010, with the first models focusing on LTE. Certain influential LTE power models are included, especially if they are the foundation of newer models. This is also due to the relative lack of power consumption models that capture the specific aspects of 5G systems. Some additional models that were excluded due to the aforementioned criteria are referenced, but not described or compared in detail. These are also listed in tables in the Appendix (Section A.1).

3.2.2 Grouping of the Power Consumption Models

The selected models are named after the first author (or publishing organization in case of the 3GPP) of the publication that describes it. The earliest, initial publication of the model is chosen for the name. If any relevant additions and revisions to the model exist, they are listed and described below the initial model.

Important to note is the conceptual separation of base station models and RAN models in Chapter 4. RAN models include considerations on RAN architecture or split options, or include the backhaul power consumption. As the RAN power consumption is primarily driven by the base stations, a RAN power consumption model includes a base station model. The category of base station models in this thesis includes models that capture the power consumption of a single base station without consideration of the RAN architecture. The user equipment models capture the power consumption of user equipment radio hardware. Any additional power consuming hardware (e.g., screen, input) is excluded in the considered models. System level models model the power consumption of both the UEs and base station(s) or the power consumption under consideration of the interplay (e.g., base station power consumption with UE mobility).

4 Power Consumption Models

In this chapter, the power consumption models identified in the literature survey are described. The models are grouped into the major components of a mobile network (refer to Figure 2.2 for an overview): The radio access network, the base stations as the central component of the radio access network, and the user equipment. The focus of this thesis is on the base station power models, these are outlined in Section 4.1, the RAN models are described in Section 4.2, and the user equipment models are summarized in Section 4.3. Additionally, a selection of system level models is described in Section 4.4. All power consumption models described in this section as well as additional models that are not described in detail are listed in the appendix in Section A.1.

4.1 Base Station Models

4.1.1 Introduction

Power consumption models for base stations are closely related to the RAN models (Section 4.2). This section includes models that do not differentiate different RAN architectures or functional splits and instead focus on the power consumption of a single (distributed) base station.

A list of the models presented in this section can be found in Table A.1 in the appendix.

Main Components

Figure 4.1 shows a block diagram of the main components that are typically considered in a base station power consumption model. The mains supply (AC-DC unit), the DC-DC power supply, baseband processing unit (BB), RF-transceiver chains (RF), power amplifiers (PA), active cooling, feeder cables (feed) and antennas.

The output power (P_{out}) is measured at the antenna port. The base station requires power supply from the grid or other sources (P_{in}).

For general background information on baseband processing, RF transceiver, and power amplifier, refer to Section 2.1.2. Concerning base station types and technology, see Section 2.2.8.
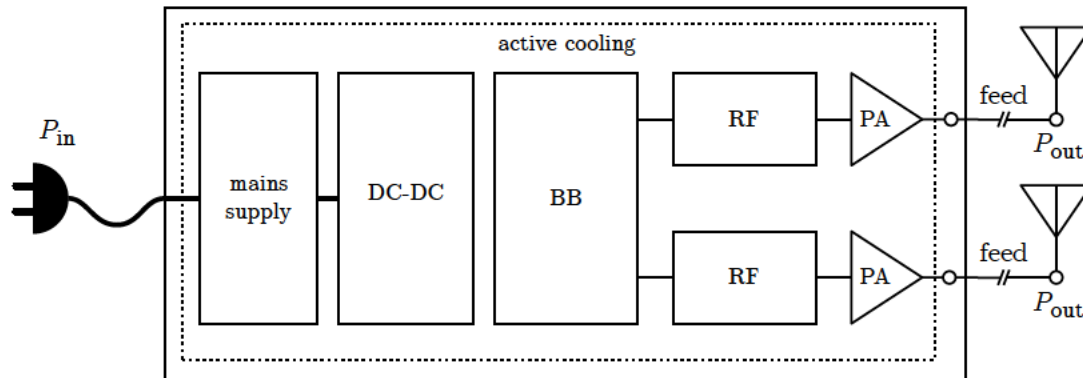
Figure 4.1: Block diagram of base station main components relevant for power consumption. Adapted from [8]

4.1.2 Auer et al. and Holtkamp et al.

Initial Model by Auer et al.

The base station power model was first presented in [8] [12]. Additional information and background is provided in [10]. It is often referred to as the EARTH model, as it was developed within the EARTH project - the model and further results of the projects are described in the project deliverables at [61]. The model is based on extensive measurements of base station hardware. The results of these measurements are discussed in [10] and [12]. Furthermore, the evaluations of the UTAMO project in [33] are in part based on the Auer model. The important aspects of the Auer power model are summarized hereafter.

The base station power consumption scales proportionally with the number of transceiver chains (N_{TRX}). The number of transceiver chains is the product of the number of sectors and the number of antennas per sector. The PA power consumption (P_{PA}), and the consumption of the RF transceiver (P_{RF}) as well as the baseband processing (P_{BB}) are

added. Losses are approximated by the loss factors (σ_{DC}) for the DC-DC power supply, (σ_{MS}) for the mains supply and (σ_{cool}) for active cooling (only applicable for macro base stations).

Based on this, the total base station power consumption is defined in equation 4.1, as proposed in [8]:

$$P_{\text{in}} = N_{\text{TRX}} \frac{P_{\text{PA}} + P_{\text{RF}} + P_{\text{BB}}}{(1 - \sigma_{\text{DC}})(1 - \sigma_{\text{MS}})(1 - \sigma_{\text{cool}})} \tag{4.1}$$

Even though the measurements within the EARTH project showed that the DC-DC conversion loss is dependent on the ratio of the maximum power to the actual output power, the DC-DC conversion loss is parameterized as a fixed value in the final model. The power consumption of the DC-DC converter varies only slightly as a function of the used bandwidth of the base station. Similarly, the AC-DC converter power consumption is modeled as a fixed value, even though the measurements showed a dependency of the consumed power to the output power. here, the power consumption is a linear function of the used bandwidth.

The cooling power consumption is difficult to model as it varies greatly depending on the geographic location, positioning inside or outside of buildings, and the size of the base station cabinet. Additionally, the recommended and actual operating temperatures of the components vary. Another challenge is that the active cooling is a very slow process compared to the signal processing procedures of a base station. Simply modeling the cooling power consumption with a dependency on the instantaneous power consumption of the other components may be misleading. Therefore, the model simply uses a fixed loss value for the approximation of the cooling power consumption of macro base stations.

The PA power consumption (P_{PA}) depends on the output power (P_{out}), the efficiency of the power amplifier (η_{PA}) and the feeder cable loss (σ_{feed}). The efficiency is assumed to be constant. The feeder cable loss only occurs in macro base stations (with a factor of 0.5), because the feeder loss for smaller base stations is typically negligible. In case an RRH is used, no feeder cable loss occurs as no coaxial feeder cable is employed.

$$P_{\text{PA}} = \frac{P_{\text{out}}}{\eta_{\text{PA}} \cdot (1 - \sigma_{\text{feed}})} \tag{4.2}$$

The measurements of base station hardware showed that the power consumption increases approximately linearly with the bandwidth, while the power amplifier contributes most to this variation of power consumption. Based on this, the power consumption of a base

station is approximated by a static component P_0 and a load-dependent component with gradient Δ_{p}. In sleep mode ($P_{\mathrm{out}} = 0$) the power consumption is further reduced to $P_{\mathrm{sleep}} < P_0$.

$$P_{\mathrm{in}} = \begin{cases} N_{\mathrm{TRX}} \cdot (P_0 + \Delta_{\mathrm{p}} \cdot P_{\mathrm{out}}), & 0 < P_{\mathrm{out}} \leq P_{\mathrm{max}} \\ N_{\mathrm{TRX}} \cdot P_{\mathrm{sleep}}, & P_{\mathrm{out}} = 0 \end{cases} \tag{4.3}$$

With the output power (P_{out}) proportional to the load share (χ). The downlink base station load is defined by $\chi = P_{\mathrm{out}}/P_{\mathrm{max}}$ and it is proportional to the utilized frequency resources. It is assumed that the ratio of used bandwidth to total system bandwidth is equivalent to the ratio of output power to maximum output power. The base station model is illustrated in the graph in Figure 4.2, which shows the linear load-dependent share of base station power consumption and the load-independent idle power (P_0).

$$P_{\mathrm{out}}(\chi) = P_{\mathrm{max}} \cdot \chi \tag{4.4}$$
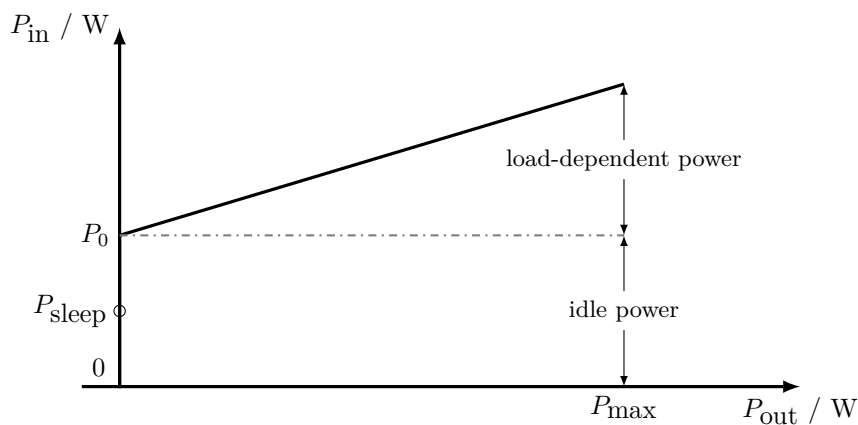
Figure 4.2: Load-dependent linear power model. Adapted from [62]

Holtkamp et al. Extensions

Holtkamp et al. extended the model by taking into account the reduced efficiency of the PA at lower transmit power and adding scaling rules for the baseband and transceiver power consumption in [62]. The model is also described in the dissertation [10] with

additional background on the initial measurements conducted for the Auer model and the Desset model (Section 4.1.3).

The maximum efficiency of the power amplifier ($\eta_{\text{PA,max}}$) is attained at $P_{\max} = P_{\text{PA,limit}}$ for a single antenna $N_{\text{ant}} = 1$. The factor γ describes the decrease of the efficiency (Equation 4.5).

$$\eta_{\text{PA}} = \eta_{\text{PA,max}} \left[1 - \gamma \log_2 \left(\frac{P_{\text{PA,limit}}}{P_{\max}/N_{\text{ant}}} \right) \right] \tag{4.5}$$

The power consumed for the baseband processing (and RF transceivers) is proportional to the bandwidth (B) and the number of antennas (N_{ant}). The baseline value is denoted by P'_{BB} and the same equation is used for the RF transceiver power consumption.

$$P_{\text{BB}} = N_{\text{ant}} \frac{B}{10 \text{ MHz}} P'_{\text{BB}} \tag{4.6}$$

Holtkamp et al. compare the model to the more complex subcomponent model by Desset described in Section 4.1.3. They conclude that the linear load-dependency is sufficient and closely matches the complex model, except for the case of four antennas or more. This is due to the non-linear power amplifier power consumption in the complex model. The PA efficiency is reduced when employing more antennas, which yields a steeper slope in the complex model that cannot be captured with the linear model.

Further Revisions and Additions

Olsson et al. and Tombaz et al. - Changes to the Sleep Mode In 2016 the model was revisited [63]. Here, the authors provided a more detailed sleep mode description to model the advances in LTE base stations. The modelled feature is described as cell discontinuous transmission (DTX) or micro sleep. In this case, the output power is reduced to $P_{\text{sleep}} = \delta P_0$ with $0 < \delta < 1$. Olsson et al. propose a value of $\delta = 0.84$, based on the maximum possible micro sleep duration in LTE.

In [64], the model is adapted to future 5G from a 2015 perspective by Tombaz et al. - taking into account assumptions on beamforming and the effects of "ultra-lean design". The same approach regarding the sleep mode is presented here as well. A lower value of $\delta = 0.29$ is chosen, as the average sleep mode duration is assumed to be longer.

Furthermore, Tombaz et al. propose two more sleep power levels in an updated paper in 2016. The first one is $\delta = 0.69$, corresponding to 1 ms DTX duration. It is defined that the value $\delta = 0.29$ corresponds to 100 ms DTX duration, and the final value of $\delta = 0.84$ to the maximum DTX duration of LTE at 0.2 ms.

Sharma et al. - Modeling Effects of High-Volume Traffic According to Sharma et al., the possible decrease in efficiency at high-frequency and high-volume traffic in 5G should be taken into account, using the mode proposed in [65]. It is assumed that the base station uses mMIMO and beamforming, while one antenna per 10^4 UEs is employed. Load-independent power consumption is not considered. The load of the base station is defined as the number of connected UEs. According to [65] the power consumption increase is non-linear at high loads. The deviation from linearity is concluded to be weak but noticeable. The authors propose advanced cooling as a way to mitigate the effect. A second model is presented in the paper, which assumes this cooling technique. It shows a lower deviation from linearity.

NTT DOCOMO et al. - Load Definition and Carrier Aggregation In [66] the load is defined as the percentage of resource elements transmitted in downlink and the corresponding power boosting level (p_k).

$$\chi = \frac{\sum_{k=0}^{12N_{\mathrm{RB}}^{\mathrm{DL}}} n(k)_{\mathrm{RE}}^{\mathrm{DL}} \cdot p_k}{12N_{\mathrm{RB}}^{\mathrm{DL}}} \tag{4.7}$$

The total number of resource elements (sub-carriers) in the frequency-domain is $12N_{\mathrm{RB}}^{\mathrm{DL}}$ for LTE, as each resource block contains twelve sub-carriers. If resource element k is used, $n(k)_{\mathrm{RE}}^{\mathrm{DL}}$ is set to 1.

In case of carrier aggregation, the total power consumption for the base station is multiplied with the number of active component carriers.

Zhao et al. - Virtualized Baseband Unit In [67] the initial model by Auer was adapted to 5G virtual base station concept based on assumptions from a 2014 perspective. Zhao et al. argue that the initial model by Auer must be adapted, as the following aspects are not covered by it: The centralization of BBUs reduces the power consumption of

baseband processing per base station, and the computational resources of the baseband units can be dynamically allocated. The BBU power consumption, implemented on a general purpose CPU, depends on the number of active CPU cores (N_{cores}), the minimum power consumed per core ($P_{\mathrm{core,min}}$), the CPU load (ρ_{CPU}), the CPU speed (s) and an exponential coefficient of the CPU speed (β):

$$P_{\mathrm{BBU}} = N_{\mathrm{cores}}(P_{\mathrm{core,min}} + \Delta_{\mathrm{BBU}} \cdot \rho_{\mathrm{CPU}} \cdot s^{\beta}) \tag{4.8}$$

The slope (Δ_{BBU}) is calculated with the maximum power consumed per core ($P_{\mathrm{core,mmax}}$) and the reference CPU speed (s_0):

$$\Delta_{\mathrm{BBU}} = \frac{P_{\mathrm{core,max}} - P_{\mathrm{core,min}}}{s_0^{\beta}} \tag{4.9}$$

The CPU load is the fraction of the actual instructions per unit time ($f(r)$) and the maximum available instructions per unit time ($N_{\mathrm{cores}} \cdot s$):

$$\rho_{\mathrm{CPU}} = \frac{f(r)}{N_{\mathrm{cores}} \cdot s} = \frac{c_0 + \kappa \cdot r}{N_{\mathrm{cores}} \cdot s} \tag{4.10}$$

Where r represents the data rate and c_0 and κ are auxiliary coefficients that describe the instruction speed of the processor. The instructions per unit time are therefore assumed to be linearly dependent on the transmission rate. The result of the simulations in [67], using this model, is that more than 60% energy savings compared to the initial Auer model can be achieved with a virtual base station approach. The employed CPU architecture (e.g., x86 or ARM) is not specified.

4.1.3 Desset et al. and Debaillie et al.

This base station power consumption model was first defined by Desset et al. in [49] in the year 2012. The work in [68] laid the groundwork for the revised model by Debaillie et al. in [31] which was published in 2015. It is frequently used in industry, as indicated in [69] and [70]. The Desset model in [49] was also developed as part of the EARTH project (see Auer model, Section 4.1.2) to form a high-level energy efficiency evaluation framework (E3F). It is not to be confused with the Auer model, as both are referred to as the "EARTH model".

Common Parts in Desset et al. and Debaillie et al.

The main components are identified as in the Auer model: The total power consumption of the base station is the sum of the baseband processing power consumption (P_{BB}), the power consumed by the RF transceivers (P_{RF}), the power amplifiers (P_{PA}), as well as the losses cumulated in (P_{overhead}).

The power consumption of the PA is modeled using a table containing measurements of output power and corresponding consumed power. The table data is not publicly available. To utilize the model, measurements of the power amplifier need to be performed or the power consumption of the PA could be approximated using an analytical power amplifier model (see Section 4.1.7 for power amplifier models).

The baseband processing power consumption is calculated with a scaling expression that includes reference values (x_{ref}) and scaling factors ($s_{i,x}$). The scaling is performed on a reference power consumption ($P_{i,\mathrm{ref}}$), where i represents the i-th subcomponent from the set of subcomponents (I_{BB}). The variable x represents the parameters on which the scaling depends. This yields the equation 4.11 defined in [49]:

$$P_{\mathrm{BB}} = \sum_{i \in I_{\mathrm{BB}}} P_{i,\mathrm{ref}} \prod_{x \in X} \left(\frac{x_{\mathrm{act}}}{x_{\mathrm{ref}}} \right)^{s_{i,x}} \tag{4.11}$$

The same scaling expression is applied to the RF transceiver power consumption, only the subcomponents are different. Reference power values for the baseband processing ($P_{i,\mathrm{ref}}$) are calculated based on an estimation of the computational complexity that is expressed in GOPS (Giga operations per second). The efficiency of the chip technology determines the power consumption, the efficiency is expressed in a value in GOPS/W. The efficiency is assumed to increase with more recent technology nodes.

The total baseband processing power is split into a dynamic part and a leakage part. The dynamic power consumption share of the baseband unit is the sum of the consumed power of its subcomponents, computed with Equation 4.11. Leakage power depends on the CMOS generation and is calculated using a reference value and an estimation of the corresponding efficiency for a CMOS generation. The leakage power is assumed to increase with newer technology nodes.

The efficiencies of mains supply η_{MS}, active cooling η_{cool} and DC-DC converter η_{DC} are considered to calculate P_{overhead}.

$$P_{\mathrm{overhead}} = (P_{\mathrm{BB}} + P_{\mathrm{RF}} + P_{\mathrm{PA}}) \cdot [(1 + \eta_{\mathrm{cool}})(1 + \eta_{\mathrm{DC}})(1 + \eta_{\mathrm{MS}}) - 1] \qquad (4.12)$$

The model differentiates between uplink and downlink: In the uplink case, some scaling exponents are different and certain subcomponents of RF transceiver and baseband processing are not required, which reduces the power consumption.

Revisions by Debaillie et al.

The model by Debaillie et al. from 2015 aims to overcome the limitations of the initial model by Desset et al. from 2012. The limitations and the motivation for the improved model are explained in [68]. The Debaillie model was developed within the GreenTouch project and therefore sometimes referred to as the "GreenTouch model", it is described in [31].

The key points that motivate the new model are mentioned in [68]:

- Desset model was focused on existing base station technology. The new model should extend predictions to the year 2020 and consider the improvements in technology. Innovative base station architectures and different parameter ranges should be taken into account.

- Power saving due to component deactivation was only considered rudimentary. The new model should include more sophisticated modeling of time-domain transitions (sleep modes).

- The Desset model followed a top-down approach and was based on power consumption figures without considering the required computations in baseband processing in detail. The number of computations and their efficiency were overestimated by a factor of about 15 in the Desset model. The new model follows a bottom-up approach and is expected to yield more accurate results.

- mMIMO should be considered for the new model. This is realized in [71], where the model is adapted to large-scale antenna systems, commonly referred to as mMIMO. The changes are also taken into account in the Debaillie model in [31].

The parameters that can be tuned to calculate the baseband processing and the RF transceiver power consumption differ from the Desset model. Bandwidth, spectral efficiency, number of antennas, load, number of spatial streams, and quantization are the six parameters of the Debaillie model. In the previous Desset model the five parameters are bandwidth, modulation type, coding-rate, time-domain duty-cycling, and frequency-domain duty-cycling. The load is defined differently in the Debaillie model as well: It is the share of used time and frequency resources, whereas for the Desset model it is the product of time-domain and frequency-domain duty-cycling. The number of considered subcomponents and the corresponding reference values for baseband processing and RF transceiver are changed in the Debaillie model as well. For mMIMO a "training phase" (channel estimation) is added - which is modeled with different reference values for the baseband processing in the Debaillie model.

Furthermore, the model introduces four sleep modes. This feature is not based on base station technology in 2015, but rather defined with future improvements in mind. According to [31], some base stations in 2015 had the capability to hibernate or sleep, though rather slow and not suitable for a dynamic and frequent utilization that adapts to the traffic load. For this reason, the different sleep modes in the Debaillie model are envisioned at the hardware subcomponent level. Each subcomponent is modeled with a deactivation power and transition latency. The components are grouped into categories with similar latencies, and each group represents a sleep mode. The latency describes, whether the respective component can turn on/off fast enough to enter and exit the sleep mode. The latencies (or minimum sleep durations) are 71.4 µs (OFDM symbol duration in LTE), 1 ms (sub-frame duration or transition time interval in LTE), 10 ms (duration of a frame in LTE), and 1 s (long-term sleep).

Further Revisions

Ge et al. - Changes to Power Amplifier and Baseband Modeling   The model was slightly adapted in [72] to evaluate computation power consumption in 5G small cell networks. Here, the fixed efficiency power amplifier model (Equation 4.2) is used. The baseband processing power is calculated using the product of the information throughput of semiconductor chips and the active switching power of transistors, based on the GOPS values from the Desset model.

4.1.4 Piovesan et al.

Piovesan et al. present an artificial neural network model, as well as an analytic model for 5G active antenna units (AAUs) in [73]. The analytic model is summarized hereafter. The artificial neural network model is based on measurements from 5G active antenna units in China. The corresponding data is not published - only the architecture and training of the neural network is described in [73] and [74].

The machine learning model is not discussed further here, as the authors state that it "lacks tractability to drive energy efficiency feature standardization, development and/or optimization" [73].

The analytic model is based on the machine learning model and the data collected. The total power consumption of the AAU (P_{AAU}) is the sum of the static power consumption (P_0), the baseband processing power consumption (P_{BB}), the transceiver power consumption (P_{RF}), the static power amplifier power consumption ($P_{\text{PA,static}}$), and the consumed power of the power amplifiers to generate the transmit power ($P_{\text{PA,dynamic}}$). This is expressed in Equation 4.13. Unique to this model is, that it considers multi-carrier power amplifiers (MCPA), where a single amplifier takes several carriers as input.

$$P_{\text{AAU}} = P_0 + P_{\text{BB}} + P_{\text{RF}} + P_{\text{PA,static}} + P_{\text{PA,dynamic}} \tag{4.13}$$

The power consumption of the RF transceiver chains (P_{RF}) is simply a fixed value per chain multiplied with the number of available chains. The power consumption of the power amplifiers is split into a static and output power dependent part. The static part ($P_{\text{PA,static}}$) is the product of active RF chains and a constant power value. The dynamic power consumption of the multi-carrier power amplifiers for each component carrier is the quotient of the transmit power for the (c)-th component carrier ($P_{\text{TX},c}$) and the efficiency of the power amplifiers and antennas (η). The total power consumption of the MCPA is the sum of the power consumed per carrier (Equation 4.14).

$$P_{\text{PA,dynamic}} = \frac{1}{\eta} \sum_{c=1}^{C} P_{\text{TX},c} \tag{4.14}$$

Multi-carrier power amplifiers increase the energy efficiency compared to conventional single-carrier implementations. The total transmit power of the MCPA is higher, which enables the amplifier to operate at increased efficiency.

Parameter values for the model are only given as normalized values for privacy reasons - without a reference. Therefore, the parameter values would need to be acquired through measurements or other sources to effectively utilize the model. Furthermore, the model was compared to the Björnson model described in Section 4.4.2. According to [73], the Björnson model overestimated the power consumption with a factor of 2.5 compared to the actual measurements over a 24-hour period. The error of the Piovesan model is reported as less than 1% in [73].

4.1.5 3GGP

The 3GPP proposed a base station power consumption model in 2022 in their *Study on network energy savings for NR (Release 18)* [75]. Various 3GPP documents referenced in the study provide additional information on the process of developing the model and the discussions of the 3GPP members. Initial introduction and discussion is provided in [69]. The structure is based on the 3GPP user equipment model (Section 4.3.2), which was developed earlier.

The model includes reference configurations, multiple power states including sleep or non-sleep modes with relative power, and associated transition time and additional transition energy as well as parameter scaling rules. The concept of additional transition energy and the transitions in the model is illustrated in Figure A.1 in the appendix. The 3GPP defined for their evaluations that a non-sleep mode occurs between adjacent sleep modes. This contradicts the approach from the Debaillie base station model, which assumes sequential sleep modes. The reason for this decision is not clear based on the final study in [75] and the initial introduction in [69]. Furthermore, the 3GPP study states that the transition between power states and the transition times are implementation specific. The number and characteristics of power states may differ depending on the base station type. Three sleep modes are defined in the final model in [75]. A fourth sleep mode ("hibernation" with lower power consumption than deep sleep) was initially discussed in [69] but only mentioned as an optional addition to the model to be decided by the reporting companies in [75]. As indicated in [69] the concept of the sleep modes is based on the Debaillie base station model (Section 4.1.3).

In Figure 4.3 the states and transitions of the 3GPP model are illustrated in a state machine. The transition from active downlink or uplink to the micro sleep mode has no associated transition time or energy. The transition to light or deep sleep is possible when the respective sleep duration (denoted as T_{sleep} in Figure 4.3) is longer than the corresponding transition time ($T_{\text{light,trans}}$ or $T_{\text{deep,trans}}$). The state machine shows the transitions back to the active state after each sleep state, as defined in [75]. There is neither transmission nor reception during a sleep state. The model assumes that the base station determines the target sleep mode before entering it based on the current traffic load. The state machine in Figure 4.3 only shows one active state for simplification - the states active transmission (downlink) and reception (uplink) have different associated power levels and are therefore two distinct states. The states of active transmission and reception correspond to 100% load - which is defined as the share of utilized Physical Resource Blocks (PRBs) in this case.
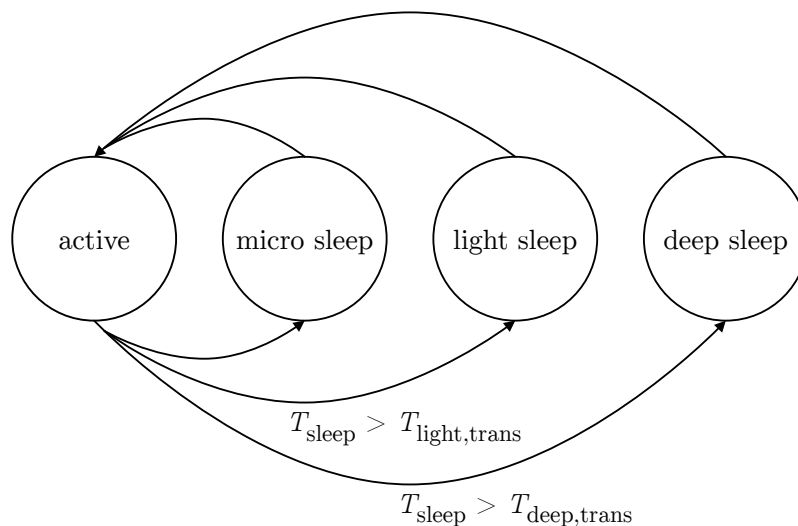
Figure 4.3: State machine of the 3GPP base station power consumption model. Based on [76] [75]

Non-sleep mode power consumption values can be scaled based on:

- Number of used physical antenna elements or radio units (RUs),

- used bandwidth/resource blocks for downlink/uplink in a slot/symbol for one component carrier.,

- number of components carriers (CCs) active for carrier aggregation,

- power spectral density or transmit power,

- number of symbols occupied in a slot.

For active downlink transmission, the base station power consumption is the sum of the static and the dynamic power consumption. The static part is a constant value, based on the micro sleep power level. The dynamic part of the power consumption is scaled based on a reference configuration. The scaling depends on the share of active radio units (antenna elements), the ratio between the utilized radio frequency bandwidth and the maximum system bandwidth, and the ratio of the power spectral density (transmit power) per radio unit between the downlink transmission and the reference configuration value.

The equations and parameter values are not directly based on measurements, but are rather the result of the discussions referenced in the 3GPP study in [75]. To understand the reasoning behind the chosen values and equations, it is necessary to refer to these discussions, as the study itself does not give reasons for the decisions taken during the development of the model. There are two categories of base stations with parameter values used as reference configurations, and three sets of these configurations with detailed specifications. The values are based on the averaged values of the input of the member companies. There is no consensus on the time unit (symbol level, slot-level, ms-level) of the relative power values in the 3GPP study.

4.1.6 Björnson et al., Hossain et al., and Peesapati et al.

Initial Model by Björnson et al. and Changes by Hossain et al.

Based on the power consumption model by Björnson in [36], a base station power consumption model is proposed by Hossain in [77]. The model by Björnson also serves as the basis for the system level model by Björnson described in Section 4.4.2.

The power consumption of the base station (P_{in}) in the model by Hossain is the sum of the baseband unit power consumption (P_{BB}), the transceiver chain power consumption (P_{TC}), the power amplifier power consumption ($P_{\text{PA}}(p)$) dependent on the output power (p) multiplied with the number of antennas (M), and the load-independent power (cooling, control signal, DC-DC conversion loss etc.).

$$P_{\text{in}} = P_{\text{BB}} + P_{\text{TC}} + M \cdot P_{\text{PA}}(p) + P_{\text{other}} \tag{4.15}$$

The baseband power consumption (P_{BB}) and the transceiver chain power consumption (P_{TC}) are calculated as in the Björnson model. The equations are similar to the system level model described in Section 4.4.2, though excluding the terms for the user equipment power.

Björnson et al. model the power amplifier using a fixed efficiency in [36]. Hossain et al. use the equations that were later summarized by Rottenberg (see Section 4.1.7). "Traditional PA", referring to a class B power amplifier (equation 4.19), and the envelope-tracking PA (equation 4.20) are considered in [77]. The remaining term P_{other} is simply given as a constant value in Watt.

López-Pérez et al.: Adding Multi-Carrier   The Björnson et al. model is adapted in [78] to consider multi-carrier architectures. The model realizes the three different carrier aggregation types of 5G NR (inter-band, intra-band contiguous, and intra-band non-contiguous). The power consumption parameter values are fitted from measurements, though the values are not disclosed for privacy reasons.

Revisions by Peesapati et al.

The model described in [24] and [79] adds sleep modes to the Hossain model. Baseband processing and the power amplifier are modeled as in the Hossain model. The definition of the four sleep modes and the corresponding parameter values for the sleep duration are adopted from the Debaillie model (Section 4.1.3). The sleep mode power levels are derived from the assumptions by Tombaz et al. in [80] on DTX in 5G from a 2016 perspective (see Auer / Holtkamp extensions in Section 4.1.2).

4.1.7 Rottenberg - Power Amplifier Models

Rottenberg presents a base station power model in [81], which is summarized here. Unique to this is the variety of considered power amplifier classes. Sleep modes from the 3GPP model (Section 4.1.5) and corresponding parameter values from a 3GPP reference configuration are used, the Auer model and Debaillie models are also included in parts.

A general power consumption model for power amplifiers is introduced, which can be adapted to fit specific types of amplifiers:

$$P_{\text{PA}} = \underbrace{P_{\text{PA},0}}_{\text{load-independent}} + \overbrace{\beta p^{\alpha}}^{\text{load-dependent}} \;, \quad 0 \leq p \leq P_{\text{max}} \tag{4.16}$$

Where $\alpha \in \,]0, 1]$ and $\beta \geq 0$.

$P_{\text{PA},0}$ is the load-independent power consumption. The second term is dependent on the load (p). The general model can also be fitted for power amplifiers based on measurements and datasheet values according to [81]. Generally, a large back-off is needed in OFDM systems, which means that the maximum output power (P_{max}) is much smaller than the saturation power of the amplifier (P_{sat}): $P_{\text{max}} \ll P_{\text{sat}}$.

Further models for other types, which can be derived from the general model in Equation 4.16, are summarized in the following based on [81].

Ideal Power Amplifier For an idealized power amplifier, the consumed power is proportional to the output power.

$$P_{\text{PA}}^{\text{ideal}}(p) = p \tag{4.17}$$

Class A Power Amplifier Power consumption is independent of the load, with a maximum efficiency of 50%.

$$P_{\text{PA}}^{\text{A}} = 2P_{\text{sat}} \tag{4.18}$$

Class B Power Amplifier The class B power amplifier is often employed in base stations, the power consumption scales with the square root of the output power.

$$P_{\text{PA}}^{\text{B}}(p) = \frac{4}{\pi} \sqrt{P_{\text{sat}}} \sqrt{p} \tag{4.19}$$

Envelope-Tracking Power Amplifier A curve fitted model with a PA dependent parameter $a \approx 0.0082$ is defined for the envelope tracking power amplifier[1]. The maximum efficiency of the power amplifier ($\eta_{\max}$) is parameterized.

$$P_{\mathrm{PA}}^{\mathrm{ET}}(p) \approx \frac{aP_{\mathrm{sat}}}{(1+a)\eta_{\max}} + \frac{1}{(1+a)\eta_{\max}}p \qquad (4.20)$$

Doherty Power Amplifier The power consumption of an ℓ-stage Doherty power amplifier[2] can be calculated as follows.

$$P_{\mathrm{PA}}^{\mathrm{Doherty}}(p) = \frac{4P_{\mathrm{sat}}}{\ell\pi} \begin{cases} \sqrt{p/P_{\mathrm{sat}}}, & 0 < p/P_{\mathrm{sat}} \leq 1/\ell^2 \\ (\ell+1)\sqrt{p/P_{\mathrm{sat}}} - 1, & 1/\ell^2 < p/P_{\mathrm{sat}} \leq 1 \end{cases} \qquad (4.21)$$

4.1.8 Further Models

Arnold et al. In [84] power models for macro and micro base stations for GSM and UMTS are presented. The predictions included for LTE systems deviate significantly from the subsequently published LTE models (Auer and Holtkamp in Section 4.1.2).

Deruyck et al. In [9] and [6] the power consumption of base stations for different technologies (WiMAX, fixed WiMAX, UMTS, HSPA, and LTE) is modelled. Extending this, [85] proposes a power consumption model for macrocell and microcell base stations which is again utilized to compare WiMAX, LTE, and HSPA technologies. The model is based on extensive measurements. However, the power consumption of a base station is assumed to be constant (sum of component power consumption taken from datasheets) for the model, therefore it differs significantly from the more recent models.

Jung et al. The model described in [86] calculates the power consumption for macro-, micro-, and RRH-based base stations. It aims to improve the previous models mentioned above by Arnold et al. [84] and Deruyck et al. [9] [6]. The paper by Jung et al. [86] does not reference the previous work of Auer and Holtkamp, however the general assumptions on the different base station types are similar. The differences to the models described in

---

[1]Background on envelope-tracking power amplifiers in the context of OFDM applications is given in [82]
[2]Background on Doherty power amplifier efficiency is well-described in [83]

Section 4.1.2 are the modeling of the cooling unit (depending on the temperature), the feeder cable, and the baseband processing.

Ayala-Romero et al. An experimental evaluation of power consumption in a virtualized base station is provided in [87] and summarized hereafter. A test setup based on the open-source platform "srsLTE" is used, with which the CPU power consumption at the BBU in the uplink is measured. The default scheduler of the platform is utilized, though potential improvements of the scheduler are described. Power consumption increases linearly with SNR until a certain point: At 28 dBs or higher, the consumed power is constant. This is due to the fact that higher modulation and coding schemes (MCS) are used with increasing SNR - up until a certain SNR value. The power consumption for the highest SNR is reduced when decreasing the airtime, and a lower airtime also reduces the slope of the power consumption. Airtime is defined as the "percentage of subframes needed to support the traffic, given the instant data rate" [87]. A tradeoff between the power consumption of the UE and the base station was identified: The UE can save energy using a lower transmission power, but this deteriorates the SNR and leads to an increased power consumption at the base station. Based on the measurements, a linear mixed-effect model is proposed. Further findings of the paper include: The power consumption depends on the type of platform used (small-factor PC or general-purpose server) and the share of power consumed by the CPU varies between about 30% and 50%. The Python code and data set for the model are available online[3].

Dzaferagic et al. In [88] the power consumption of a virtual base station scheduler is modeled using a black-box model (neural network) as a function of the following parameters: Airtime, SNR, and the modulation and coding scheme. The authors compare the black-box model to the regression approach. They conclude that the black-box model is advantageous when "domain knowledge is not available or is hard to acquire" [88].

Saraiva et al. Further linear mixed-effect models for LTE base stations are described in [89] and [90].

---

[3]Link to GitHub repository: github.com/jaayala/power_ul_dataset (visited on 16/06/2023)

4.1.9 Summary

The base station models vary in their approaches and potential use cases. In the following summary, the models are grouped according to these aspects.

There are main component models that model the power consumption of the main base station components (power amplifier, analog frontend, baseband unit, active cooling, power supply) separately. Subcomponent models exhibit an even higher granularity, the baseband processing and analog frontend are modeled based on subcomponent power consumption. System models only give overall figures for the whole base station.

- Main component models: Auer/Holtkamp

- Subcomponent models: Desset/Debaillie, Björnson/Hossain/Peesapati

- System models: 3GPP

The approach can further be categorized into top-down models and bottom-up models. Top-down models are based on measurements or theoretical discussions on the total power consumption levels in the case of the 3GPP model. Bottom-up models are based on estimations of low-level power consumption values for hardware subcomponents, computational efficiency of hardware, and computational complexity of operations.

- Top-down: Auer/Holtkamp, Desset, Piovesan, 3GPP

- Bottom-up: Debaillie, Björnson/Hossain/Peesapati

Based on this, the potential main use cases of the models can be categorized. Quantification models are most suitable for quantifying overall power consumption of base station or even networks as part of large-scale evaluations. The number and complexity of parameters is limited, and simple usage with load profiles or traffic models is possible to estimate total energy consumption. Exploration models on the other hand are rather suited to examine the effects of varying parameters, for example to predict power consumption of future base stations under consideration of improvements in efficiency for certain subcomponents. The exploration models feature low-level parameters or a general complexity that makes them unwieldy for large-scale quantification efforts of network energy consumption.

- Quantification: Auer and Holtkamp, Debaillie, (Piovesan)

- Exploration: Desset and Debaillie, 3GPP, Björnson/Hossain/Peesapati

However, the main component models can generally be combined to tailor the model to the specific use case. An exception to this is the 3GPP model, as it does not feature main component power consumption and only includes power values in relative units instead of Watt. Therefore, the 3GPP model is suitable for exploration of energy saving impacts of fine granularity changes to the 5G protocol stack or physical layer setup, such as the evaluation of synchronization signal periodicity.

The models by Auer, Holtkamp and Debaillie are well-developed as they have been used in academic research as well as industry. The Auer and Holtkamp model is more suitable for large scale system level/network level evaluation of energy consumption - it is widely used and cited by almost all the considered subsequent publications on base station power consumption. The Debaillie model features finer granularity scaling of parameters and is therefore more suited for evaluation of specific hardware setups or prediction of the power consumption of future base station technology.

All models, except the 3GPP model, include a (traffic) load scaling of power consumption. However, there is no standard load definition. This is discussed in further detail in Section 5.2.1. A more detailed comparison of the models and their parameters is conducted in that section as well.
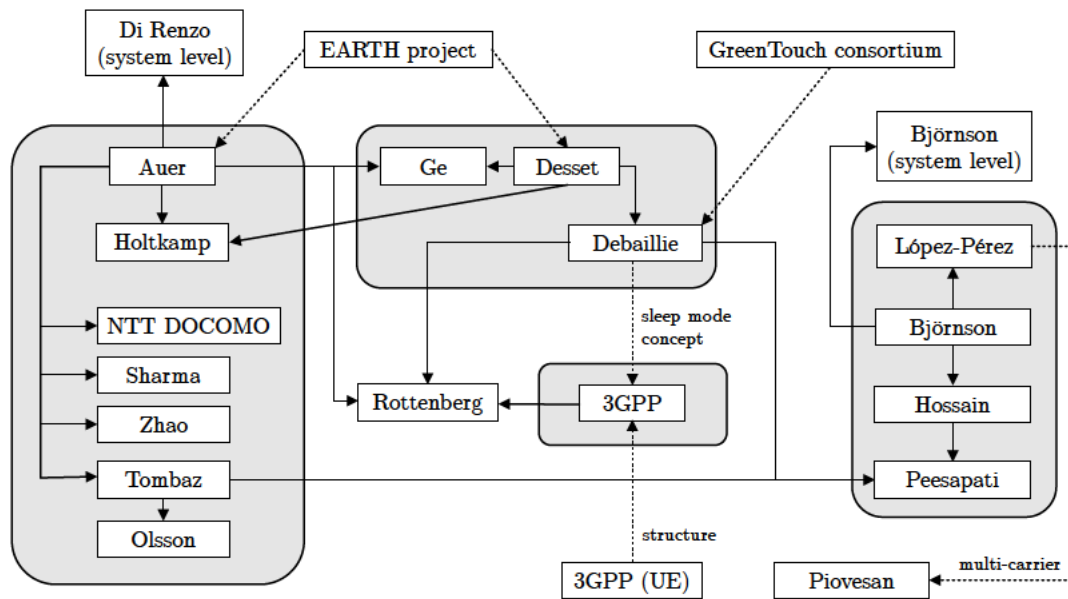
Figure 4.4: Diagram of the relationships between the base station power consumption models

Figure 4.4 illustrates the relationships between the base station power consumption models. An arrow is drawn in the diagram, if a significant part of the original model has been used or modified in the new model. Dotted lines signify weaker relationships, where only certain concepts are adopted, but the new model has notable differences for main parts. Additionally, the EARTH project and GreenTouch consortium are included in the diagram to clarify the origin/context of the respective models. Several models are enclosed by gray rectangles, if major parts or the general methodology of the enclosed models are very similar.

4.2 Radio Access Network Models

Extending the power consumption models specific to distributed base stations (Section 4.1), this section outlines models that capture the power consumption of the radio access network for different architectures and considering the transport networks.

4.2.1 Introduction

Regarding RAN power consumption models for 5G, two aspects are relevant beyond the aspects already covered in the base station models (Section 4.1):

- Location of the baseband (digital signal) processing (distributed RAN and centralized RAN - for background information on RAN architectures, refer to Section 2.2.7)

- Configuration of the front- and backhaul

The radio unit or analog frontend contribution of the power consumption and any other redundant parts of the models already covered in the base station model section will not be repeated here.

In contrast to the base station models, a fairly extensive survey on models regarding different RAN architectures is available - therefore the description of the models included in the survey by López-Pérez et al. [91] will be limited to a brief summary.

4.2.2 López-Pérez et al. Survey

The survey in [91] divides the models into two categories: Models for distributed RAN and for centralized RAN.

Models for Distributed RAN

The DRAN models are the conventional base station power models, as the total DRAN power consumption is simply the sum of the base station's power consumption. The models included in the survey in [91] are:

- Auer et al. (Section 4.1.2)

- Yu et al. [92] (not included in this work as it does not offer significant additional insights - the major contribution of carrier aggregation power consumption is also covered by other models)

- Tombaz et al. (extension of the Auer et al. model in Section 4.1.2)

- Björnson et al. and Hossain et al. (Section 4.1.6)

Models for Centralized RAN

Generally, the power consumption of a C-RAN network is the sum of the power consumption of the radio units (P_{RU}), the fronthaul power consumption (P_{FH}), and the power consumed by the virtualized baseband units (or baseband unit pool) (P_{vBBU}) as shown in [91]:

$$P_{\text{C-RAN}} = \sum P_{\text{RU}} + \sum P_{\text{FH}} + \sum P_{\text{vBBU}} \tag{4.22}$$

The radio unit part can be modeled with the base station models presented in Section 4.1 (excluding the baseband processing part and generally without active cooling for the radio unit). Therefore, only the fronthaul and baseband unit pool remain relevant for this section of the thesis.

The models considered in [91] for the centralized RAN architecture are:

- Fiorani et al. [93] [94]: Power consumption for different RAN splits considering the required transport network capacities.

- Younis et al. [95]: Power consumption of virtualized BBU pool and fronthaul links based on measurement of test setup.

- Sigwele et al. [96]: Power consumption of C-RAN based on power consumption figures from literature for optical networks (fronthaul) and general purpose processors (virtualized BBU). Also includes power consumption of the cooling and the dispatcher/controller of the BBU pool.

- Sabella et al. [97] and Werthmann et al. [98]: Backhaul power consumption and server power consumption (linear model) for centralized BBU pool and power consumption of the backhaul network (based on fixed value for network switches power consumed for each communication link for idle, low and high traffic states).

Generally, the power consumption of a general purpose CPU is assumed to be a linear function of the CPU utilization [96] [95] - idle power and slope of the power consumption function depend on the type of the processor. The listed models assume that the processor is the major contributor to power consumption of a virtualized C-RAN implementation. The Fiorani and Younis models are described briefly in the following paragraphs.

Fiorani et al. The model introduced in [93] and [94] expands on the Auer et al. model for the RRU (Section 4.1.2). The BBU is modeled under consideration of different RAN architectures.

Four different RAN architectures are analyzed in [94]: Distributed RAN and C-RAN with three different functional splits. The functional splits are named A2, A3, and A4. For A2 the layer 1, 2, and 3 functions and the FFT are centralized. In A3 the FFT is not centralized and in A4 the FFT and layer 1 are not centralized. The A1 architecture is the distributed RAN. Furthermore, A2 corresponds to split option 8, A3 roughly corresponds to split option 7, and A4 corresponds to split option 6.

It should be noted that the terminology used in [94] and [93] is completely different to the definitions of the 3GPP functional split options - the papers were published in 2016 and the first versions of the 3GGP Release 15 for 5G were not published until 2018 (see Section 2.2.1. The results of the Fiorani et al. model should therefore not be used without considering the current specifications and practical implementations of functional split options.

The energy consumption of C-RAN is modeled with three benefits over distributed architecture achieved through the centralization of the baseband computation hardware: The stacking gain, pooling gain, and cooling gain. The centralized and distributed power consumption values are calculated based on fractional increases or decreases, depending on which functionalities are located at the respective sites. Additionally, the consumed power of the optical fronthaul network is modeled. It is a function of the transport capacity required for each distributed base station site and the number of base stations

in the network. It is not clear from [93] and [94], how the required transport capacity is derived. Further relevant parameter values are based on assumptions.

Younis et al. A power model for a downlink C-RAN system is proposed in [95] (preliminary version) - a longer description of the model is published in [99].

The computation capacities of the virtual machines in the BBU pool can be dynamically adjusted. The authors conclude that the consumed power of the BBU pool depends on the computing workloads for baseband signal processing [95].

The authors conducted experiments to analyze the CPU utilization of an LTE BBU implementation in a virtualization environment and a remote radio head (RRH) based on a software defined radio platform. The setup is not a commercial solution that is used in practice, but a small and flexible configuration to enable the measurements. The results of the experiments show that the CPU utilization increases linearly with the SINR (signal-to-interference-plus-noise-ratio), the PRB utilization, and the MCS (modulation and coding scheme) index. This results in Equation 4.23, defined in [99].

$$\mathrm{CPU}\% = I^{\mathrm{snr}} + G \cdot r + D \tag{4.23}$$

According to Equation 4.23, CPU utilization increases with the achievable data rate (r). The parameters I^{snr} (depends on the SINR), G, and D (depending on MCS) are constants derived from the measurements of the C-RAN test bed [99].

Furthermore, the power consumption for the virtualized BBU pool is calculated based on the CPU utilization (it is simply multiplied with a constant). The power consumption for the fronthaul is modeled as a constant per-user power value. However, parameter values are not given for the derived equations. Only a few selected values for the parameters of equation 4.23 are listed in [99].

4.2.3 Further models

Israr et al. Israr, Yang, and Israr propose power consumption quantification models of distributed HetNet, C-RAN and H-CRAN in [100]. Two-tier HetNet is defined by the authors as a network including pico and macro base stations. The C-RAN power consumption is calculated as in equation 4.22. Additionally, heterogeneous C-RAN is defined as a network consisting of macro base stations, remote radio units, small cell base stations and the centralized BBU cloud. The model utilizes a similar linear load-dependent model as in Auer et al. (Section 4.1.2) for the base station / remote radio unit power consumption.

4.2.4 Summary

Compared to distributed RAN, where the power consumption mainly depends on the base stations, which can be modeled with the base station models from Section 4.1, the centralized RAN power consumption modeling requires additional considerations. Radio access network models generally extend upon base station power consumption models. In the case of a fully centralized RAN only the analog frontend and power amplifier component models remain relevant. Thus, the centralized baseband unit and the transport networks connecting the distributed RRUs and the centralized components are of special interest to evaluate the power consumption of 5G RAN.

Power consumption of a virtualized BBU pool is assumed to mostly depend on the CPU power consumption and cooling. Either only the CPU power is modeled as a linear function (as in the Younis model) or the power consumption of a server based on idle power consumption and linear increase with CPU utilization is assumed.

The functional split options defined by the 3GPP and further specified by other organizations have not been analyzed in detail in the considered power consumption models. The Fiorani model is the only one that considers different splits, but it was developed before the current functional split specifications for 5G were published. Therefore, it likely requires some adaptation to reflect the current state of technology. The power consumption of transport networks (fronthaul, backhaul, midhaul) is included in several of the models. Fairly simplified network architectures are assumed, and modeling is mostly based on fixed values for network devices. The transport network power consumption increases with the capacity of the network.

None of the considered models are based on measurements of 5G hardware. Even the most recently published models (Younis and Israr) are utilizing an LTE setup and parameter values from literature, respectively. The novel specifications of centralized RAN, as well as current hardware and virtualization technology, are not reflected or evaluated in any of the models. Therefore, none of the models identified in the literature survey are suitable for evaluation of 5G centralized RAN power consumption without significant additional modeling effort. However, the parameters and causal relationships identified in the available publications are a solid theoretical foundation for future models.

4.3 User Equipment Models

In this section power consumption models for user equipment of cellular networks are summarized.

4.3.1 Introduction

For general background information on user equipment and Radio Resource Control (RRC) in 5G refer to Section 2.2.9. An overview of the main power saving techniques for user equipment in 5G is given in Section 2.3.1.

Lauridsen provided an analysis of power consumption in user equipment focusing on LTE [101]. It includes an overview of various power models, considering different radio access technologies in [101] Table 2.2. Most of the models listed use specific smartphone models and are based on measurements. The number of parameters and the generality of most of these models is limited.

4.3.2 3GPP Model

The 3GPP defined a UE power model for 5G in [102]. It is suitable to calculate UE power consumption depending on the physical layer setup, Radio Resource Management (RRM) and mobility measurement procedures and three sleep modes - deep, light, and micro sleep. The structure and presentation of the model is similar to the 3GPP base station model (Section 4.1.5). It includes reference configurations for frequency ranges FR1 and FR2. Power consumption values are given relative to deep sleep mode. For the state transitions, transition times and additional transition energy is given. Scaling rules are provided to scale the non-sleep power consumption values based on bandwidth, carrier aggregation, antenna scaling and physical layer setup. The transition between sleep-states and active states is defined in the same way as in the 3GPP base station model. The concept of additional transition energy is illustrated in Figure A.1 in the appendix. Lauridsen, Laselva, Frederiksen, *et al.* use the model in [103] to examine the potential of different power saving schemes through simulation and to optimize DRX parameters.

4.3.3 Lauridsen et al.

The model proposed by Lauridsen is arguably the most well-developed and documented power model for user equipment that features main component power consumption of the radio hardware based on measurements of LTE smartphones. The model is presented with slight variations and additions in [104], [105], and [106]. The dissertation [101] includes and summarizes all of these publications and additionally describes further relevant aspects such as power saving in LTE and predictions for 5G user equipment from a 2015 perspective.

For the power model, the following parameters were identified as important: Transmit and receive power levels, downlink and uplink data rate, RRC state changes, Discontinous Reception (DRX), scanning and measuring of cells, cell bandwidth. The power consumption model includes power consumption of two identified main components: Baseband processing (BB) and RF transceiver (including the power amplifier - in contrast to the base station models). The Figure 4.5 illustrates the included main components of the model for transmission (uplink) and reception (downlink). The ADC and DAC are included as separate and bandwidth-dependent components. The bandwidth-dependency is assumed as a constant reduction of power consumption for lower bandwidths in [105].
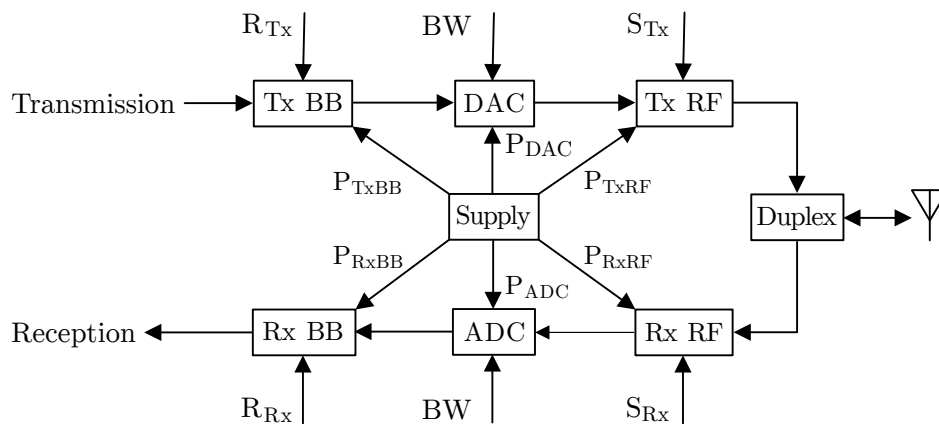
Figure 4.5: Power consumption and input parameters of Lauridsen et al. LTE UE power model. Adapted from [104] Fig. 1

The power consumption is defined using the power consumed in RRC connected (P_{con}) and idle states (P_{idle}). Additionally, the DRX power consumption is calculated (P_{DRX}). The binary variables (m) indicate in which mode the user equipment currently is. This results in Equation 4.24, as defined in [101].

$$P_{\text{in}} = m_{\text{con}} \cdot P_{\text{con}} + m_{\text{idle}} \cdot P_{\text{idle}} + m_{\text{DRX}} \cdot P_{\text{DRX}} \qquad (4.24)$$

The power in connected mode is calculated based on the components in Figure 4.5. The baseband power consumption (P_{RxBB} and P_{TxBB}) depends on the data rate (denoted by R). The RF receiver and transmitter power consumption depends on the downlink received signal power and uplink transmission signal power, respectively - the signal powers are denoted by S in Figure 4.5. The average DRX power (P_{DRX}) based on parameterized time durations for the sleep, wake-up, synchronization, the DRX on duration, and the power-down time. Thus, the DRX parameters can be varied to reflect the different possible configurations.

In [107] the model is adapted to NB-IoT.

4.3.4 Dusza et al.

In [108] an LTE UE power consumption model considering the uplink transmit power and carrier aggregation is proposed. It is based on the previous work of the authors in [109] and is further developed in [110]. The model is very similar in approach and methodology to the Lauridsen model for the power consumption in uplink. The main differences are that it only covers the uplink, does not differentiate components, and uses different power states. The downlink power consumption is modeled as a constant value in the Dusza model. In [111] this model is extended for downlink power consumption. A different extension is proposed in [112], where the model is adapted to mixed uplink/downlink transmissions and carrier aggregation in LTE-Advanced.

4.3.5 Further Models

Mehmood et al. The work in [113] proposes an analytical model that covers the power-saving mechanisms of discontinuous reception in LTE. It focuses on machine-type communication applications and its requirements. It also features a literature review of power consumption models that cover DRX mechanism.

Andres-Maldonado et al. An analytic model specifically for NB-IoT is defined in [114]. The model utilizes five power levels: Transmission, reception, uplink gap, inactive, and standby. The behavior of the UE is modelled using a Markov chain. By applying a traffic model, the probability for the states is determined. The energy consumption is the average power and duration for each state.

Jano et al. The Andres-Maldonado et al. model also serves as the basis for the work in [115] - the authors propose and evaluate a Markov Chain based energy consumption model suitable for RedCap IoT devices in 5G networks.

Accurso et al. - Survey In [116] a survey on tradeoffs between energy consumption and network performance in Cellular-IoT is presented, including some relevant power consumption models.

Jacobsen et al. The work in [117] presents a generic evaluation methodology for energy consumption specific to mMTC devices.

Joda et al. A power consumption model for downlink energy consumption of user equipment with carrier aggregation is presented in [118]. For carrier aggregation, the power consumption is the summation of the consumed power for all active component carriers. Power consumption for a single component carrier is a function of the received power level, the data rate and the bandwidth of the component carrier. The model extends on the Lauridsen model and therefore only features the two RRC states idle and connected - even though it claims to model 5G user equipment. The missing RRC inactive state, which is defined for 5G (see section 2.2.9), is not mentioned in [118].

Skrimponis et al. In [119] initial power estimates for mobile mmWave devices are provided. Power consumption is estimated for user equipment in a multi-carrier 5G NR system similar to current 5G deployments and a hypothetical 6G system operating at 140 GHz. There is no model included, though the estimations may be helpful to advance other power models.

4.3.6 Summary

The user equipment models are only suitable to explore the setup, effect of changes to the protocols or power saving measures. Accurate reporting or quantification of the total device power consumption is only possible if the complete device power consumption is included. The models considered here only include the radio hardware part. It has been shown in [101] that the wireless radio components consume a significant share of the total power of commercial smartphones.

Based on the literature survey, two models are identified as particularly relevant and suitable for 5G UE power consumption modeling: The Lauridsen model and the 3GPP model.

The Lauridsen model is the most well documented and developed model that considers main component power consumption of user equipment radio hardware. The Dusza model was developed around the same time but independent to the Lauridsen model, it is similar in approach and methodology (measurement of smartphones and LTE sticks with varying parameters). But some differences are observable with regard to the modeling (most importantly, different number and definition of power states). The Lauridsen or Dusza model can be adapted to newer or different UE hardware by conducting the power measurements - which is necessary as the parameter values differ significantly for different devices. The model is suitable for several use cases, including: Battery lifetime estimations, system level network modeling, exploring tradeoffs between base station and user equipment energy consumption, and evaluating power saving measures. The 3GPP model is the only model that considers the 5G specific UE procedures and configurations. It is very similar to the 3GPP base station model in the way it is described and used. It also utilizes relative power values. It is therefore only suitable for very specific low-level evaluation purposes, such as deriving parameters for DRX or optimization of scheduling.

Additionally, several models with considerations for low power specifications - such as NB-IoT or 5G NR RedCap devices, are listed in Section 4.3.5. These are not discussed further here, as additional background on the energy saving mechanisms is required to evaluate these power models.

Generally, the user equipment models require very specific traffic profiles and models to be utilized. The modeling of the intended traffic of the user equipment is discussed in most of the aforementioned models.

4.4 System Level Models

This section summarizes three system level models of wireless communication networks that can be used to compute power consumption, energy consumption, or even energy efficiency based on parameterized network configurations. System level models are suitable for optimizing currently deployed networks, and for planning future networks.

4.4.1 Di Renzo et al.

An analytic system model of the energy efficiency of downlink cellular networks is described in [120] and [121] - the important aspects are summarized hereafter.

The fundamental premise of the model is that a base station operates in two modes. It is in an idle mode if no UEs are associated and in transmission mode if one or more UEs are connected [121]. A simple linear power model for the base station is assumed, the Auer et al. model is referenced (Section 4.1.2) as the foundation for this. The power consumption of the base station results from the sum of the transmit power P_{tx}, the static power consumption P_{circ}, and the idle power consumption P_{idle}, which are parameterized.

Central to the paper is the definition of the so-called coverage probability and resulting potential spectral efficiency, which considers the strong interaction between the transmit power and the density of the base stations. The potential spectral efficiency is defined as the network information rate per unit area (in bit/sec/m^2) at the minimum signal quality for reliable transmission [121]. It is assumed that the following conditions are met, for the closed-form expression of the potential spectral efficiency to be valid: "Single-antenna transmission, singular path loss model, Rayleigh fading, fully-loaded base stations, cell association based on the highest average received power" [121]. The network power consumption per unit area P_{grid} (Watt/m^2) is calculated as the average number of base stations per unit area (using the density of the base stations λ_{BS}) and the power consumption of a base station that depends on the mode (idle or transmission). The density of the UEs is indicated with λ_{MT}, where MT stands for mobile terminal. Mobile terminal is an (older) alternative designation for user equipment. Two different load models are provided. The load model 1 results in a high energy efficiency at low to medium potential spectral efficiency. Load model 2 provides a higher energy efficiency at medium and high potential spectral efficiency.

Load model 1 (Equation 4.25) assumes the exclusive allocation of bandwidth and transmit power to one randomly selected UE.

$$P_{\text{grid}}^{(1)} = \lambda_{\text{BS}}(P_{\text{tx}} + P_{\text{circ}})\mathcal{L}(\lambda_{\text{MT}}/\lambda_{\text{BS}}) + \lambda_{\text{BS}}P_{\text{idle}}(1 - \mathcal{L}(\lambda_{\text{MT}}/\lambda_{\text{BS}})) \qquad (4.25)$$

Load model 2 (Equation 4.26) describes the equal allocation of bandwidth and transmit power among all the UEs.

$$P_{\text{grid}}^{(2)} = \lambda_{\text{BS}}P_{\text{tx}}\mathcal{L}(\lambda_{\text{MT}}/\lambda_{\text{BS}}) + \lambda_{\text{MT}}P_{\text{circ}} + \lambda_{\text{BS}}P_{\text{idle}}(1 - \mathcal{L}(\lambda_{\text{MT}}/\lambda_{\text{BS}})) \qquad (4.26)$$

The probability of a base station in transmission mode $\mathbb{P}_{\text{BS}}^{(\text{tx})}$ is given by Equation 4.27.

$$\mathbb{P}_{\text{BS}}^{(\text{tx})} = \mathcal{L}(\lambda_{\text{MT}}/\lambda_{\text{BS}}) \qquad (4.27)$$

The probability function $\mathcal{L}(\lambda_{\text{MT}}/\lambda_{\text{BS}})$ is defined as follows, with $\alpha = 3.5$.

$$\mathcal{L}(\lambda_{\text{MT}}/\lambda_{\text{BS}}) = 1 - \left(1 + \frac{\lambda_{\text{MT}}/\lambda_{\text{BS}}}{\alpha}\right)^{-\alpha} \qquad (4.28)$$

As the base station is either in transmission or idle mode, thus the probability of a base station in idle mode $\mathbb{P}_{\text{BS}}^{(\text{idle})}$ is the complementary probability to the probability in transmission.

$$\mathbb{P}_{\text{BS}}^{(\text{idle})} = 1 - \mathcal{L}(\lambda_{\text{MT}}/\lambda_{\text{BS}}) \qquad (4.29)$$

Using the network power consumption calculated with the load models, the network energy efficiency (bit/Joule) can be derived by dividing the potential spectral efficiency by the network power consumption.

4.4.2 Björnson et al.

The work in [38] proposes a system level model that models the power consumption in uplink and downlink of a single-cell multi-user MIMO system. The base station employs an array of antennas, communicating with a number of single-antenna UEs that are selected with round-robin scheduling from a larger set of UEs within the coverage area of the base station. The source code for the model is available online[4]. The important considerations of the model are outlined based on [38] hereafter.

Björnson et al. argue in [38] that simply setting $P_{\mathrm{CP}} = P_{\mathrm{FIX}}$ would lead to a theoretically unbounded energy efficiency when increasing the number of antennas. This is assumption is false, as each antenna requires additional circuit components that consume power and the computational complexity of the signal processing increases with the number of active antennas. However, the misleading assumption of a constant circuit power that is independent of the number of antennas, is proposed in earlier models.

The circuit power (P_{CP}) expressed in Equation 4.30, depends on the number of base station antennas (M), number of active UEs (K), and the user gross rates ($\bar{R}$). It is the sum of the static power consumption (P_{FIX}), the transceiver chain power consumption (P_{TC}), the channel estimation power consumption (P_{CE}), the coding and decoding power consumption ($P_{\mathrm{C/D}}$), the backhaul power consumption (P_{BH}), and the linear processing power consumption (P_{LP}).

$$P_{\mathrm{CP}} = P_{\mathrm{FIX}} + P_{\mathrm{TC}} + P_{\mathrm{CE}} + P_{\mathrm{C/D}} + P_{\mathrm{BH}} + P_{\mathrm{LP}} \tag{4.30}$$

The power consumption of the transceiver chains (P_{TC}), given in Equation 4.31, is calculated as follows. The number of base station antennas is multiplied with the power consumed by the transceiver circuit components for each chain (see Section 2.1.2 for background on wireless transceivers). As the local oscillator is shared among the chains, its power consumption is added only once (P_{SYN}). If multiple oscillators are used for the base station, the power consumption for the oscillators can be included in P_{BS} instead. The power required for the transceiver by each single-antenna UE (P_{UE}) is multiplied with the number of UEs.

---

[4]Link to GitHub repository: github.com/emilbjornson/is-massive-MIMO-the-answer (visited on 16/06/2023)

$$P_{\text{TC}} = M P_{\text{BS}} + P_{\text{SYN}} + K P_{\text{UE}} \tag{4.31}$$

Channel estimation power consumption (Equation 4.32) depends on the relative pilot sequence length for uplink and downlink ($\tau^{(\text{ul})}$ and $\tau^{(\text{dl})}$), the number of coherence blocks per second ($\frac{B}{U}$), and the computational efficiencies of base station and UE defined as arithmetic complex-valued operations per Joule (L_{BS} and L_{UE}). The first term describes the required power in the uplink, where the base station receives the pilot signal and estimates the channel for each UE. The second term is the downlink power, where each active UE processes the received pilot sequence.

$$P_{\text{CE}} = \frac{B}{U} \frac{2\tau^{(\text{ul})} M K^2}{L_{\text{BS}}} + \frac{B}{U} \frac{4\tau^{(\text{dl})} K^2}{L_{\text{UE}}} \tag{4.32}$$

The base station applies coding and modulation to K sequences of symbols in downlink, each UE decodes its sequence. In the uplink direction, the opposite process is completed. The power consumption for the coding/decoding (Equation 4.33) is proportional to the number of bits and thus the average sum rate $\left(\mathbb{E}\left\{ R_k^{(\text{ul})} + R_k^{(\text{dl})} \right\} \right)$. The coding and decoding power (W/bit/s) (P_{COD} and P_{DEC}) is multiplied with the average sum rate.

$$P_{\text{C/D}} = \sum_{k=1}^{K} \left(\mathbb{E}\left\{ R_k^{(\text{ul})} + R_k^{(\text{dl})} \right\} \right) (P_{\text{COD}} + P_{\text{DEC}}) \tag{4.33}$$

The backhaul power consumption (Equation 4.34) is split into a load-independent and load-dependent part. The load-independent part is included in P_{FIX}. The load-dependent part (P_{BH}) is proportional to the average sum rate. The backhaul traffic power in Watt/bit/s (P_{BT}) accounts for uplink and downlink.

$$P_{\text{BH}} = \sum_{k=1}^{K} \left(\mathbb{E}\left\{ R_k^{(\text{ul})} + R_k^{(\text{dl})} \right\} \right) P_{\text{BT}} \tag{4.34}$$

The linear processing power consumption (P_{LP}, Equation 4.35) accounts for the process of precoding and processing the transmitted and received vectors of information symbols at the base station.

$$P_{\text{LP}} = B \left(1 - \left(\tau^{(\text{ul})} + \tau^{(\text{dl})} \right) \frac{K}{U} \right) \frac{2MK}{L_{\text{BS}}} + P_{\text{LP}-\text{C}} \tag{4.35}$$

$P_{\text{LP-C}}$ denotes the power consumption of the linear processing computing power, which depends on the type of precoding method utilized. The paper gives equations for maximum ratio transmission / maximum-ratio combining (MRT/MRC) and zero-force (ZF) precoding.

The average sum rate (Equation 4.36) is calculated with the sum of the pilot sequence lengths for uplink and downlink (τ_{sum}) and the average user gross rate ($\bar{R}$). It is assumed that a uniform gross rate is guaranteed to all connected UEs through power allocation. If fixed power allocation is used, the model is also valid.

$$\mathbb{E} \left\{ R_k^{(\text{dl})} \right\} + \mathbb{E} \left\{ R_k^{(\text{ul})} \right\} = R_k^{(\text{dl})} + R_k^{(\text{ul})} = \left(1 - \tau_{\text{sum}} \frac{K}{U} \right) \bar{R} \tag{4.36}$$

4.4.3 Sanguinetti et al.

The distribution of the energy consumption in a MIMO system with UEs moving within the cell according to a Brownian motion is determined by the model in [122]. The source code for the model is available online[5]. The central assumption of the model is that due to the movement of the UEs, the path losses change, which results in a fluctuation of the base station power consumption. A constant data rate is guaranteed for all UEs and it is assumed that perfect channel state information is available to the base station. It is concluded that the energy consumption converges in distribution to a Gaussian random variable. Zero-force precoding is utilized at the base station and a fixed data rate is guaranteed for all the UEs. The simplicity of the results of this model is due to the assumption of zero-force precoding at the base station, as other precoding schemes increase the complexity. This is an ongoing research activity, according to the authors. Another open research question is the impact of different user mobility models on energy consumption dynamics.

---

[5]Link to GitHub repository: github.com/lucasanguinetti/energy_consumption_in_MU_MIMO_-with_mobility (visited on 16/06/2023)

4.4.4 Summary

System level models are suitable for optimization problems and provide a way to quantify the effect of different factors on network power consumption and energy efficiency. Three system level models, which are modeling very different scenarios, were selected based on the literature survey.

The Di Renzo model is convenient for system level network planning optimization, as it calculates the network energy efficiency depending on the transmission power and density of base stations. The Björnson model shows how the optimal energy efficiency is achieved based on selecting the number of mMIMO base station antennas, number of active UEs, and the data rate per UE. The Sanguinetti model shows that the energy consumption of a base station converges to a Gaussian distribution, based on the fluctuations in energy consumption that depend on UE mobility.

All the models are based on considerable simplifications that may restrict the general application of them: In the Di Renzo model, only the downlink is considered, and it assumes simplified cell association and single-antenna base stations that are always fully loaded. The Björnson model assumes that any number of UEs may be served with any data rate. And the Sanguinetti model assumes zero-force precoding at the base station.

If the evaluation of more complex scenarios is required, network simulation or extensive measurements on test setups is needed - especially for 5G specific procedures instead of the fairly generic assumptions of the models. The models may be adapted to slightly different cases. But this requires thorough understanding of the fairly complex mathematical formulation of the models and may lead to more complicated models - that are not easily applicable.

5 Implementation, Comparison, and Discussion of the Models

The second major contribution of this thesis, the implementation of power consumption models, is described in this section. Based on the implementation, selected models are compared and discussed.

5.1 Implementation

Selected power consumption models were implemented in Python. Additional documentation and information regarding the scripts can be found in the `README.md` file supplied with the source code. The source code of the implementations is on CD, which is available to be seen at the supervising examiners office. The implemented models are listed in Table A.8 in the Appendix. No RAN models were implemented, as none of the identified models in Section 4.2 are suitable for further evaluations of 5G systems - or the aspects are already covered by the base station models.

5.2 Comparison and Discussion

5.2.1 Base Station

The base station models are compared by means of the main components: Power supply and cooling, baseband processing, analog frontend/RF transceiver, power amplifier. Additionally, the sleep modes and load dependency as well as the load definition are compared. The base station models differ in their modeling methodology, and the included components and published parameters vary. Therefore, only models that include the respective main components and the necessary parameters are included in the comparison.

Common Parameter Values for Comparison - Reference Scenario

Unless stated otherwise, the following general parameter values are defined for the comparison of the base station models:

- Bandwidth: $B = 20$ MHz

- Spectral efficiency: $\eta_{\mathrm{SE}} = 6$ bit/s/Hz

- Upper bound of the data rate: $R_{\max} = B \cdot \eta_{\mathrm{SE}} = 120$ Mbit/s

- Base station configuration:

  - 1 sector

  - No carrier aggregation

- Power amplifier:

  - Maximum transmission power: $P_{\max} = 41$ dBm

  - Saturation power: $P_{\mathrm{sat}} = 49$ dBm

  - Back-off: $P_{\max}/P_{\mathrm{sat}} = 8$ dB

The bandwidth and spectral efficiency are chosen based on the reference configurations of the Auer and Debaillie models - the bandwidth of 20 MHz is also a common choice in other models. The values do not necessarily reflect 5G configurations - they are simply chosen for the sake of a common reference. Number of sectors is set to one, as the number of sectors is simply multiplied with the power consumption of a single sector - for example, in the models by Auer [12] and Debaillie [31]. Carrier aggregation is not used, as not all models consider it and if it is considered, the total power consumption is simply multiplied with the number of component carriers. The power amplifier parameter values are selected to reflect a typical large base station type, based on the values given for the Auer model [8] and the Rottenberg power amplifier models [81]. Parameters that are not common for the different models and can not be calculated/derived from other values are set to the default values given by the respective models. Further parameter value considerations are explained in the respective sections.

Base Station Classes and Cell Types

The parameters for the Auer/Holtkamp, Desset/Debaillie, and 3GPP models are defined for different base station classes (cell types). It is important to note that the models assume different maximum transmit powers for the same cell type (see Table 5.1).

Table 5.1: Maximum transmit power for base station types defined by different base station models

Model	Macro	RRH	Micro	Pico	Femto	LSAS	Unspecified
Auer and Holtkamp [10]	43 dBm	43 dBm	38 dBm	21 dBm	17 dBm		
Desset [49]	46 dBm		41 dBm	21 dBm	20 dBm		
Debaillie [31]	49 dBm			30 dBm	24 dBm	41 dBm	
3GPP [75]							55; 49; 33 dBm

The defined types also differ: The RRH is considered a separate type in the Auer model (though the only difference to the macro cell base station is the lack of active cooling). The Debaillie models also considers LSAS (large scale antenna systems, also known as mMIMO) base stations a different category. The 3GPP defines three different reference configurations in [75], though it is not clear which cell types or base station classes they are referring to.

This means that simply comparing parameter values or resulting power values for the same base station type among different models may lead to (very) different results. The power amplifier that determines the output power is a major contributor to the power consumption during transmission - even differences of a few dB in maximum output power corresponds to significant differences in maximum power consumption.

Power Supply and Cooling

Power supply and active cooling of base station components are either modeled using loss/efficiency factors or fixed values in Watt. For the models that use loss factors, the defined values are listed in Table 5.2. The loss factor is multiplied with the total power consumption of the other components to obtain the respective power consumption for the power supply or cooling - this value is then added to the total. Therefore, a load dependency is assumed. in case of fixed power values, no load dependency is assumed. The AC-DC or main supply loss is specified in a range of 8% to 11%. DC-DC conversion loss is denoted between 5% and 9%. The higher values are used for smaller base stations.

Cooling loss for macro base stations is defined at 10%, or in case of the Debaillie model as approximately 8% [31] and only activated upwards of 200 W for three sector base station.

The resulting efficiency for macro/large base stations between 75,8% and 77,9% (up to 84,6% for Debaillie in case of less than 200 W) is lower than for smaller base station types (micro, pico, femto) and the RRH - this is due to the absence of active cooling for these types. The total efficiency in this context is the product of the AC-DC, DC-DC and cooling efficiency values.

Table 5.2: Base station models parameter values for losses of AC-DC conversion, DC-DC conversion, cooling, and resulting total efficiency.

Parameter	Auer [8]					Desset [49]		Debaillie [31]
	Macro	RRH	Micro	Pico	Femto	Large	Small	Large
AC-DC loss	9.0%	9.0%	9.0%	11.0%	11.0%	10.0%	10.0%	8.0%
DC-DC loss	7.5%	7.5%	7.5%	9.0%	9.0%	5.0%	5.0%	8.0%
Cooling loss	10.0%	0.0%	0.0%	0.0%	0.0%	10.0%	0.0%	∼8.0%*
Total efficiency	75.8%	84,2%	84,2%	81,0%	81,0%	77,0%	85,5%	77,9% (84,6%)**

* Debaillie state that a "similar efficiency factor" as for the AC-DC and DC-DC conversion is used. Cooling is only activated above 200 W for a 3-sector base station [31]
** Value in parentheses for below 200 W, without cooling

The UTAMO project report [33] indicates that cooling is generally adapted to the load. However, the power consumption of ventilators is not proportional to the load but is assumed to increase disproportionately at loads larger than 50%. The analysis of datasheets and literature sources shows that typical loss values for cooling are 7% to 15%. For AC-DC power supply efficiency is dependent on the ratio of the nominal load and typical values for 50% nominal load are between 85% and 96%.

The values considered in the models seem reasonable based on this. Depending on the age and other properties of the analyzed base station, the loss factors might need slight adjustments. Accurate modeling of the cooling power consumption is difficult as the required cooling at any point in time depends not only on the current load but also on environmental factors (air temperature, location of the base station). Additionally, the cooling demand changes much more slowly than the power consumption of the radio related hardware - a direct dependency on the instantaneous power consumption of the base station (or a constant loss value) may be too simplistic.

Baseband Processing

The power consumption of the baseband processing is defined as a constant value in the Auer, Holtkamp, and Piovesan models. In the Holtkamp model, it is scaled linearly with the bandwidth and the number of employed antennas.

Desset and Debaillie model the baseband processing based on subcomponents (each subcomponent describes a specific digital operation e.g., channel coding, predistortion, equalization, FFT/IFFT etc.). It is scaled with several parameters. The parameters and subcomponents differ slightly between Desset and the later Debaillie model. As the Debaillie model is newer and provides more accurate values for the baseband processing according to [68] and [31], the Desset model is not considered here. In the Debaillie model, the baseband processing power scales with the bandwidth, the spectral efficiency, the number of antennas, the load, the number of spatial streams, and the quantization bits. The power consumption is reduced in case mMIMO is employed, because some subcomponents are not required and the number of quantization bits is reduced. According to [73], the power consumption values for mMIMO calculated with the Debaillie model are probably underestimated.

The Björnson/Hossain/Peesapati models calculate the baseband processing power consumption as the sum of the power required for channel estimation, coding and decoding and linear processing. It depends on the number of antennas at the base station, the number of users, the data rate per user, and the bandwidth. The model equations are equal for the three variants, though the parameter values of the Hossain model are used for this comparison. The Holtkamp model only scales the baseband processing power of the reference configuration with the number of antennas and the bandwidth.

The 3GPP model does not differentiate the baseband power consumption, and the Piovesan power model simply uses a constant parameter value that is not scaled. Therefore, these two models are not considered here.

The scaling of the baseband processing power consumption with the bandwidth for the different models is shown in Figure 5.1. The plot shows that the baseband processing power consumption is proportional to the bandwidth for all three considered models. However, the calculated power consumption varies significantly between the models. The two mMIMO models (Debaillie with LSAS configuration and Hossain) show a similar power consumption - for these models, the number of antennas corresponds to the number of antenna elements, not the number of antenna arrays. As the power consumption

per antenna element is lower than per a conventional antenna port, 16 antennas and spatial streams (users) were configured for this comparison. The standard Debaillie model configuration for large base stations and the Holtkamp model for macro base stations, differ significantly - whereas the Holtkamp model exceeds 800 W, the Debaillie model values remain at less than 300 W for up to 100 MHz bandwidth. The Holtkamp model results are very sensitive to the initial value of the reference configuration (base station type), which is simply multiplied with the number of antennas and the bandwidth (divided by 10 MHz).
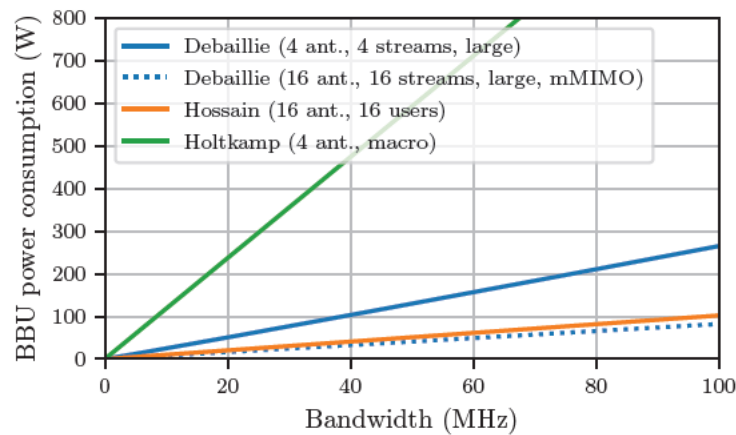

Figure 5.1: Baseband unit power consumption as a function of the bandwidth for different models

The Björnson/Hossain/Peesapati model features scaling of baseband processing based on the number of simultaneously served users. The Debaillie model includes the number of spatial streams as a parameter, which also denotes the number of simultaneously served users. The power consumption versus this parameter is plotted in Figure 5.2. The data rate per UE for the Hossain model is calculated using the upper bound of the total data rate (spectral efficiency multiplied with bandwidth) divided by the number of UEs. It should be noted that the Hossain model assumes a computational efficiency of 12.8 GFLOPS/W and for the baseline configuration in the Debaillie model 8 GOPS/W is assumed. GFLOPS includes the floating point operations only, and GOPS includes all operation types. A conversion between GFLOPS and GOPS is not possible without additional considerations. The power consumption for an increasing number of simultaneously served users is paradoxically higher in the Hossain model. This is due to the different scaling assumed by the models: The Debaillie model assumes that the power consumption for the channel estimation and precoding scales linearly with the number of users.

The Hossain model assumes a quadratic increase of channel estimation power consumption with the number of users, and the precoding power contains quadratic and cubic terms. The coding and decoding power for the Hossain and Debaillie model is proportional to the number of users. The Björnson base station [36] and system level models [38] give reasoning on how the power consumption equations are derived, whereas the Debaillie et al. paper [31] does not explain the specific scaling for each subcomponent.
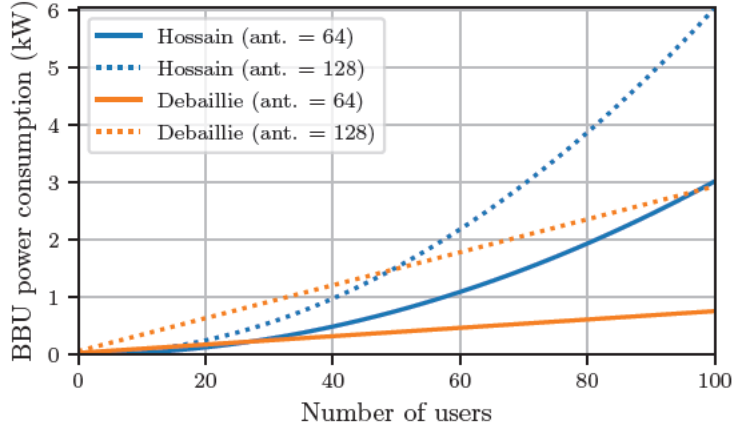
Figure 5.2: Baseband unit power consumption as a function of the number of simultaneously served users and for a varying number of antennas, calculated with the Hossain and Debaillie base station models

The Zhao model offers an extension to the Auer model, where the power consumption of a virtualized baseband unit running on a general purpose CPU is calculated. The plot in Figure 5.3 shows that the power consumption calculated with this model increases linearly with the transmission data rate. The number of cores determines the maximum achievable data rate. The number of active cores is set to the maximum available cores in this case. Comparing the Zhao model to the Auer, Debaillie, and Hossain models discussed before, the difference in the parameters is apparent. For the Zhao model, the power consumption depends on the data rate and the number of CPU cores - the number of antennas is not relevant. The number of users and bandwidth both influence the data rate, however additional assumptions are required to determine the data rate based on bandwidth and number of users.

Figure 5.3: Virtualized baseband unit power consumption as a function of the data rate, calculated with the Zhao base station model.
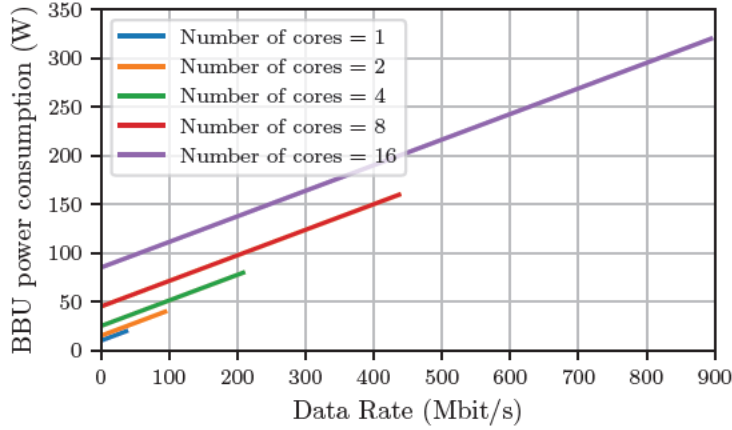
Analog Frontend / RF Transceiver

The RF transceiver power is a constant value in the Auer and Holtkamp models, derived from measurements. In the Holtkamp model, it is scaled linearly with the bandwidth and the number of employed antennas. Similarly, a constant power value per chain is multiplied with number of chains in the Piovesan model. The Desset and Debaillie power models follow a subcomponent approach and give power values for each subcomponent of the transceiver. The values for the default configuration of the Auer/Holtkamp, Desset, and Debaillie power consumption models - without any scaling applied - are listed in Table 5.3.

Table 5.3: RF transceiver power consumption per chain for different base station models

Model / comm. direction	Macro	RRH	Micro	Pico	Femto	Large	Small
Auer and Holtkamp [10]							
TX power consumption (W)	6.8	6.8	3.4	0.4	0.2		
RX power consumption (W)	6.1	6.1	3.1	0.4	0.3		
Desset [49]							
TX power consumption (W)	5.7		2.9	0.4	0.2		
RX power consumption (W)	5.1		2.6	0.4	0.2		
Debaillie [31]							
TX power consumption (W)						6.87	0.740
RX power consumption (W)						4.70	0.763

The RF transceiver power depends on the bandwidth for the Debaillie and the Holtkamp model. The RF transceiver power consumption versus the bandwidth for these models is shown in the plot in Figure 5.4. Additionally, the power calculated with the Hossain model is plotted, which does not define a bandwidth dependency of the RF transceiver. This does not mean that the model disputes a bandwidth dependency. However, the circuit power of the transceiver chains, which is given as a single value for 20 MHz in the Hossain model, would likely need to be adapted to consider different bandwidths. How the circuit power scales with bandwidth is not given in the Hossain model. The plot shows that the power required by the RF transceiver is proportional to the bandwidth for the Holtkamp and Debaillie models. For the Hossain model, it is constant and only increases with the number of antennas - the latter is also the true for the other two power models. The model equations of the Björnson/Hossain/Peesapati power models are equal for the three variants, though the parameter values of the Hossain model are used for this comparison. As the Hossain model considers mMIMO deployment, the number of antennas corresponds to the number of antenna elements. The Holtkamp model does not consider mMIMO and the Debaillie model does not differentiate it for the analog frontend.
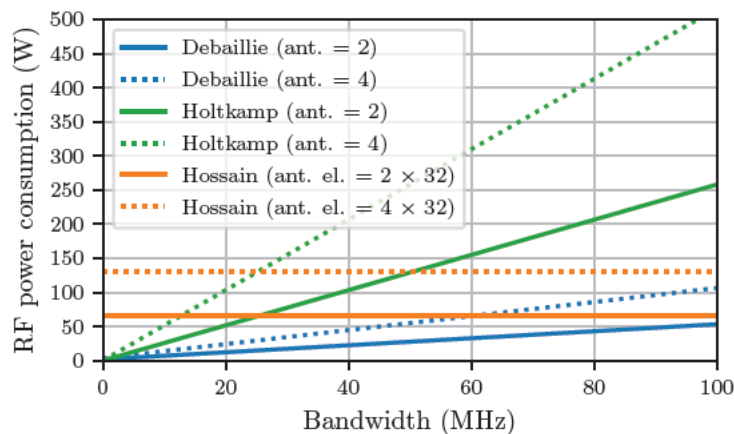

Figure 5.4: Base station RF transceiver power consumption as a function of the bandwidth for different base station models

Power Amplifier

The power amplifier is considered separately from the other RF components, as it generally constitutes a large share of the base station power consumption. This underlines the importance of an accurate power amplifier model. The modeling of the power amplifier differs: The Auer model utilizes a fixed efficiency value to calculate the power consumption based on the output power of the amplifier - this is a common approach that is also utilized in other models. The assumed efficiency values have a wide range and depend on the base station type. Degradation of the efficiency for lower output power is taken into account in the Holtkamp model, where the maximum efficiency is decreased by a certain factor for every halving of the output power. Additionally, models for different types of power amplifiers are listed by Rottenberg in [81]. The three types are class B, envelope-tracking, and Doherty power amplifier. Debaillie and Desset models use a table of measurements that is not publicly available. The defined back-off for the power amplifier ranges from 8 dB (smaller base stations) to 12 dB (larger base stations) for the models.

A comparison of the power consumption calculated with the power amplifier models versus the output power is shown in the plot in Figure 5.5. The default parameter values for the envelope-tracking power amplifier are used ($\eta_{\max} = 0.4$ and $a = 0.0082$). For the Holtkamp model, the default parameter values for the macro base station are set for the comparison ($\eta_{\mathrm{PA,max}} = 0.36$ and $\gamma = 0.15$). The feeder cable loss is set to zero for the Auer and Holtkamp models, as only the power amplifier itself is compared. A two-way Doherty power amplifier is considered, and the remaining parameter values for all models are set as follows: $P_{\max} = 41$ dBm ≈ 12.6 W and $P_{\mathrm{sat}} = 49$ dBm ≈ 79.4 W.

Especially noticeable in the plot in Figure 5.5 is the steep increase in power consumption for small output powers in the Holtkamp model. This is due to the assumed decrease in efficiency following a logarithmic function - this leads to a modeling artifact: The efficiency function decreases However, this is not how the efficiency scaling of the Holtkamp model is actually intended to be used (based on [62]). It should rather only be utilized to calculate a constant (maximum) operating efficiency from the maximum efficiency of the power amplifier given in the datasheet (or similar). Based on the lower efficiency derived from this scaling, the fixed-efficiency Auer model should be used. The Holtkamp model efficiency scaling is included in the comparison to show that it is not suitable to estimate the efficiency for output powers significantly lower than the saturation power of the power amplifier. Compared with the other models, the efficiency reduction of the Holtkamp

model seems overestimated (see Figure 5.6). The Auer and envelope-tracking power amplifiers exhibit a linear power consumption function. The class B power consumption is a root function, and the curve of the Doherty amplifier with two stages features a corner at about 20 W output power. The unique behavior of the Doherty amplifier is due to its architecture, which combines two amplifiers. The power consumption values shown in the plot should not be compared between all models, as they simply depend on the choice of parameters. The efficiency (or maximum efficiency) is parameterized for the Auer, Holtkamp and envelope-tracking power amplifier models. Therefore, only the class B and Doherty amplifiers may be compared, the models only depend on the common parameters of maximum output power and saturation power.
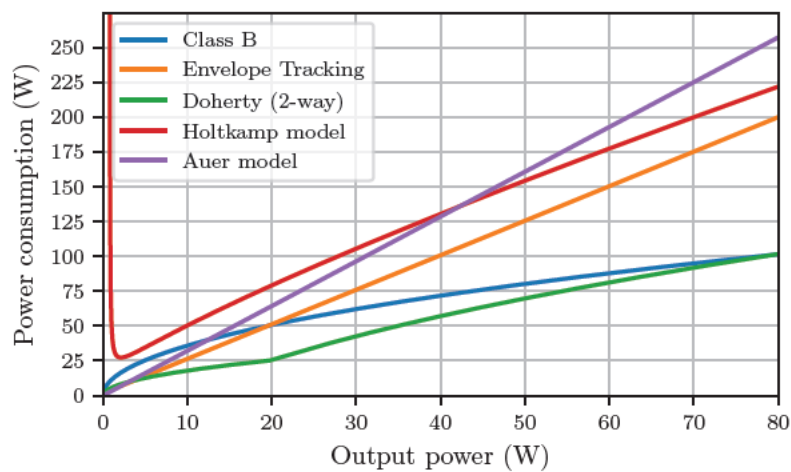
Figure 5.5: Comparison of power consumption for different power amplifier models. With maximum output power of 41 dBm, 8 dB back-off and saturation power of 49 dBm. The Holtkamp model is utilized beyond the intended output power range, which results in the steep increase in power consumption for small output power values.

To further clarify the differences between the power amplifier models, the power consumption is plotted versus the efficiency in Figure 5.6 (output power in dBm) and Figure A.2 (in the Appendix, output power in W). The efficiency is defined as output power divided by power consumption. The plot illustrates why the Doherty amplifier is advantageous to the class B amplifier due to the second maximum of efficiency at a lower output power, this is generally desirable for signals with a high peak-to-average power ratio (PAPR). In contrast to this, the efficiency for the envelope-tracking, class B, and Holtkamp model is maximal at the saturation power. The fixed efficiency Auer model does not capture these

differences in efficiency, and it should be assumed that efficiency is either significantly over- or underestimated for at least part of the output power range. If the exact power amplifier type is unknown, a fixed efficiency may still be a reasonable choice for modeling the power amplifier. In addition to the compared analytic models in this section, a curve fitted model based on measurements is a viable alternative - for example applied in the Desset and Debaillie models.

The UTAMO project models the power amplifier using a fixed efficiency in [33]. The compiled efficiency values show a wide range of 15% to 60%, depending on the output power and carrier frequency. Amplifiers operating in the mmWave spectrum exhibit a lower efficiency. The aspect of operating frequency is not considered in the aforementioned analytic models.
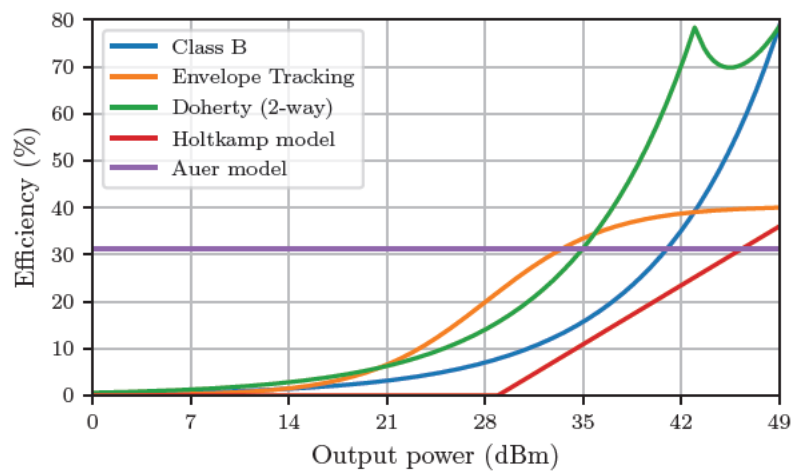
Figure 5.6: Comparison of efficiency for different power amplifier models versus output power in dBm

Sleep Modes

Base station sleep modes are often discussed in the context of energy efficiency and power consumption optimization of base stations. The concept is not new: The EARTH project envisaged sleep modes (different lengths of discontinuous transmission) in 2010 in their report [25]. Consequently, the Auer model (and Holtkamp model) feature a single sleep mode, though this is not necessarily based on the contemporary technology. The later proposed sleep modes in the Debaillie model are often cited, and the respective minimum

time durations are used in other models (such as the Peesapati model). The 3GPP model also based the sleep models in their model on the Debaillie et al. definitions. A comparison of the minimum time durations defined by the Debaillie and 3GPP models is shown in Table 5.4. The 3GPP assumes significantly longer sleep durations, especially for the second base station category. The sleep modes are generically referred to as SM1 to SM4 (where power level and minimum duration are descending from SM1 to SM4) in the following comparisons, as the exact definition and naming differs between the models.

Table 5.4: Minimum duration for the sleep modes (SM1- SM4) defined in the base station models

Model	No. of sleep modes	SM1	SM2	SM3	SM4
Debaillie [31]	4	71.4 µs	1 ms	10 ms	1 s
3GPP [75] [69]	3 (4)**	0 s	6 ms; 640 ms *	50 ms; 10 s *	1 s **

* First value for base station category 1, second value for base station category 2
** Hibernate proposed in initial discussion, not defined in final 3GPP study

It should be noted that these definitions are not based on functionalities implemented in actual base station hardware. The propositions by Debaillie et al. in [31] are based on theoretical grouping of components with similar power-on/power-off times - further details on which components are considered are not described. The 3GPP durations are based on discussions of the member companies. The discussions may include reasoning of individual companies, but the final values are not further justified in the final study in [75]. The values of the Peesapati model are also based on assumptions for LTE. Only the Piovesan modes are based on measurements, although no minimum sleep durations or transition times are given and the power values are normalized without a disclosed reference (and therefore only useable for relative comparisons).

Apart from the durations, the level of the sleep modes can be compared. The Figure 5.7 illustrates the different sleep mode levels in a bar chart. The relative levels in the chart are in relation to the idle/no load power consumption. A fourth sleep mode (SM4) is not defined in the Peesapati and Piovesan models. The power level of the fourth sleep mode of the 3GPP is barely visible in the bar chart, as it is only about 0.13% of the idle power. For the 3GPP model and the Debaillie model, the sleep mode power depends on the configuration - some of these are included in the bar chart for comparison.

For the 3GPP model, the "micro sleep" level (SM1) is multiplied with a factor of 1.5 for the reference idle/no load power. The idle state of a base station is considered a "pseudo-state" in the initial introduction of the model in [2], which should not be defined.

However, the final definition of the model gives a value for the static (load-independent) power of the base station. For the baseline, it is equal to the micro sleep level - this is not comparable with other models, as the power amplifiers are completely turned off in the 3GPP definition for the mode. Alternatively, the factor of 1.5 may be used - which is done in this comparison. The assumption is, that the factor accounts for the "idle" power consumed by power amplifier and low noise amplifier (though this is not explicitly stated in [75]). All the other values are directly taken from the parameter value definitions of the models or calculated based on these.
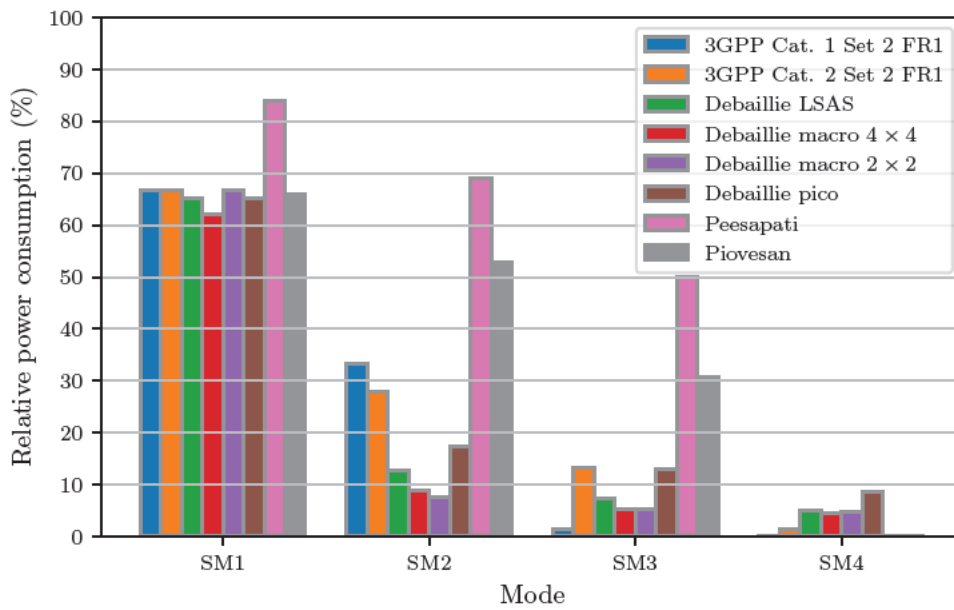
Figure 5.7: Comparison of base station sleep mode power levels relative to idle (no load) power consumption for different models and configurations

The first sleep mode exhibits a similar power level for all power models, except for the Peesapati model that defines a value of 84% relative to the idle power - the other levels are in the range of 60% to 70%. For the other modes, the relative power consumption varies quite significantly between the models and configurations. The Peesapati and Piovesan model levels are especially high in relation to the others for the SM2 and SM3.

In conclusion, there is no consistent definition of the sleep mode power levels and minimum durations. If sleep modes are to be evaluated in a base station power model, measurements are needed to derive the respective parameter values, as there is no consensus in the analyzed models. Alternatively, datasheets and other documentation may be a possible

source, if available - there is no information on the sleep mode specifics in publicly available documentation to the best knowledge of the author.

The descriptions of the sleep modes for the 3GPP and Piovesan models are listed hereafter. They show that even the definition of which components may be turned off is not unified in the publications. Also note that the "channel shutdown" defined in the Piovesan model has no corresponding state in the 3GPP definitions.

The 3GPP model sleep mode definitions from [69]:

- Micro sleep: No transmission or reception within current symbol. The power amplifier and low noise amplifier are turned off.

- Light sleep: No transmission or reception at least within next SM2 time period (refer to Table 5.4). Additional components (e.g., transceiver chains) are turned off.

- Deep Sleep: No transmission or reception at least within next SM3 time period. Additional components are turned off. A minimum of active components (e.g., the clock) remain.

- Hibernate: No transmission or reception at least within next SM4 time period. All hardware/software components are turned off.

The Piovesan model sleep modes are defined as follows in [73]:

- Channel shutdown: Limits the multiplexing and beamforming capabilities. Some multi-carrier power amplifiers turned off. (only applicable for mMIMO or MIMO)

- Symbol shutdown: All multi-carrier power amplifiers are turned off.

- Carrier shutdown: Additionally, the analog RF transceivers are turned off.

- Deep dormancy: Additionally, the baseband processing is turned off. Only the baseline power consumption remains.

Table 5.5: Load definitions of base station models

Model	Definition of load
Auer	% of used bandwidth, defined as equivalent to % of maximum transmit power
NTT DOCOMO	% of REs transmitted and power boosting level per RE
Sharma	Number of connected UEs
Desset	% of used time and frequency resources (product of time- and frequency-domain duty cycling)
Debaillie	% of used frequency resources and/or traffic load
3GPP	% of used PRBs (only 100% PRB state defined)
Piovesan	% of used PRBs
Peesapati	Traffic load
Hossain	Base station: "M/G/m/m queue"; Network: Traffic load

Definition of Load and Load Dependency

All the base station models considered in this thesis are assuming a (partially) load-dependent power consumption for the base station. Though, the exact definition of "load" varies between the models. Some definitions are listed in short form in Table 5.5. This shows, that a unified, precise and well-understood definition of the load is required.

As outlined in Section 2.2.4 in the background chapter, the assumption that the share of utilized frequency resources (PRBs) is a one-to-one correspondence to the ratio of transmit power to maximum transmit power may be too simplistic under certain conditions.

The linear equation (Equation 2.1 in Section 2.2.4) may not be valid for advanced scheduling algorithms and adaptive power amplifiers. Additionally, the offset of the function and the dependence of its slope on the EPRE (energy per resource element) lead to (slight) inaccuracies when assuming that the ratio of transmit power to maximum transmit power is equal to the frequency resource load. On the other hand, this is an approach that is used in several well-developed models and therefore still reasonable to apply. The traffic load is usually given in bit/s, for example in [25], and therefore needs to be converted first to a load in terms of used frequency resources or similar.

Load dependency is dominated by the power amplifier in downlink. It is linear in the Auer, Holtkamp and Björnson models. Depending on the employed power amplifier model, it is non-linear in the Hossain and Peesapati models. The power models by Desset and Debaillie are the only ones that describe a load dependency for main components other

than the power amplifier. The baseband processing is dependent on the load in both models. The RF transceiver power consumption is assumed to scale with frequency-domain duty-cycling in the Desset model. The load dependency of the main components for the different models is listed in Table 5.6.

Table 5.6: Load-dependency of base station components defined by base station models

Model	Load-dependent	Load-independent
Auer, Holtkamp, Björnson	PA	BB, RF
Desset	PA, BB, RF	
Debaillie	PA, BB	RF
Piovesan	PA	BB, RF
Hossain and Peesapati	PA	BB, RF
3GPP	No component and load modeling	

The plot in Figure 5.8 compares the power consumption as a function of the load for the Auer, Holtkamp, and Debaillie models. For this comparison, the 3-sector macro base station (large base station for Debaillie model) parameter value setup is used. The Debaillie model is combined with the class B power amplifier power model (Equation 4.19) as it is a common power amplifier type for base stations. The Holtkamp model uses slightly different parameter values compared to the Auer model, as it is fitted to the Desset model results (the predecessor of the Debaillie model). The largest difference between Auer and Holtkamp models is at the sleep mode power (about 200 W) and the idle power consumption (about 100 W). The Debaillie model deviates greatly from both the Auer and Holtkamp models. The idle power is significantly lower for the Debaillie model at about 64 W, compared to the 877 W for the Holtkamp model and 782 W for the Auer model. The large disparity between the Debaillie model and the other power models may be caused by several reasons: The power amplifier is the largest contributor to the power consumption. For a 3-sector base station with 2 antennas per sector, six power amplifiers are required in total. Therefore, deviations in the power amplifier modeling are further amplified. The class B power amplifier power model can not be approximated with a linear function without over- or underestimating the power consumption for part of the output power range. This is the case for the Auer and Holtkamp models (though the type of power amplifier is not specified for these models). Additionally, as shown in the previous sections, the power consumption modeling of the other main components (baseband processing and analog frontend) differs between the power models. Lastly, the disparity could simply be attributed to the fact that the Debaillie model was developed a few years after the Auer and Holtkamp models - thus, different hardware was considered.
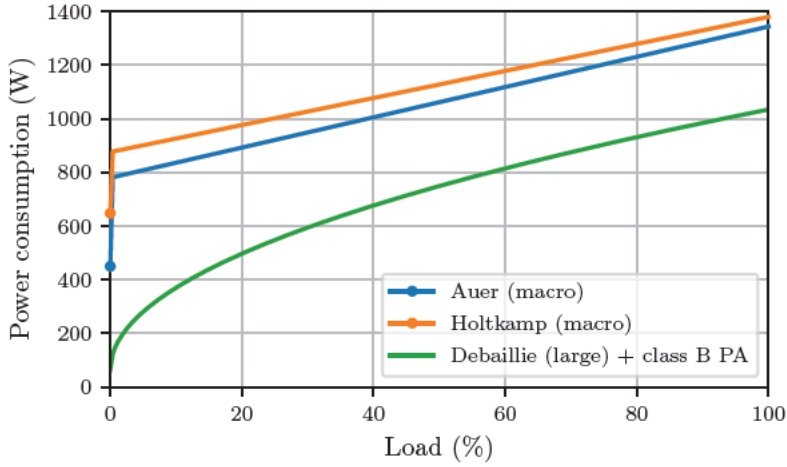
Figure 5.8: Comparison of downlink load dependency of macro base station power consumption for Auer, Holtkamp, and Debaillie power models. Sleep mode power consumption for Auer and Holtkamp models is indicated with a dot. (Parameters: Three sectors, two antennas per sector, maximum power amplifier output power 46 dBm, back-off 8 dBm, bandwidth 10 MHz)

Uplink and Downlink

The plots shown in Figure A.3 and A.4 show the power consumption of a base station versus the load (or output power) in downlink. However, the power consumption in uplink (reception) is different, mainly because the RF receiver chain does not contain a power amplifier and the required baseband processing for reception is dissimilar to the transmission case. The EARTH project [12] shows this in the initial measurements from which the Auer model is derived. The Debaillie model (and previous Desset model) is the only one that features a detailed modeling for the power consumption in uplink for the RF transceiver and baseband processing based on subcomponents.

For models that do not feature such a distinction, only the power amplifier power consumption can be ignored, and otherwise the power is the same as in the downlink for all components. Figure A.5 shows a plot of the power consumption in the uplink versus the load, computed with the Debaillie model.

For both plots in Figure A.3 and A.4, the class B power amplifier model (Equation 4.19) is combined with the respective power consumption models. Additionally, Figure A.6 shows the power consumption of a small base station in downlink for comparison to the large base station in Figure A.4, both computed with the Debaillie model.

5.2.2 User Equipment

Transmit Power Dependency

The Lauridsen model shows that the power consumption of the user equipment depends on the transmit power. The same is true for the Dusza model. The power amplifier is the main contributor to the UE cellular modem power consumption during transmission. The Dusza model provides parameter values for different UEs. The resulting plot for two different LTE data sticks is shown in Figure 5.9. Additionally, the LTE smartphone power model from Lauridsen is plotted.

The curves of the power consumption for all different UEs share common properties, such as the stepped increase of power consumption and the largest slope at transmission powers higher than 16 dBm. The two slopes of the curves and the step at 16 dBm transmission power for the LTE data sticks (Dusza model) are a result of multiple power amplifier stages employed in user equipment to enhance the efficiency, as discussed in [108]. Additionally, supply voltage and bias switching are employed to optimize the power consumption of UE modems [108]. The Lauridsen model for an LTE smartphone uses a quadratic function to model the power consumption between transmit powers of 1.1 dBm and 15.6 dBm next to the two linear functions for at lower and higher transmission powers. Furthermore, when comparing the curves for different UEs and carrier frequencies, the differences in power consumption are significant (up to 1 W at maximum transmission power). Therefore, if a specific device should be modeled, it likely requires measurements of that device at the respective carrier frequency to derive accurate parameter values. The Dusza and Lauridsen models only include values for LTE devices - no measurement data is provided for 5G UEs.

The Lauridsen model additionally allows for the separate calculation of power consumption for the components RF transceiver and baseband processing in uplink and downlink. The respective modeling equations are included in the implementation for this thesis.

The resulting plots are also included in the publication [101], and therefore not discussed here. Any further evaluations of the user equipment models of Lauridsen and the 3GPP depend on the chosen traffic model and the specific DRX configuration. Therefore, these aspects are not further discussed here, as it requires considerations beyond the scope of this thesis.
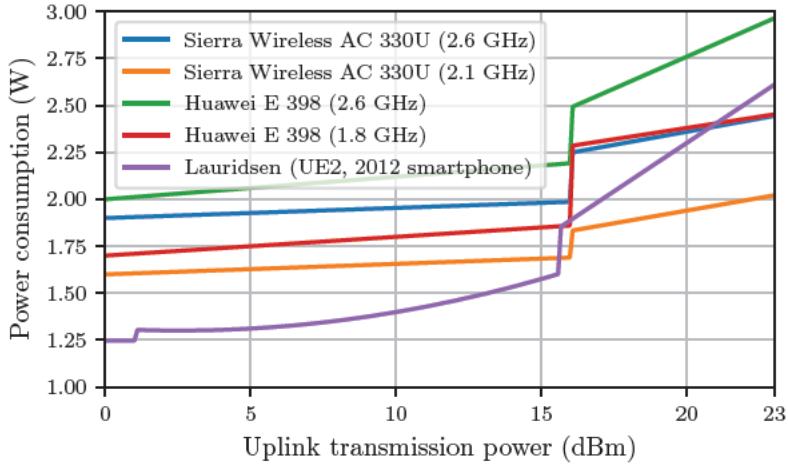
Figure 5.9: User equipment power consumption (LTE data sticks from Dusza model and smartphone from Lauridsen model) as a function of the uplink transmission power. Carrier frequency for Dusza model indicated in parentheses. Parameters for Lauridsen model from [105], for a bandwidth of 20 MHz.

5.2.3 System Level

Network Energy Efficiency

Using the Di Renzo system level model, the network energy efficiency for a given base station and UE density can be calculated. Deriving from the potential spectral efficiency, the "bit/energy" metric (or EE_{DV} defined by the 3GPP/ETSI - Section 6.1) is computed. In Figure 5.10, the energy efficiency versus the transmit power of the base stations is plotted. The energy efficiency remains nearly constant for a wide range of the transmit power (10 dBm to 40 dBm) and decreases for lower and higher transmit powers. The energy efficiency is generally higher for the load model 1, where the bandwidth and transmit power is allocated exclusively to one UE. The default parameter values for the Di Renzo model given in [121] are used to generate the plots.

The network energy efficiency is plotted against the cell radius (base station density) in Figure 5.11. The maximum of energy efficiency for the given setup depends on the load model. The plot shows that there is a distinct optimum for the energy efficiency.
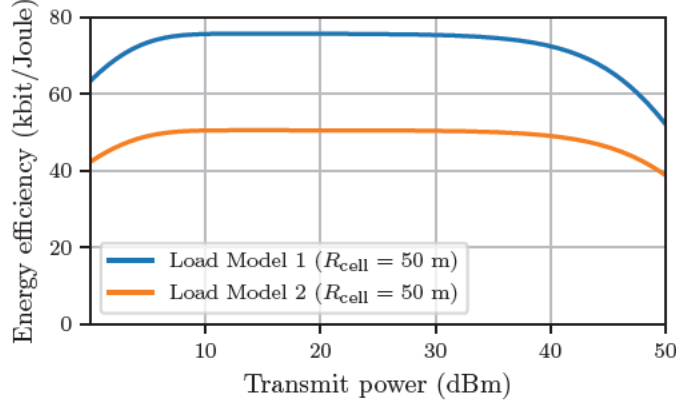
Figure 5.10: Network energy efficiency as a function of the base station transmit power (Di Renzo model)
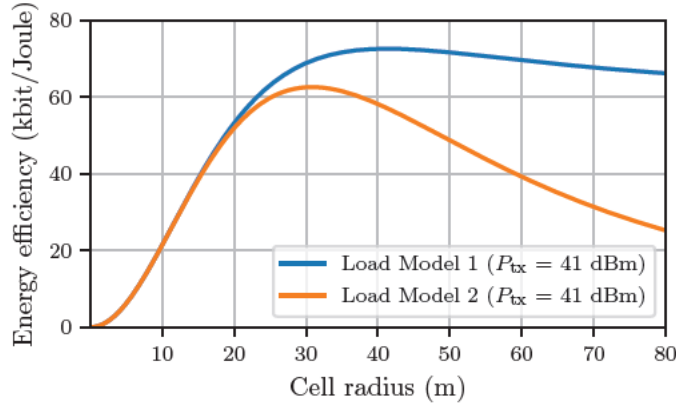
Figure 5.11: Network energy efficiency as a function of the cell radius (Di Renzo model)

The plots shown in Figure 5.10 and 5.11 are derived from the power consumption per coverage area and the potential spectral efficiency, calculated with the Di Renzo model. The respective plots are included in the appendix in Figures A.7 and A.8.

Furthermore, alternative energy efficiency metrics can be utilized with the model. The plot in Figure 5.12 shows the EE_{mMTC} metric (Equation 6.6 in Chapter 6) versus the density of the UEs. The EE_{mMTC} metric divides the number of registered UEs by the energy consumption. The definition is slightly altered to utilize it with the Di Renzo model: The number of UEs per cell is derived from the density of the base stations and density of the UEs. Instead of the energy consumption, the power consumption per

coverage area (P_{grid}) is used to calculate the EE_{mMTC} - which is therefore expressed in 1/W (Number of UEs per Watt power consumption). Furthermore, the plot in Figure 5.12 shows that the load model 1 of the Di Renzo model results in an unbounded energy efficiency for increasing UE density, if the total number of UEs in the cell is considered for the energy efficiency (dotted blue curve). As noted before (Section 4.4.1), the load model 1 assumes that the base station only serves one UE simultaneously. For this reason, the number of UEs should be set to one per cell to calculate the EE_{mMTC}. This is done for the solid blue curve in Figure 5.12. The metric EE_{mMTC}, as defined by the 3GPP/ETSI defines that the number of *registered* UEs should be used for the metric [123] [124]. This definition may not be suitable for all scenarios, as the plot in Figure 5.12 shows - here the number of *simultaneously served* UEs is the more suitable option. As the UEs are registered at the core network, the specific scheduling of the base station resources is not taken into account when using the number of registered UEs. Utilizing the simultaneously served UEs, the energy efficiency at increasing UE density converges to the same value (about 0.006 UEs/W) for both load models, as shown in Figure 5.12.
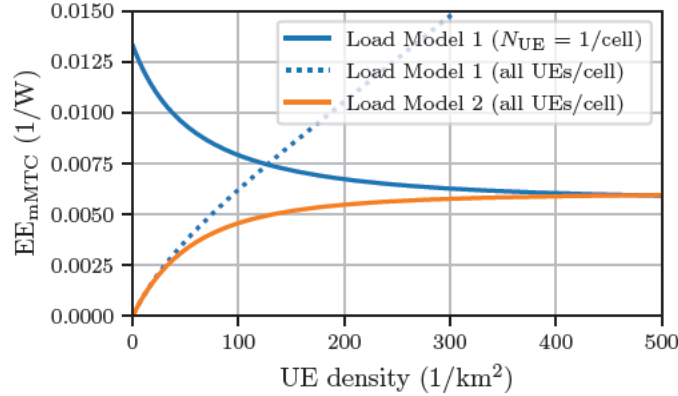
Figure 5.12: Energy efficiency (EE_{mMTC}) as a function of the UE density for a cell radius of 50 m and transmit power of 41 dBm (Di Renzo model)

The Di Renzo system level model is suitable for simplified network energy efficiency evaluations and may be further extended to suit more specific use cases, such as including the uplink and modeling multiple network slices. A simple modification is the combination of the Di Renzo model with the base station models. In the Di Renzo model, the static circuit power and the idle power is parameterized. These values may be calculated for different base station configurations using the base station models discussed in Section 4.1.

The aforementioned examples of calculating the network energy efficiency show that the choice of the metric or key performance indicator is important when assessing the energy efficiency of a mobile network. Further energy efficiency metrics specifically for mMTC and URLLC are discussed in the following Chapter 6.

5.2.4 Summary and Outlook

The comparison showed that all main components of a base station are modeled differently in the considered power models, using different parameters and parameter values. A particular challenge for the comparison and further modeling is the variety of possible base station configurations (e.g., number of antennas, bandwidth, power amplifier type and output power etc.), which influence the power consumption. As there is very limited data on power consumption of current base station components publicly available, it was not feasible to verify the modeling results against actual measurements. Data sheets can serve as a rough orientation for RRH and BBU power consumption, although a direct comparison to data sheet values is not feasible due to unspecified parameters in the data sheets (e.g., power amplifier type and efficiency). Furthermore, the data sheets only specify power consumption for the complete hardware unit, not the main components or subcomponents separately. The implementation of the power consumption models can consequently be used as the basis for additional comparisons. The modeling of the base station main components can be arbitrarily combined and further applied to enhance the system level models by Di Renzo et al. or the other system level models described in Section 4.4. When combining models, the comparisons conducted in this chapter can serve as an orientation when choose suitable models for the intended task. The implemented base station models cover all main approaches identified in the literature survey in Section 4.1, therefore the implementation for this thesis can readily be adapted and expanded to form a complete energy consumption simulation model / evaluation framework. For this, traffic models are needed to supplement the power consumption models - the functionality to convert traffic load to base station load also needs to be added to the implementation. However, the first step towards further development of the power consumption models is the determination of the intended modeling use cases and scenarios. The subsequent choice of a model from the presented ones mainly depends on the required level of granularity and the intended network configurations to be considered. Furthermore, the aspects of base station sleep modes and base station load need to be defined, as the compared models do not agree on common definitions.

6 Energy Efficiency Metrics

This chapter first introduces the most common energy efficiency metric for conventional mobile broadband focused networks. Then Section 6.2 outlines the metrics defined by the 3GGP (and subsequently ETSI) for URLLC and mMTC network slices.

6.1 Common Metric for Mobile Broadband Applications

Björnson, Hoydis, and Sanguinetti define the energy efficiency (EE) of a cellular network as "the number of bits that can be reliably transmitted per unit of energy" (bit/Joule) [32]. This is expressed in Equation 6.1.

$$\text{EE} = \frac{\text{Throughput (bit/s)}}{\text{Power consumption (W)}} \tag{6.1}$$

This metric is measured in bit/Joule, and generally values in the order of kbit/Joule or Mbit/Joule are to be expected for current wireless communication systems, according to [32].

The definition of efficiency depends on the chosen performance or profit quantity. The throughput or achievable data rate is the performance indicator for mobile broadband applications. This energy efficiency metric can therefore be regarded as a mobile broadband (or eMBB) metric. As mobile broadband is traditionally the central use case of wireless communication systems, this metric is widespread and generally accepted when assessing the energy efficiency.

The ETSI also defines this metric in [124] with the data volume (DV) and the energy consumption (EC):

$$\text{EE}_{\text{DV}} = \frac{\text{DV}}{\text{EC}} \tag{6.2}$$

There is one difference in the expression of the two definitions: To calculate the ETSI metric in Equation 6.2 the data volume over a certain time period (in bit) and the energy consumption (in Joule) over the same time period is measured. The definition in Equation 6.1 is defined on instantaneous throughput and power values.

Additional work on efficiency metrics is presented in the results of the EARTH project in [125]. Here, the metric of choice for mobile broadband networks is concluded to be power per coverage area (W/m^2). Component level, node level, and network level metrics are discussed, though only for mobile broadband networks and not for alternative use cases.

6.2 3GPP/ETSI Metrics for URLLC and mMTC

Generally, the network slice energy efficiency 6.3 can be expressed as defined in [123].

$$\text{EE}_{\text{generic slice KPI}} = \frac{\text{Performance of network slice}}{\text{Energy consumption of network slice}} \tag{6.3}$$

For URLLC and mMTC slices, data volume is not the most relevant key performance indicator (KPI). Therefore, other metrics have been proposed for these network slices by the 3GPP. These are outlined hereafter based on [123] and [91].

In URLLC the latency is a central metric, therefore the reciprocal end-to-end latency (T_{e2e}) is divided by the energy consumption (EC):

$$\text{EE}_{\text{URLLC,Latency}} = \frac{1}{T_{\text{e2e}} \cdot \text{EC}} \tag{6.4}$$

Alternatively, the metric $EE_{\text{URLLC,DV,Lat}}$ also takes into account the data volume (DV).

$$\text{EE}_{\text{URLLC,DV,Lat}} = \frac{\text{DV}}{T_{\text{e2e}} \cdot \text{EC}} \tag{6.5}$$

According to [91] a metric that captures the system reliability in combination with the delay would be required for URLLC applications.

For mMTC the number of UEs (N_{UE}) is a relevant quantity. The 3GPP proposes a metric that simply divides the number registered UEs by the energy consumption:

$$EE_{\text{mMTC}} = \frac{N_{\text{UE}}}{EC} \tag{6.6}$$

The survey in [91] concludes that mMTC requires a metric which captures the number of connected UEs combined with the area covered by the network. The coverage area energy efficiency (EE_{CoA}) is defined by the 3GPP in [123]:

$$EE_{\text{CoA}} = \frac{CoA}{EC} \tag{6.7}$$

Furthermore, a coverage area quality factor that estimates the quality of coverage (CoA_{Q}) is defined in [123]:

$$CoA_{\text{Q}} = (1 - FR_{\text{RRC}})(1 - FR_{\text{RABS}})(1 - FR_{\text{RABR}}) \tag{6.8}$$

With the RRC setup failure ratio (FR_{RRC}), the failure ratio of the radio access bearer setup (FR_{RABS}), and the failure ratio of the radio access bearer release (FR_{RABR}) [91].

Based on this, we propose a simple combination of the EE_{CoA}, the CoA_{Q}, and the EE_{mMTC}:

$$EE_{\text{mMTC,CoA,Q}} = \frac{CoA \cdot CoA_{\text{Q}} \cdot N_{\text{UE}}}{EC} \tag{6.9}$$

This combination of metrics ensures that the coverage area is taken into account as well as the number of registered UEs (serving the same number of UEs over a larger coverage area should be considered advantageous). Additionally, the coverage area quality factor is multiplied to ensure that a network with lower coverage quality receives a lower energy efficiency and vice versa.

6.3 Summary

The 3GPP has proposed energy efficiency metrics for the different 5G use cases as network slice metrics. The proposed key performance indicator for URLLC is the total end-to-end latency, alternatively combined with the data volume. The key performance indicator for mMTC is the number of served UEs.

The survey by López-Pérez et al. concludes that additional metrics are required, as there is a lack of specific and well understood metrics for URLLC and mMTC. Based on the 3GPP/ETSI metrics, we propose a metric (Equation 6.9) that combines the performance indicators of coverage area, coverage quality and number of handled connections to assess the energy efficiency of mMTC network slices. The metrics currently available for URLLC and mMTC are not applied widely in literature, therefore further evaluation is needed to determine the validity and limitations of these metrics.

Generally, the challenge when defining an energy efficiency metric, is to derive a meaningful key performance indicator that can also easily be derived from measurements or calculations. The key performance indicator used for the energy efficiency metric should capture the relevant Quality of Service parameters of the considered network use case.

7 Summary, Conclusions, and Future Work

To conclude the thesis, the previous chapters are summarized. Conclusions are drawn based on the results and potential future work is discussed.

7.1 Summary

In Chapter 2, an overview on the fundamental aspects of cellular networks in general and 5G specifically was provided to define the contributions and scope in Chapter 3. The first major contribution is provided in Chapter 4, which describes the power consumption models identified as part of the literature survey. The power models were grouped into the following categories, following the general system structure of cellular networks: Base station, radio access network, user equipment, and system level. For the base station models, it was shown that they can be categorized into main component models, subcomponent models, and system models - based on the granularity of the modeling. The approaches of the base station models vary between bottom-up theoretical, estimation-based models or top-down measurement-based models. Base station models rather suitable for quantification of current configurations are described, as well as models more suitable for the detailed exploration of different configurations and future developments. Radio access network models extend upon the base station models. For 5G, centralized radio access network architectures and functional splits are of interest. The identified RAN power models are not suitable for the evaluation of networks based on 5G specifications without additional work, as the parameter values and considerations are largely outdated. Transport network modeling is very simplified in the discussed radio access network power models. The user equipment models are suitable for detailed evaluation of power saving mechanisms such as discontinuous reception (DRX) and estimations of battery lifetime, or integration into system level models. The described user equipment power models are either based on theoretical estimations or measurements of LTE hardware and only include the radio hardware. Furthermore, three system level models were described that

enable the evaluation of networks in terms of energy consumption and energy efficiency. These models were developed to solve complex theoretical optimization problems and are therefore based on simplifications in key aspects, which may restrict their general application. In Chapter 5, the power consumption models are compared and discussed. This constitutes the second major contribution of this thesis, where the comparison is based on the implementation of selected power models. The focus of the comparison was set on the base station power models. The comparison showed that for every main component of a base station, different power consumption modeling approaches exist. The computed power values vary between the models. This is the result of a multitude of reasons, such as different underlying assumptions and parameter values. Additionally, the differences in power consumption for different base station configurations underlined the importance of specifying the exact configuration when evaluating and reporting the energy consumption. Furthermore, energy efficiency metrics are discussed in Chapter 6. Energy efficiency metrics for mMTC and URLLC network slices were identified. Relevant metrics have been proposed by the 3GPP and ETSI. Though the significance of these metrics has not been evaluated and further research on energy efficiency metrics for novel 5G use cases is required.

7.2 Conclusions

In light of the increasing importance of sustainability in wireless communication systems, an important aspect is the quantification of the energy consumption of mobile networks. To estimate the energy consumption of different network configurations, power consumption models are an important tool. As the wireless communication systems are rapidly evolving in their specification and implementation due to new use cases, requirements, and higher performance demands, power models need to reflect the current state of technology. Therefore, when evaluating the energy consumption of current 5G mobile networks, it is important to verify that the underlying assumptions of the power models are valid for the respective system configuration. The literature survey and the comparison of models based on the implementation is a step towards this verification, as it enables further discussion and development of the power models for the intended use case.

For this thesis, analytic models of the power consumption for base station, radio access network, user equipment, and the system level were identified and discussed. As the majority of the total mobile network energy consumption is generally attributed to

the radio access network and specifically the base stations, the focus was set on power consumption models for base stations. The comparison of the power models showed that there are several approaches to the modeling of the base station power consumption. The main power consuming components of a base station are categorized in the same manner by almost all the discussed models, though the parameters and parameter values vary. As the main components are common for the models, they can be easily combined to form new models.

Furthermore, a lack of radio access network power models that accurately resemble current specifications of 5G RAN architectures and functional split options was identified. The user equipment models are mostly based on measurements of LTE hardware. They exhibit distinct approaches to the modeling of the different UE power states that are a result of the Radio Resource Control (RRC) protocol and the Discontinuous Reception (DRX) mechanism for LTE or 5G. The UE power models are most appropriate for the evaluation of power saving mechanisms and parameters specific to the 5G protocol stack. Battery lifetime estimations may also be conducted using the UE models. System level models are helpful for simplified network planning and optimization, though the identified models are all based on simplified assumptions that may not be true to the network configuration to be modeled.

It is important to note that the energy efficiency (energy/bit) of mobile networks has improved disproportionately compared to the increase in energy consumption for the recent 4G and 5G cellular network generations. However, the total energy consumption by mobile networks has steadily increased and is projected to grow further in the future, as for example shown by the UTAMO project report in [33]. This means that the strong increase in efficiency is largely due to the improvements in terms of coverage, bandwidth, and spectral efficiency - and not due to a reduction in total energy consumption. The increase in energy consumption is a consequence of the ever-increasing traffic volume and number of mobile network users, which requires deployment of additional and more capable network infrastructure. The total network energy consumption and the power consumption of individual devices and network hardware should not be neglected. Power consumption models and derived energy consumption models are suitable to evaluate both the total energy consumption and the energy efficiency. The energy efficiency of novel network use cases, for 5G specifically URLLC and mMTC, requires new metrics to quantify the energy efficiency. As the main performance indicator for these mobile network use cases is not the data rate, Chapter 6 discussed possible alternative metrics that have

been proposed in the literature. However, the metrics require additional examination, especially as they have not been used widely in scientific publications.

Beyond the reduction of energy consumption itself, employing renewable energy sources to power network equipment can help in reducing the associated greenhouse gas emissions of wireless access network operation. Power consumption models can also aid in the planning and optimization for the integration of renewable energy sources into wireless access networks. For example, by calculating the required capacity of battery storage or dimensioning photovoltaic systems to power base stations.

Choosing the appropriate communication technology for the respective task can reduce the total network energy consumption. For example, the UTAMO project results in [33] show that the required energy consumption per bit of wired networks (fiber optic cable or copper wires) is lower than that of all currently available wireless technologies. Power consumption models can further assist in deciding on the appropriate technology from an energy consumption standpoint, based on the specific requirements and intended network configuration.

In the context of sustainability, the aspect of sufficiency should not be overlooked next to the optimization of efficiency. The work in [126] identified four types of digital sufficiency for information and communication technology: Hardware sufficiency, software sufficiency, user sufficiency, and economic sufficiency. Beyond the evaluation of operational energy consumption, life-cycle evaluations for the network hardware, considering the required energy for manufacturing and installation, are relevant for hardware sufficiency. Software sufficiency and user sufficiency are key facets to enable energy consumption reduction of mobile networks, as the increase in traffic volume may be curbed through reduction of data usage by software applications without human intervention and data traffic generated through user behavior. Further research into specific strategies to improve the sufficiency of mobile networks is required, as it is currently largely overlooked in favor of efficiency optimization. Analyzing the complex implications and interactions of the types of sufficiency, in addition to the aspects of energy efficiency and power consumption, is a step towards developing future network technologies under consideration of a holistic understanding of sustainability.

7.3 Future Work

The comparison and discussion of the power consumption models in this thesis motivates the development of a software framework that calculates the power consumption of mobile networks using parameterized network configurations as input.

As the discussion of the power models showed, the accurate modeling of the base station and RAN power consumption requires measurements of current base station hardware under varying operating parameters. The parameter values of the base station and RAN power models considered in this thesis are largely based on older technology, or estimations based on outdated assumptions. The measurements could follow the methods specified for wireless access equipment by the ETSI in [127] and [128]. Reference configurations for base stations and reference scenarios for measurements and evaluations could be based on the definitions of the 3GPP in [75] or those of the EARTH project in [129]. If no measurements are possible and data is not available, the overview of datasheets compiled by the UTAMO project in [33] provides a starting point.

Novel 5G configurations and technologies, specifically mMIMO and mmWave deployments as well as the RAN functional splits require additional attention, as the power consumption models identified in this work do not sufficiently include these aspects or lack tractable parameter values. As the 5G core and radio access network enables the utilization of network function virtualization on general purpose hardware, the power consumption of general purpose platforms and the impact of different software implementations and virtualization platforms on power consumption requires further research.

Additionally, traffic models are required to derive the energy consumption based on the power models. The modeling of traffic should consider the intended use case of the network. The publications covering the power consumption models presented in this thesis often include traffic models as well, which could constitute the groundwork for this. Lastly, the specifics of mMTC are only considered in some user equipment models, but not for the base stations or on system level. Further evaluations of the power consumption and traffic profiles of mMTC and URLLC network slices are needed to evaluate the energy consumption of these novel use cases.

The contributions of this thesis on the identification, comparison, and discussion of relevant power consumption models for 5G systems serve as the foundation of future research on the aforementioned aspects.

Bibliography

[1] L. M. P. Larsen, H. L. Christiansen, S. Ruepp, and M. S. Berger, "Toward Greener 5G and Beyond Radio Access Networks—A Survey," *IEEE Open Journal of the Communications Society*, vol. 4, pp. 768–797, 2023, ISSN: 2644-125X. DOI: 10.1109/OJCOMS.2023.3257889.

[2] Ericsson, "Ericsson Mobility Report," Nov. 2022. [Online]. Available: https://www.ericsson.com/4ae28d/assets/local/reports-papers/mobility-report/documents/2022/ericsson-mobility-report-november-2022.pdf.

[3] B. M. Khorsandi, M. Hoffmann, M. Uusitalo, *et al.*, "Targets and requirements for 6G - initial E2E architecture," Deliverable D1.3, Feb. 28, 2022. [Online]. Available: https://hexa-x.eu/wp-content/uploads/2022/03/Hexa-X_D1.3.pdf (visited on 03/26/2023).

[4] Nokia, "5G network energy efficiency," Nokia, White Paper, 2016. [Online]. Available: https://onestore.nokia.com/asset/200876.

[5] H. Asplund, D. Astely, P. von Butovitsch, *et al.*, *Advanced Antenna Systems for 5G Network Deployments: Bridging the Gap Between Theory and Practice*. Elsevier Science, 2020, ISBN: 978-0-12-822386-4.

[6] M. Deruyck, E. Tanghe, W. Joseph, and L. Martens, "Modelling and optimization of power consumption in wireless access networks," *Computer Communications*, vol. 34, no. 17, pp. 2036–2046, Nov. 1, 2011, ISSN: 0140-3664. DOI: 10.1016/j.comcom.2011.03.008.

[7] Q. Bai, "Energy Efficient Design and Operation of Wireless Communication Systems," Technische Universität München, 2016. [Online]. Available: https://mediatum.ub.tum.de/1303443 (visited on 05/19/2023).

[8] G. Auer, V. Giannini, C. Desset, *et al.*, "How much energy is needed to run a wireless network?" *IEEE Wireless Communications*, vol. 18, no. 5, pp. 40–49, Oct. 2011, ISSN: 1558-0687. DOI: 10.1109/MWC.2011.6056691.

[9] M. Deruyck, E. Tanghe, W. Joseph, *et al.*, "Model for power consumption of wireless access networks," *IET science, measurement & technology*, vol. 5, no. 4, pp. 155–161, 2011.

[10] H. Holtkamp, "Enhancing the Energy Efficiency of Radio Base Stations," arXiv, Nov. 14, 2013. [Online]. Available: `http://arxiv.org/abs/1311.3534` (visited on 02/10/2023).

[11] J. Joung, C. K. Ho, and S. Sun, "Spectral Efficiency and Energy Efficiency of OFDM Systems: Impact of Power Amplifiers and Countermeasures," *IEEE Journal on Selected Areas in Communications*, vol. 32, no. 2, pp. 208–220, Feb. 2014, ISSN: 1558-0008. DOI: `10.1109/JSAC.2014.141203`.

[12] G. Auer, V. Giannini, I. Godor, *et al.*, "Cellular Energy Efficiency Evaluation Framework," in *2011 IEEE 73rd Vehicular Technology Conference (VTC Spring)*, May 2011, pp. 1–6. DOI: `10.1109/VETECS.2011.5956750`.

[13] M. Sauter, *Grundkurs Mobile Kommunikationssysteme: 5G New Radio und Kernnetz, LTE-Advanced Pro, GSM, Wireless LAN und Bluetooth.* Wiesbaden: Springer Fachmedien, 2022, ISBN: 978-3-658-36962-0. DOI: `10.1007/978-3-658-36963-7`.

[14] M. Kottkamp, A. Pandey, D. Raddino, A. Roessler, and R. Stuhlfauth, *5G New Radio: Fundamentals, Procedures, Testing Aspects*, 5th ed. Rohde & Schwarz GmbH & Company KG, 2022, ISBN: 978-3-939837-15-2. [Online]. Available: `https://www.rohde-schwarz.com/5G-ebook`.

[15] 3GPP. "The 3GPP's System of Parallel Releases," 3GPP. (2022), [Online]. Available: `https://www.3gpp.org/specifications-technologies/releases` (visited on 05/10/2023).

[16] 3GPP. "Release 17," 3GPP. (2022), [Online]. Available: `https://www.3gpp.org/specifications-technologies/releases/release-17` (visited on 05/10/2023).

[17] 3GPP. "Release 18," 3GPP. (2023), [Online]. Available: `https://www.3gpp.org/specifications-technologies/releases/release-18` (visited on 05/10/2023).

[18] Nokia. "6G explained," Nokia. (2023), [Online]. Available: `https://www.nokia.com/about-us/newsroom/articles/6g-explained/` (visited on 05/11/2023).

[19]   W. Lei, A. C. Soong, L. Jianghua, *et al.*, *5G System Design: An End to End Perspective* (Wireless Networks). Cham: Springer International Publishing, 2021, ISBN: 978-3-030-73702-3. DOI: `10.1007/978-3-030-73703-0`.

[20]   M. Sauter, "Long Term Evolution (LTE) und LTE-Advanced," in *Grundkurs Mobile Kommunikationssysteme: 5G New Radio und Kernnetz, LTE-Advanced Pro, GSM, Wireless LAN und Bluetooth*, M. Sauter, Ed., Wiesbaden: Springer Fachmedien, 2022, pp. 1–114, ISBN: 978-3-658-36963-7. DOI: `10.1007/978-3-658-36963-7_1`.

[21]   R. Ratasuk, N. Mangalvedhe, G. Lee, and D. Bhatoolaul, "Reduced Capability Devices for 5G IoT," in *2021 IEEE 32nd Annual International Symposium on Personal, Indoor and Mobile Radio Communications (PIMRC)*, Sep. 2021, pp. 1339–1344. DOI: `10.1109/PIMRC50174.2021.9569595`.

[22]   F. Launay, *NG-RAN and 5G-NR: 5G Radio Access Network and Radio Interface*, 1st ed. Wiley, Aug. 4, 2021, ISBN: 978-1-78630-628-9. DOI: `10.1002/9781119851288`.

[23]   ETSI, "Study on scenarios and requirements for next generation access technologies," ETSI, Technical Report TR 138 913 V17.0.0, May 2022. [Online]. Available: `https://portal.etsi.org/webapp/workprogram/Report_WorkItem.asp?WKI_ID=65613` (visited on 06/02/2023).

[24]   S. K. G. Peesapati, "Energy Efficiency of 5G Radio Access Networks," 2020. [Online]. Available: `http://urn.kb.se/resolve?urn=urn:nbn:se:kth:diva-289433` (visited on 02/09/2023).

[25]   G. Auer, O. Blume, V. Giannini, *et al.*, "Energy efficiency analysis of the reference systems, areas of improvements and target breakdown," D3.2, Dec. 31, 2010. [Online]. Available: `https://cordis.europa.eu/docs/projects/cnect/3/247733/080/deliverables/001-EARTHWP2D23v2.pdf` (visited on 04/06/2023).

[26]   ETSI, "Physical layer procedures for data," ETSI, Technical Specification TS 138 214 (17.5.0), Mar. 28, 2023. [Online]. Available: `https://portal.etsi.org/webapp/workprogram/Report_WorkItem.asp?WKI_ID=68324` (visited on 05/31/2023).

[27]   A. Sirotkin, Ed., *5G Radio Access Network Architecture: The Dark Side of 5G*. Hoboken, NJ, USA: Wiley-IEEE Press, 2020, 1 p., ISBN: 978-1-119-55091-4.

[28] X. Cao, L. Liu, Y. Cheng, and X. Shen, "Towards Energy-Efficient Wireless Networking in the Big Data Era: A Survey," *IEEE Communications Surveys & Tutorials*, vol. 20, no. 1, pp. 303–332, 2018, ISSN: 1553-877X. DOI: `10.1109/COMST.2017.2771534`.

[29] ETSI, "Base Station (BS) radio transmission and reception (FDD)," ETSI, Technical Specification TS 125 104 17.0.0, Apr. 4, 2022. [Online]. Available: `https://www.etsi.org/deliver/etsi_ts/125100_125199/125104/17.00.00_60/ts_125104v170000p.pdf`.

[30] ETSI, "Base Station (BS) radio transmission and reception," ETSI, Technical Specification TS 138 104 V16.14.0, Jan. 2023. [Online]. Available: `https://www.etsi.org/deliver/etsi_ts/138100_138199/138104/16.14.00_60/ts_138104v161400p.pdf` (visited on 03/27/2023).

[31] B. Debaillie, C. Desset, and F. Louagie, "A Flexible and Future-Proof Power Model for Cellular Base Stations," in *2015 IEEE 81st Vehicular Technology Conference (VTC Spring)*, May 2015, pp. 1–7. DOI: `10.1109/VTCSpring.2015.7145603`.

[32] E. Björnson, J. Hoydis, and L. Sanguinetti, "Massive MIMO Networks: Spectral, Energy, and Hardware Efficiency," *Foundations and Trends® in Signal Processing*, vol. 11, no. 3-4, pp. 154–655, 2017, ISSN: 1932-8346. DOI: `10.1561/2000000093`.

[33] L. Stobbe, N. Richter, M. Quaeck, *et al.*, *Umweltbezogene Technikfolgenabschätzung Mobilfunk in Deutschland* (Texte 26/2023). Umweltbundesamt, Feb. 2023, 293 pp. [Online]. Available: `https://www.umweltbundesamt.de/publikationen/umweltbezogene-technikfolgenabschaetzung-mobilfunk`.

[34] ETSI, "Physical layer procedures for control," ETSI, Technical Specification TS 138 213 (17.5.0), Mar. 28, 2023. [Online]. Available: `https://portal.etsi.org/webapp/workprogram/Report_WorkItem.asp?WKI_ID=68322` (visited on 05/31/2023).

[35] E. Björnson, L. Sanguinetti, and M. Kountouris, "Deploying Dense Networks for Maximal Energy Efficiency: Small Cells Meet Massive MIMO," *IEEE Journal on Selected Areas in Communications*, vol. 34, no. 4, pp. 832–847, Apr. 2016, ISSN: 1558-0008. DOI: `10.1109/JSAC.2016.2544498`.

[36] E. Björnson, L. Sanguinetti, J. Hoydis, and M. Debbah, "Designing multi-user MIMO for energy efficiency: When is massive MIMO the answer?" In *2014 IEEE Wireless Communications and Networking Conference (WCNC)*, Apr. 2014, pp. 242–247. DOI: `10.1109/WCNC.2014.6951974`.

[37] E. Björnson, L. Sanguinetti, and M. Kountouris, "Energy-efficient future wireless networks: A marriage between massive MIMO and small cells," in *2015 IEEE 16th International Workshop on Signal Processing Advances in Wireless Communications (SPAWC)*, Jun. 2015, pp. 211–215. DOI: `10.1109/SPAWC.2015.7227030`.

[38] E. Björnson, L. Sanguinetti, J. Hoydis, and M. Debbah, "Optimal Design of Energy-Efficient Multi-User MIMO Systems: Is Massive MIMO the Answer?" *IEEE Transactions on Wireless Communications*, vol. 14, no. 6, pp. 3059–3075, Jun. 2015, ISSN: 1558-2248. DOI: `10.1109/TWC.2015.2400437`.

[39] P. Frenger, Ylva Jading, and J. Bengtsson. "5G energy consumption: The impact of 5G NR," Ericsson Blog. (Oct. 8, 2021), [Online]. Available: `https://www.ericsson.com/en/blog/2021/10/5g-energy-consumption-impact-5g-nr` (visited on 06/20/2023).

[40] E. Björnson and E. G. Larsson, "How Energy-Efficient Can a Wireless Communication System Become?" In *2018 52nd Asilomar Conference on Signals, Systems, and Computers*, Oct. 2018, pp. 1252–1256. DOI: `10.1109/ACSSC.2018.8645227`.

[41] European 5G Observatory. "5G Private networks – 5G Observatory." (), [Online]. Available: `https://5gobservatory.eu/5g-private-networks/` (visited on 06/03/2023).

[42] E. Kolta, T. Hatt, and S. Moore, "Going green: Benchmarking the energy efficiency of mobile networks (second edition)," GSMA Intelligence, 2023, p. 25. [Online]. Available: `https://data.gsmaintelligence.com/research/research/research-2023/going-green-benchmarking-the-energy-efficiency-of-mobile-networks-second-edition-` (visited on 03/26/2023).

[43] C. Han, T. Harrold, S. Armour, *et al.*, "Green radio: Radio techniques to enable energy-efficient wireless networks," *IEEE Communications Magazine*, vol. 49, no. 6, pp. 46–54, Jun. 2011, ISSN: 1558-1896. DOI: `10.1109/MCOM.2011.5783984`.

[44] S. Han, T. Xie, and C.-L. I, "Greener Physical Layer Technologies for 6G Mobile Communications," *IEEE Communications Magazine*, vol. 59, no. 4, pp. 68–74, Apr. 2021, ISSN: 0163-6804, 1558-1896. DOI: `10.1109/MCOM.001.2000484`. [Online]. Available: `https://ieeexplore.ieee.org/document/9433520/` (visited on 06/02/2023).

[45] L. Williams, B. K. Sovacool, and T. J. Foxon, "The energy use implications of 5G: Reviewing whole network operational energy, embodied energy, and indirect

effects," *Renewable and Sustainable Energy Reviews*, vol. 157, p. 112 033, Apr. 1, 2022, ISSN: 1364-0321. DOI: `10.1016/j.rser.2021.112033`.

[46] W. S. Jevons and A. W. Flux, *The Coal Question; an Inquiry Concerning the Progress of the Nation, and the Probable Exhaustion of Our Coal-Mines*, in collab. with New York Public Library. New York, A. M. Kelley, 1965, 377 pp. [Online]. Available: `http://archive.org/details/coalquestionani00jevogoo g` (visited on 06/03/2023).

[47] L. Golard, J. Louveaux, and D. Bol, "Evaluation and projection of 4G and 5G RAN energy footprints: The case of Belgium for 2020–2025," *Annals of Telecommunications*, Nov. 29, 2022, ISSN: 1958-9395. DOI: `10.1007/s12243-022-00932-9`.

[48] Huawei, "5G Power Whitepaper," White Paper, Feb. 27, 2019. [Online]. Available: `https://www.huawei.com/minisite/5g-ultra-lean-site-2019/ pdf_v1.0/5G-Power-White-Paper-en.pdf` (visited on 04/25/2023).

[49] C. Desset, B. Debaillie, V. Giannini, *et al.*, "Flexible power modeling of LTE base stations," in *2012 IEEE Wireless Communications and Networking Conference (WCNC)*, Paris, France: IEEE, Apr. 2012, pp. 2858–2862, ISBN: 978-1-4673-0437-5. DOI: `10.1109/WCNC.2012.6214289`.

[50] R. Bolla, R. Bruschi, F. Davoli, C. Lombardo, J. F. Pajo, and O. R. Sanchez, "The dark side of network functions virtualization: A perspective on the technological sustainability," in *2017 IEEE International Conference on Communications (ICC)*, May 2017, pp. 1–7. DOI: `10.1109/ICC.2017.7997129`.

[51] R. Mijumbi. "On the Energy Efficiency Prospects of Network Function Virtualization." arXiv: `1512.00215`. (Dec. 1, 2015), preprint.

[52] A. N. Al-Quzweeni, A. Q. Lawey, T. E. H. Elgorashi, and J. M. H. Elmirghani, "Optimized Energy Aware 5G Network Function Virtualization," *IEEE Access*, vol. 7, pp. 44 939–44 958, 2019, ISSN: 2169-3536. DOI: `10.1109/ACCESS.2019. 2907798`.

[53] R. Bolla, R. Bruschi, F. Davoli, C. Lombardo, and J. F. Pajo, "Debunking the "Green" NFV Myth: An Assessment of the Virtualization Sustainability in Radio Access Networks," in *2020 6th IEEE Conference on Network Softwarization (NetSoft)*, Jun. 2020, pp. 180–184. DOI: `10.1109/NetSoft48620.2020.9165481`.

[54] R. Bolla, R. Bruschi, C. Lombardo, and B. Siccardi, "6G Enablers for Zero-Carbon Network Slices and Vertical Edge Services," *IEEE Networking Letters*, pp. 1–1, 2023, ISSN: 2576-3156. DOI: `10.1109/LNET.2023.3262861`.

[55] G. Bianchi, C. Bianco, M. Boldi, *et al.*, "Sustainability, a Key Issue of 5G Network Ecosystem," in *The 5G Italy Book 2019: A Multiperspective View of 5G*, Dec. 2019, pp. 59–93. [Online]. Available: `https://iris.polito.it/handle/11583/2853946` (visited on 03/25/2023).

[56] H. A. Suraweera, Jing Yang, A. Zappone, and J. Thompson, Eds., *Green Communications for Energy-Efficient Wireless Systems and Networks*. Institution of Engineering and Technology, Oct. 27, 2020, ISBN: 978-1-83953-067-8. DOI: `10.1049/PBTE091E`.

[57] D. Renga and M. Meo, "Modeling renewable energy production for base stations power supply," in *2016 IEEE International Conference on Smart Grid Communications (SmartGridComm)*, Nov. 2016, pp. 716–722. DOI: `10.1109/SmartGridComm.2016.7778846`.

[58] M. Meo and D. Renga, "Renewable energy-enabled wireless networks," *Green Communications for Energy-Efficient Wireless Systems and Networks*, pp. 113–143, Oct. 27, 2020. DOI: `10.1049/PBTE091E_ch5`.

[59] M. H. Alsharif, J. Kim, and J. H. Kim, "Green and Sustainable Cellular Base Stations: An Overview and Future Research Directions," *Energies*, vol. 10, no. 5, p. 587, 5 May 2017, ISSN: 1996-1073. DOI: `10.3390/en10050587`.

[60] ITU-T, "L.1380: Smart energy solution for telecom sites," ITU-T, Nov. 2019. [Online]. Available: `https://www.itu.int/rec/T-REC-L.1380-201911-I/en` (visited on 06/03/2023).

[61] EU Publications Office. "Energy Aware Radio and neTwork tecHnologies," CORDIS EU Research Results. (May 25, 2022), [Online]. Available: `https://cordis.europa.eu/project/id/247733/reporting` (visited on 04/08/2023).

[62] H. Holtkamp, G. Auer, V. Giannini, and H. Haas, "A Parameterized Base Station Power Model," *IEEE Communications Letters*, vol. 17, no. 11, pp. 2033–2035, Nov. 2013, ISSN: 1558-2558. DOI: `10.1109/LCOMM.2013.091213.131042`.

[63] M. Olsson, S. Tombaz, I. Gódor, and P. Frenger, "Energy performance evaluation revisited: Methodology, models and results," in *2016 IEEE 12th International Conference on Wireless and Mobile Computing, Networking and Communications (WiMob)*, Oct. 2016, pp. 1–7. DOI: `10.1109/WiMOB.2016.7763182`.

[64] S. Tombaz, P. Frenger, F. Athley, E. Semaan, C. Tidestav, and A. Furuskar, "Energy Performance of 5G-NX Wireless Access Utilizing Massive Beamforming and an Ultra-Lean System Design," in *2015 IEEE Global Communications Conference (GLOBECOM)*, Dec. 2015, pp. 1–7. DOI: `10.1109/GLOCOM.2015.7417240`.

[65] D. Sharma, S. Singhal, A. Rai, and A. Singh, "Analysis of power consumption in standalone 5G network and enhancement in energy efficiency using a novel routing protocol," *Sustainable Energy, Grids and Networks*, vol. 26, p. 100 427, Jun. 1, 2021, ISSN: 2352-4677. DOI: `10.1016/j.segan.2020.100427`.

[66] NTT DOCOMO, Telecom Italia, Alcatel-Lucen, Ericsson, and Alcatel-Lucent Shanghai Bell, "Base Station Power Model," 3GPP, San Francisco, USA, Discussion & Decision R1-114336, Nov. 14–18, 2011. [Online]. Available: `https://www.3gpp.org/ftp/tsg_ran/WG1_RL1/TSGR1_67/Docs/`.

[67] T. Zhao, J. Wu, S. Zhou, and Z. Niu, "Energy-Delay Tradeoffs of Virtual Base Stations With a Computational-Resource-Aware Energy Consumption Model," in *2014 IEEE International Conference on Communication Systems*, Nov. 2014, pp. 26–30. DOI: `10.1109/ICCS.2014.7024759`.

[68] C. Desset, B. Debaillie, and F. Louagie, "Towards a flexible and future-proof power model for cellular base stations," in *2013 24th Tyrrhenian International Workshop on Digital Communications - Green ICT (TIWDC)*, Sep. 2013, pp. 1–6. DOI: `10.1109/TIWDC.2013.6664200`.

[69] Ericsson, "Modeling and evaluation methodology for network energy saving," 3GPP, Technical Report R1-2204881, May 2022. [Online]. Available: `https://www.3gpp.org/ftp/tsg_ran/WG1_RL1/TSGR1_109-e/Docs`.

[70] P. Frenger and R. Tano, "More Capacity and Less Power: How 5G NR Can Reduce Network Energy Consumption," in *2019 IEEE 89th Vehicular Technology Conference (VTC2019-Spring)*, Apr. 2019, pp. 1–5. DOI: `10.1109/VTCSpring.2019.8746600`.

[71] C. Desset, B. Debaillie, and F. Louagie, "Modeling the hardware power consumption of large scale antenna systems," in *2014 IEEE Online Conference on Green Communications (OnlineGreenComm)*, Nov. 2014, pp. 1–6. DOI: `10.1109/OnlineGreenCom.2014.7114430`.

[72] X. Ge, J. Yang, H. Gharavi, and Y. Sun, "Energy Efficiency Challenges of 5G Small Cell Networks," *IEEE communications magazine. IEEE Communications*

Society, vol. 55, no. 5, pp. 184–191, May 2017, ISSN: 0163-6804. DOI: `10.1109/MCOM.2017.1600788`. pmid: `28757670`.

[73] N. Piovesan, D. Lopez-Perez, A. De Domenico, X. Geng, H. Bao, and M. Debbah, "Machine Learning and Analytical Power Consumption Models for 5G Base Stations," *IEEE Communications Magazine*, vol. 60, no. 10, pp. 56–62, Oct. 2022, ISSN: 0163-6804, 1558-1896. DOI: `10.1109/MCOM.001.2200023`.

[74] N. Piovesan, D. Lopez-Perez, A. De Domenico, X. Geng, and H. Bao. "Power Consumption Modeling of 5G Multi-Carrier Base Stations: A Machine Learning Approach." arXiv: `2212.04318`. (Dec. 8, 2022), preprint.

[75] 3GPP, "Study on network energy savings for NR (Release 18)," Technical Report TR 38.864 V18.0.0, Dec. 2022. [Online]. Available: `https://portal.3gpp.org/desktopmodules/Specifications/SpecificationDetails.aspx?specificationId=3987` (visited on 03/20/2023).

[76] OPPO, "Discussion on NW energy savings performance evaluation," Toulouse, France, Discussion and Decision R1-2211458, Nov. 14, 2022.

[77] M. M. A. Hossain, C. Cavdar, E. Björnson, and R. Jäntti, "Energy Saving Game for Massive MIMO: Coping With Daily Load Variation," *IEEE Transactions on Vehicular Technology*, vol. 67, no. 3, pp. 2301–2313, Mar. 2018, ISSN: 1939-9359. DOI: `10.1109/TVT.2017.2769163`.

[78] D. López–Pérez, A. D. Domenico, N. Piovesan, X. Geng, H. Bao, and M. Debbah, "Energy Efficiency of Multi-Carrier Massive MIMO Networks: Massive MIMO Meets Carrier Aggregation," in *2021 IEEE Global Communications Conference (GLOBECOM)*, Dec. 2021, pp. 01–07. DOI: `10.1109/GLOBECOM46510.2021.9685216`.

[79] S. K. G. Peesapati, M. Olsson, M. Masoudi, S. Andersson, and C. Cavdar, "An Analytical Energy Performance Evaluation Methodology for 5G Base Stations," in *2021 17th International Conference on Wireless and Mobile Computing, Networking and Communications (WiMob)*, Oct. 2021, pp. 169–174. DOI: `10.1109/WiMob52687.2021.9606296`.

[80] S. Tombaz, P. Frenger, M. Olsson, and A. Nilsson, "Energy performance of 5G-NX radio access at country level," in *2016 IEEE 12th International Conference on Wireless and Mobile Computing, Networking and Communications (WiMob)*, Oct. 2016, pp. 1–6. DOI: `10.1109/WiMOB.2016.7763183`.

[81] F. Rottenberg. "Information-Theoretic Study of Time-Domain Energy-Saving Techniques in Radio Access." arXiv: `2303.17898`. (Mar. 31, 2023), preprint.

[82] F. Wang, A. Yang, D. Kimball, L. Larson, and P. Asbeck, "Design of wide-bandwidth envelope-tracking power amplifiers for OFDM applications," *IEEE Transactions on Microwave Theory and Techniques*, vol. 53, no. 4, pp. 1244–1255, Apr. 2005, ISSN: 1557-9670. DOI: `10.1109/TMTT.2005.845716`.

[83] F. H. Raab, "Efficiency of Doherty RF Power-Amplifier Systems," *IEEE Transactions on Broadcasting*, vol. BC-33, no. 3, pp. 77–83, Sep. 1987, ISSN: 1557-9611. DOI: `10.1109/TBC.1987.266625`.

[84] O. Arnold, F. Richter, G. Fettweis, and O. Blume, "Power Consumption Modeling of Different Base Station Types in Heterogeneous Cellular Networks," presented at the Proceedings of the ICT MobileSummit (ICT Summit'10), Florence, Italy, Jul. 18, 2010, pp. 1–8.

[85] M. Deruyck, W. Joseph, and L. Martens, "Power consumption model for macro-cell and microcell base stations," *Transactions on Emerging Telecommunications Technologies*, vol. 25, no. 3, pp. 320–333, 2014, ISSN: 2161-3915. DOI: `10.1002/ett.2565`.

[86] B. H. Jung, H. Leem, and D. K. Sung, "Modeling of Power Consumption for Macro-, Micro-, and RRH-Based Base Station Architectures," in *2014 IEEE 79th Vehicular Technology Conference (VTC Spring)*, May 2014, pp. 1–5. DOI: `10.1109/VTCSpring.2014.7022990`.

[87] J. A. Ayala-Romero, I. Khalid, A. Garcia-Saavedra, X. Costa-Perez, and G. Iosifidis, "Experimental Evaluation of Power Consumption in Virtualized Base Stations," in *ICC 2021 - IEEE International Conference on Communications*, Jun. 2021, pp. 1–6. DOI: `10.1109/ICC42927.2021.9500323`.

[88] M. Dzaferagic, J. A. Ayala-Romero, and M. Ruffini, "ML Approach for Power Consumption Prediction in Virtualized Base Stations," in *2022 IEEE Globecom Workshops (GC Wkshps)*, Dec. 2022, pp. 986–991. DOI: `10.1109/GCWkshps56602.2022.10008643`.

[89] T. Saraiva, D. Duarte, I. Pinto, and P. Vieira, "An Enhanced Power Consumption Prediction for LTE Remote Radio Unit based on Mixed Models," Jun. 26, 2019.

[90] T. Saraiva, D. Duarte, I. Pinto, and P. Vieira, "An Improved BBU/RRU Energy Consumption Predictor for 4G and Legacy Mobile Networks using Mixed Statistical Models," Feb. 17, 2020. DOI: `10.1109/ICNC47757.2020.9049673`.

[91] D. López-Pérez, A. De Domenico, N. Piovesan, *et al.*, "A Survey on 5G Radio Access Network Energy Efficiency: Massive MIMO, Lean Carrier Design, Sleep Modes, and Machine Learning," *IEEE Communications Surveys & Tutorials*, vol. 24, no. 1, pp. 653–697, 2022, ISSN: 1553-877X. DOI: 10.1109/COMST.2022.3142532.

[92] G. Yu, Q. Chen, R. Yin, H. Zhang, and G. Y. Li, "Joint Downlink and Uplink Resource Allocation for Energy-Efficient Carrier Aggregation," *IEEE Transactions on Wireless Communications*, vol. 14, no. 6, pp. 3207–3218, Jun. 2015, ISSN: 1558-2248. DOI: 10.1109/TWC.2015.2403327.

[93] M. Fiorani, S. Tombaz, J. Martensson, B. Skubic, L. Wosinska, and P. Monti, "Modeling energy performance of C-RAN with optical transport in 5G network scenarios," *Journal of Optical Communications and Networking*, vol. 8, no. 11, B21–B34, Nov. 2016, ISSN: 1943-0639. DOI: 10.1364/JOCN.8.000B21.

[94] M. Fiorani, S. Tombaz, J. Mårtensson, B. Skubic, L. Wosinska, and P. Monti, "Energy performance of C-RAN with 5G-NX radio networks and optical transport," in *2016 IEEE International Conference on Communications (ICC)*, May 2016, pp. 1–6. DOI: 10.1109/ICC.2016.7510717.

[95] A. Younis, T. X. Tran, and D. Pompili, "Bandwidth and Energy-Aware Resource Allocation for Cloud Radio Access Networks," *IEEE Transactions on Wireless Communications*, vol. 17, no. 10, pp. 6487–6500, Oct. 2018, ISSN: 1558-2248. DOI: 10.1109/TWC.2018.2860008.

[96] T. Sigwele, A. S. Alam, P. Pillai, and Y. F. Hu, "Energy-efficient cloud radio access networks by cloud based workload consolidation for 5G," *Journal of Network and Computer Applications*, vol. 78, pp. 1–8, Jan. 15, 2017, ISSN: 1084-8045. DOI: 10.1016/j.jnca.2016.11.005.

[97] D. Sabella, A. de Domenico, E. Katranaras, *et al.*, "Energy Efficiency Benefits of RAN-as-a-Service Concept for a Cloud-Based 5G Mobile Network Infrastructure," *IEEE Access*, vol. 2, pp. 1586–1597, 2014, ISSN: 2169-3536. DOI: 10.1109/ACCESS.2014.2381215.

[98] T. Werthmann, H. Grob-Lipski, and M. Proebster, "Multiplexing gains achieved in pools of baseband computation units in 4G cellular networks," in *2013 IEEE 24th Annual International Symposium on Personal, Indoor, and Mobile Radio Communications (PIMRC)*, Sep. 2013, pp. 3328–3333. DOI: 10.1109/PIMRC.2013.6666722.

[99]   A. Younis, T. X. Tran, and D. Pompili, "Energy-Efficient Resource Allocation in C-RANs with Capacity-Limited Fronthaul," *IEEE Transactions on Mobile Computing*, vol. 20, no. 2, pp. 473–487, Feb. 2021, ISSN: 1558-0660. DOI: `10.1109/TMC.2019.2942597`.

[100]   A. Israr, Q. Yang, and A. Israr, "Power consumption analysis of access network in 5G mobile communication infrastructures — An analytical quantification model," *Pervasive and Mobile Computing*, vol. 80, p. 101 544, Feb. 1, 2022, ISSN: 1574-1192. DOI: `10.1016/j.pmcj.2022.101544`.

[101]   M. Lauridsen, "Studies on mobile terminal energy consumption for LTE and future 5G," Department of Electronic Systems, Aalborg University, 2015.

[102]   3GPP, "Study on User Equipment (UE) power saving in NR (Release 16)," 3GPP, Technical Report TR 38.840 V16.0.0, Jun. 2019.

[103]   M. Lauridsen, D. Laselva, F. Frederiksen, and J. Kaikkonen, "5G New Radio User Equipment Power Modeling and Potential Energy Savings," in *2019 IEEE 90th Vehicular Technology Conference (VTC2019-Fall)*, Sep. 2019, pp. 1–6. DOI: `10.1109/VTCFall.2019.8891215`.

[104]   M. Lauridsen, L. Noël, T. B. Sørensen, and P. Mogensen, "An Empirical LTE Smartphone Power Model with a View to Energy Efficiency Evolution," *Intel Technology Journal*, vol. 18, no. 1, pp. 172–193, Mar. 2014. [Online]. Available: `https://vbn.aau.dk/files/176790997/An_Empirical_LTE_Smartphone_Power_Model_with_a_View_to_Energy_Efficiency_Evolution.pdf`.

[105]   M. Lauridsen, P. Mogensen, and L. Noel, "Empirical LTE Smartphone Power Model with DRX Operation for System Level Simulations," in *2013 IEEE 78th Vehicular Technology Conference (VTC Fall)*, Las Vegas, NV, USA: IEEE, Sep. 2013, pp. 1–6, ISBN: 978-1-4673-6187-3. DOI: `10.1109/VTCFall.2013.6692179`.

[106]   A. R. Jensen, M. Lauridsen, P. Mogensen, T. B. Sørensen, and P. Jensen, "LTE UE Power Consumption Model: For System Level Energy and Performance Optimization," in *2012 IEEE Vehicular Technology Conference (VTC Fall)*, Sep. 2012, pp. 1–5. DOI: `10.1109/VTCFall.2012.6399281`.

[107]   M. Lauridsen, R. Krigslund, M. Rohr, and G. Madueno, "An Empirical NB-IoT Power Consumption Model for Battery Lifetime Estimation," in *2018 IEEE 87th Vehicular Technology Conference (VTC Spring)*, Jun. 2018, pp. 1–5. DOI: `10.1109/VTCSpring.2018.8417653`.

[108] B. Dusza, C. Ide, L. Cheng, and C. Wietfeld, "CoPoMo: A context-aware power consumption model for LTE user equipment," *Transactions on Emerging Telecommunications Technologies*, vol. 24, no. 6, pp. 615–632, 2013, ISSN: 2161-3915. DOI: `10.1002/ett.2702`.

[109] B. Dusza, C. Ide, L. Cheng, and C. Wietfeld, "An accurate measurement-based power consumption model for LTE uplink transmissions," in *2013 IEEE Conference on Computer Communications Workshops (INFOCOM WKSHPS)*, Turin: IEEE, Apr. 2013, pp. 49–50, ISBN: 978-1-4799-0056-5. DOI: `10.1109/INFCOMW.2013.6970731`.

[110] B. Dusza, P. Marwedel, O. Spinczyk, and C. Wietfeld, "A context-aware battery lifetime model for carrier aggregation enabled LTE-A systems," in *2014 IEEE 11th Consumer Communications and Networking Conference (CCNC)*, Las Vegas, NV: IEEE, Jan. 2014, pp. 13–19, ISBN: 978-1-4799-2355-7. DOI: `10.1109/CCNC.2014.6866541`.

[111] J. Perdomo, M. Ericsson, M. Nordberg, and K. Andersson, "User Performance in a 5G Multi-connectivity Ultra-Dense Network City Scenario," in *2020 IEEE 45th Conference on Local Computer Networks (LCN)*, Sydney, NSW, Australia: IEEE, Nov. 16, 2020, pp. 195–203, ISBN: 978-1-72817-158-6. DOI: `10.1109/LCN48667.2020.9314774`.

[112] R. Falkenberg, B. Sliwa, and C. Wietfeld, "Rushing Full Speed with LTE-Advanced Is Economical - A Power Consumption Analysis," in *2017 IEEE 85th Vehicular Technology Conference (VTC Spring)*, Jun. 2017, pp. 1–7. DOI: `10.1109/VTCSpring.2017.8108515`.

[113] Y. Mehmood, L. Zhang, and A. Förster, "Power Consumption Modeling of Discontinuous Reception for Cellular Machine Type Communications," *Sensors*, vol. 19, no. 3, p. 617, 3 Jan. 2019, ISSN: 1424-8220. DOI: `10.3390/s19030617`.

[114] P. Andres-Maldonado, M. Lauridsen, P. Ameigeiras, and J. M. Lopez-Soler, "Analytical Modeling and Experimental Validation of NB-IoT Device Energy Consumption," *IEEE Internet of Things Journal*, vol. 6, no. 3, pp. 5691–5701, Jun. 2019, ISSN: 2327-4662. DOI: `10.1109/JIOT.2019.2904802`.

[115] A. Jano, P. A. Garana, F. Mehmeti, C. Mas-Machuca, and W. Kellerer, "Modeling of IoT Devices Energy Consumption in 5G Networks," 2023. [Online]. Available: `https://mediatum.ub.tum.de/doc/1705687/55ahjo0udp2jr6z1159i`

`lkwbr.Modelling_energy_consumption_of_IoT_devices_in_5G_`
`network.pdf`.

[116] N. Accurso, N. Mastronarde, and F. Malandra, "Exploring Tradeoffs between Energy Consumption and Network Performance in Cellular-IoT: A Survey," in *2021 IEEE Global Communications Conference (GLOBECOM)*, Dec. 2021, pp. 01–06. DOI: `10.1109/GLOBECOM46510.2021.9685313`.

[117] T. Jacobsen, I. Z. Kovács, M. Lauridsen, L. Hongchao, P. Mogensen, and T. Madsen, "Generic Energy Evaluation Methodology for Machine Type Communication," in *Multiple Access Communications*, T. K. Madsen, J. J. Nielsen, and N. K. Pratas, Eds., vol. 10121, Cham: Springer International Publishing, 2016, pp. 72–85, ISBN: 978-3-319-51375-1. DOI: `10.1007/978-3-319-51376-8_6`.

[118] R. Joda, M. Elsayed, H. Abou-Zeid, *et al.*, "Carrier Aggregation With Optimized UE Power Consumption in 5G," *IEEE Networking Letters*, vol. 3, no. 2, pp. 61–65, Jun. 2021, ISSN: 2576-3156. DOI: `10.1109/LNET.2021.3076409`.

[119] P. Skrimponis, S. Dutta, M. Mezzavilla, *et al.*, "Power Consumption Analysis for Mobile MmWave and Sub-THz Receivers," in *2020 2nd 6G Wireless Summit (6G SUMMIT)*, Mar. 2020, pp. 1–5. DOI: `10.1109/6GSUMMIT49458.2020.9083793`.

[120] M. Di Renzo, A. Zappone, T. T. Lam, and M. Debbah, "Stochastic Geometry Modeling of Cellular Networks: A New Definition of Coverage and its Application to Energy Efficiency Optimization," in *2018 26th European Signal Processing Conference (EUSIPCO)*, Sep. 2018, pp. 1507–1511. DOI: `10.23919/EUSIPCO.2018.8553134`.

[121] M. Di Renzo, A. Zappone, T. T. Lam, and M. Debbah, "System-Level Modeling and Optimization of the Energy Efficiency in Cellular Networks—A Stochastic Geometry Framework," *IEEE Transactions on Wireless Communications*, vol. 17, no. 4, pp. 2539–2556, Apr. 2018, ISSN: 1558-2248. DOI: `10.1109/TWC.2018.2797264`.

[122] L. Sanguinetti, A. Moustakas, E. Bjornson, and M. Debbah, "Energy Consumption in multi-user MIMO systems: Impact of user mobility," in *2014 IEEE International Conference on Acoustics, Speech and Signal Processing (ICASSP)*, May 2014, pp. 4743–4747. DOI: `10.1109/ICASSP.2014.6854502`.

[123] ETSI, "5G end to end Key Performance Indicators (KPI)," ETSI, Technical Specification TS 128 554 V17.8.0, Oct. 2022. [Online]. Available: `https://www.etsi.org/deliver/etsi_ts/128500_128599/128554/17.08.00_60/ts_128554v170800p.pdf` (visited on 03/31/2023).

[124] ETSI, "Assessment of mobile network energy efficiency," ETSI, ETSI Standard ES 203 228 V1.4.1, Apr. 2022. [Online]. Available: `https://www.etsi.org/deliver/etsi_es/203200_203299/203228/01.04.01_60/es_203228v010401p.pdf` (visited on 03/31/2023).

[125] M. A. Imran, J. Alonso-Rubio, G. Auer, *et al.*, "Most suitable efficiency metrics and utility functions," D2.4, Dec. 31, 2011. [Online]. Available: `https://cordis.europa.eu/docs/projects/cnect/3/247733/080/deliverables/001-EARTHWP2D24.pdf` (visited on 04/08/2023).

[126] T. Santarius, J. C. T. Bieser, V. Frick, *et al.*, "Digital sufficiency: Conceptual considerations for ICTs on a finite planet," *Annals of Telecommunications*, May 12, 2022, ISSN: 1958-9395. DOI: `10.1007/s12243-022-00914-x`.

[127] ETSI, "Metrics and Measurement Method for Energy Efficiency of Wireless Access Network Equipment; Part 2: Energy Efficiency - dynamic measurement method," ETSI, Technical Specification TS 102 706-2 V1.5.1, Nov. 2018. [Online]. Available: `https://www.etsi.org/deliver/etsi_ts/102700_102799/10270602/01.05.01_60/ts_10270602v010501p.pdf` (visited on 06/08/2023).

[128] ETSI, "Metrics and measurement method for energy efficiency of wireless access network equipment; Part 1: Power consumption - static measurement method," ETSI, ETSI Standard ES 202 706-1 V1.7.1, Aug. 23, 2022. [Online]. Available: `https://www.etsi.org/deliver/etsi_es/202700_202799/20270601/01.07.01_60/es_20270601v010701p.pdf` (visited on 03/20/2023).

[129] A. Ambrosy, G. Auer, O. Blume, *et al.*, "Definition and Parameterization of Reference Systems and Scenarios," D2.2, Jun. 30, 2010. [Online]. Available: `https://cordis.europa.eu/docs/projects/cnect/3/247733/080/deliverables/001-EARTHWP2D22v2.pdf`.

A Appendix

A.1 Tabular Overview of Power Consumption Models

Table A.1: Selected base station power consumption models

Model	Ref.	Section	Publ. year	Cellular gen. / techn.	UL/DL
Auer et al.	[8] [12] [10]	4.1.2	2011	LTE	DL
Desset et al.	[49]	4.1.3	2012	LTE	UL + DL
Björnson et al.	[36]	4.1.6	2014	Generic / mMIMO	DL
Debaillie et al.	[68] [71] [31]	4.1.3	2015	LTE	UL + DL
3GPP	[75] [69]	4.1.5	2022	5G	UL + DL
Piovesan et al.	[73]	4.1.4	2022	5G	DL
Rottenberg	[81]	4.1.7	2023	5G	DL

Table A.2: Revisions of base station power consumption models

Model	Original model	Ref.	Publ. year	Cellular gen.	Revisions
NTT DOCOMO et al.	Auer et al.	[66]	2011	LTE	Definition of load, carrier aggregation
Holtkamp et al.	Auer et al.	[62] [10]	2013	LTE	PA efficiency, BB, RF-transceiver scaling
Zhao et al.	Auer et al.	[67]	2014	LTE	Virtualized BBU
Olsson et al.	Auer et al.	[63]	2016	5G	Sleep mode
Tombaz et al.	Auer et al.	[64] [80]	2015, 2016	5G	Sleep mode
Ge et al.	Desset et al.	[72]	2017	5G	PA model, modified estimation of BBU computation power
Hossain et al.	Björnson et al.	[77]	2018	Generic	PA model
Peesapati et al.	Hossain et al.	[24] [79]	2020	5G	Sleep modes
Sharma et al.	Auer et al.	[65]	2021	5G	Non-linearity at high-volume traffic, load definition
López-Pérez et al.	Björnson et al.	[78]	2021	5G	Multi-carrier

Table A.3: Excluded base station power consumption models

Model	Ref.	Publ. year	Cellular gen.	Reason for exclusion
Arnold et al.	[84]	2010	GSM, UMTS, (LTE)	No relevance for 5G, predictions for LTE differ from subsequent models
Deruyck et al.	[6] [9]	2011	WiMAX, UMTS, HSPA, LTE	Sum of fixed values for component power from datasheets, therefore outdated
Jung et al.	[86]	2014	LTE	No further development or revisions, not relevant for subsequent models
Saraiva et al.	[89] [90]	2019, 2020	GSM, UMTS, LTE	Statistical model (linear mixed-effect)
Ayala-Romero et al.	[87]	2021	LTE	Statistical model (linear mixed-effect)
Dzaferagic et al.	[88]	2022	5G	Machine learning model

Table A.4: RAN power consumption models

Model	Ref.	Section	Publ. year
López-Pérez et al. Survey	[91]	4.2.2	2022

Table A.5: User equipment power consumption models

Model	Ref.	Section	Publ. year	Cellular gen.	UL/DL
Lauridsen et al.	[101]	4.3.3	2013	LTE	UL + DL
Dusza et al.	[109] [108] [110]	4.3.4	2013, 2014	LTE	UL
3GPP	[102]	4.3.2	2019	5G	UL + DL

Table A.6: Excluded user equipment power consumption models

Model	Ref.	Publ. year	Cellular gen. / techn.	Reason for exclusion
Perdomo et al.	[111]	2020	5G	Extension of Dusza
Falkenberg et al.	[112]	2020	LTE	Extension of Dusza
Jacobsen et al.	[117]	2016	mMTC	Extension of Lauridsen
Mehmood et al.	[113]	2019	LTE (MTC)	Markov-chain extension of Dusza
Andres-Maldonado et al.	[114]	2019	NB-IoT	Specific to NB-IoT
Joda et al.	[118]	2021	5G	Extension of Lauridsen
Jano et al.	[115]	2023	5G RedCap	Specific to RedCap devices

Table A.7: System level power consumption models

Model	Ref.	Section	Publ. year	UL/DL	Scenario
Sanguinetti et al.	[122]	4.4.3	2014	DL	Base station energy consumption distribution considering user mobility
Björnson et al.	[38]	4.4.2	2015	UL + DL	Joint power model for single mMIMO base station and served single-antenna UEs
Di Renzo et al.	[120] [121]	4.4.1	2018	DL	Network, base station load, and network energy efficiency model for density of base stations and UEs

Table A.8: Power consumption models implemented for this thesis

Model	Implemented part(s)	Exclusions
Base station		
Auer/Holtkamp	Complete	None
Zhao	Baseband processing	RF transceiver, power amplifier, losses (everything identical to Auer/Holtkamp)
Debaillie	RF transceiver, baseband processing, losses	Sleep modes, power amplifier, scaling with technology node, everything not fully documented in [31]
Rottenberg	Power amplifier	Sleep modes, baseband processing, RF transceiver
Björnson/Hossain/Peesapati	Complete	None
Piovesan	Complete	None
3GPP	Scaling equations	State machine
User equipment		
Dusza	Transmission power dependency, uplink power allocation equation	Power states
Lauridsen	Complete	None
System level		
Di Renzo	Complete	None

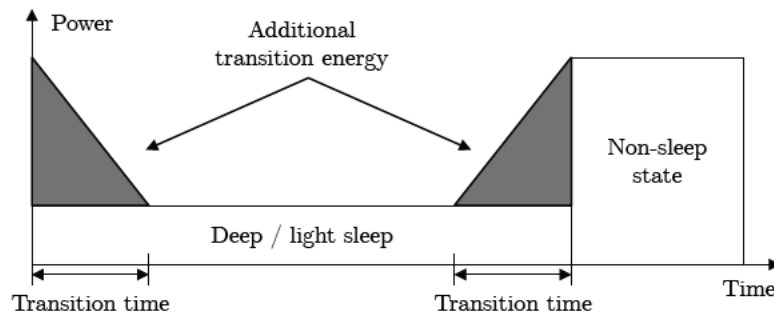## A.2 Additional Plots and Figures

Figure A.1: State transition in the 3GPP UE and base station power models. Adapted from [102] Fig. 1
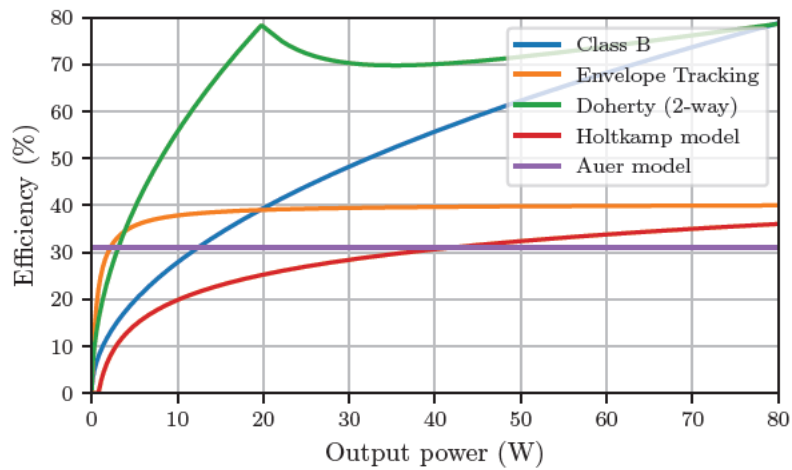

Figure A.2: Comparison of efficiency for different power amplifier models versus output power in W
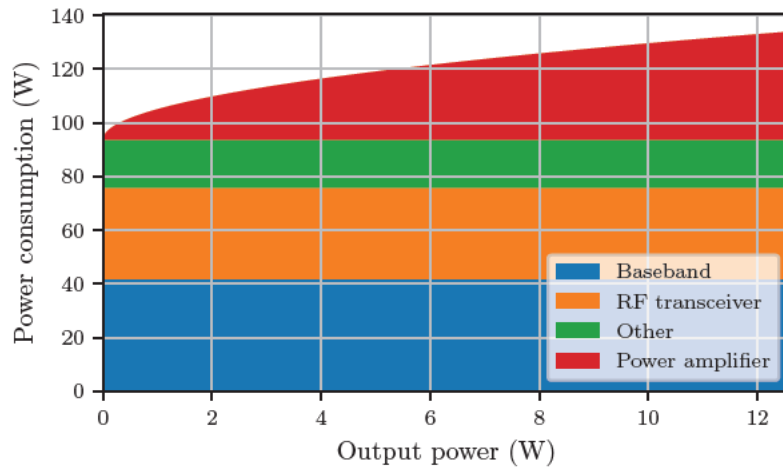
Figure A.3: Base station downlink power consumption as a function of the transmit power
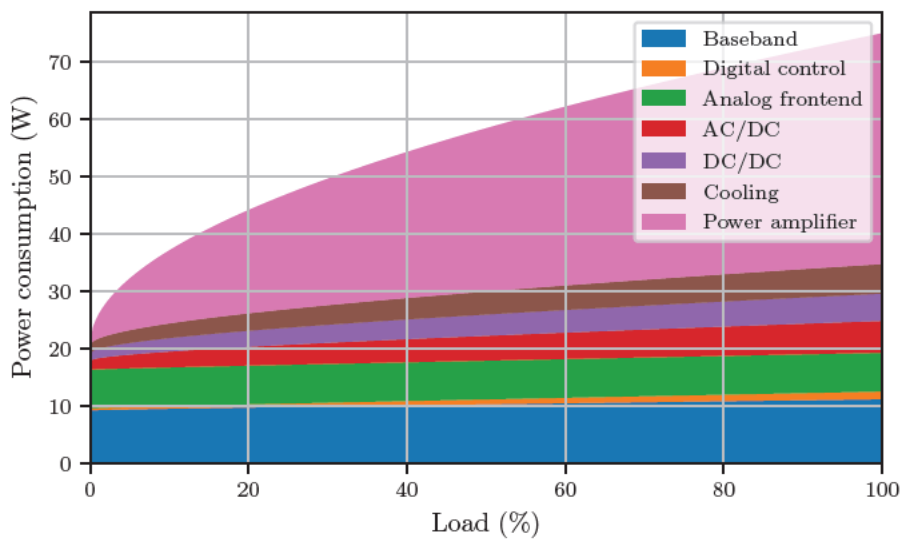(Hossain model: 32 antennas, 16 users, 120 Mbit/s, 20 MHz)

Figure A.4: Large base station downlink power consumption as a function of the load
(Debaillie model: Large base station, one sector, one antenna)
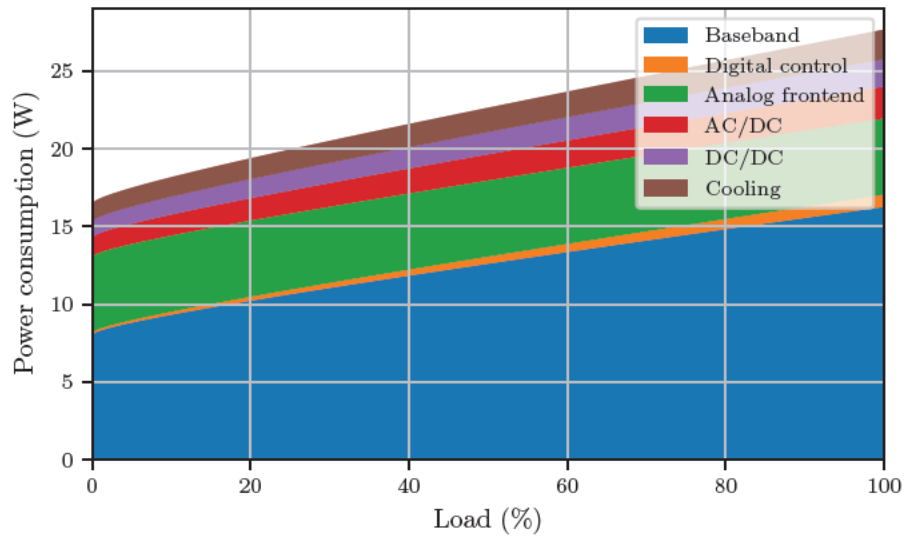
Figure A.5: Large base station uplink power consumption as a function of the load (Debaillie model: Large base station, one sector, one antenna)
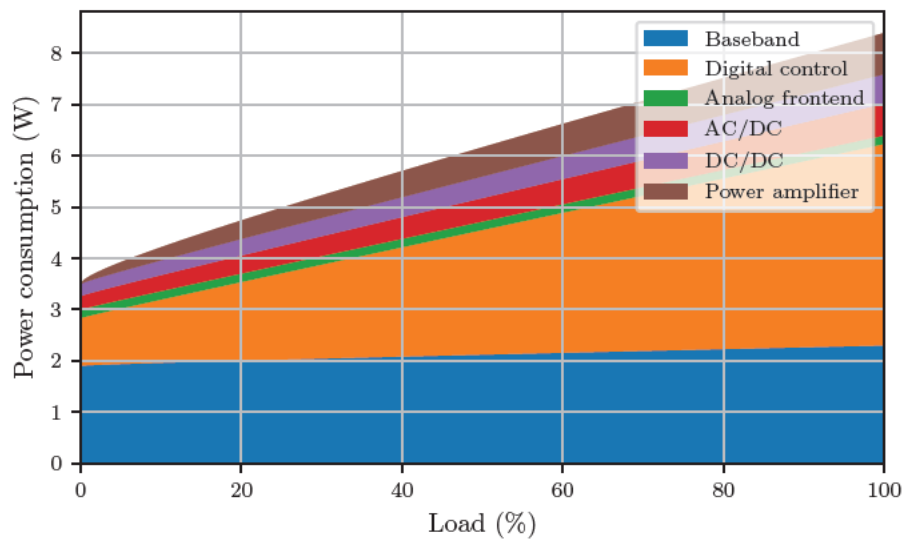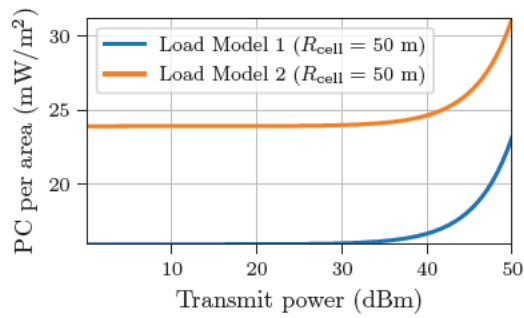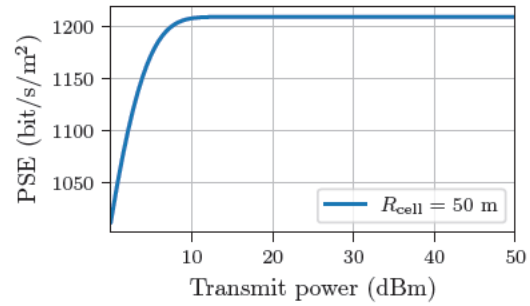

Figure A.6: Small base station downlink power consumption as a function of the load (Debaillie model: Small base station, one sector, one antenna)
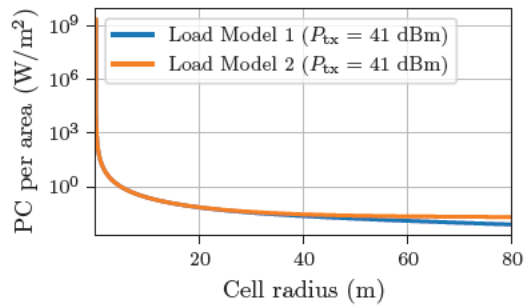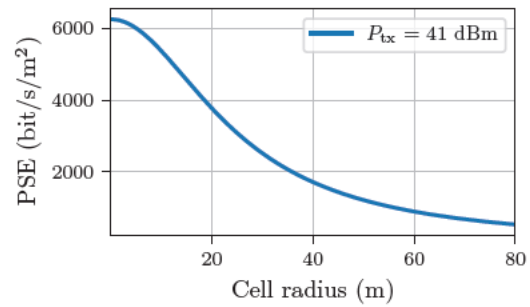
(a) Power consumption (PC) per area

(b) Potential spectral efficiency (PSE)

Figure A.7: Power consumption and potential spectral efficiency as a function of the base station transmit power (Di Renzo model)

(a) Power consumption (PC) per area

(b) Potential spectral efficiency (PSE)

Figure A.8: Power consumption and potential spectral efficiency as a function of the cell radius (Di Renzo et al. model)
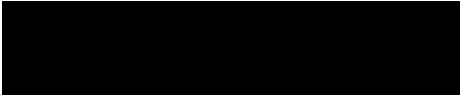
A.3 Search Strings and Keywords

Table A.9: Search strings used for literature research on power consumption models

Category	Search string
Base station	base station energy model
	cellular base station energy power model
	base station power model
	5g advanced base station power model
	6g base station power model
	5g modelling base station
	5g base station power model
	mimo base station power model
Radio Access Network	ran power energy consumption model
	radio access network power model
	wireless access network power model
User equipment	nb-iot power model
	redcap power model
	lte user equipment power model
	5g user equipment power model
	smartphone power model
Core network	5g core energy model
	5g core power model
	lte epc power model
	5gc power model
	nfv power model
	vnf power model
	network function virtualization energy consumption
	energy-efficient core networks
System level / general	5g system level modelling energy
	analytical model network power consumption
	model network power consumption 5g lte wireless
	energy consumption model 3gpp
	cellular network power consumption
	mmtc power consumption
	urllc power consumption

Declaration

I declare that this Bachelor Thesis has been completed by myself independently without outside help and only the defined sources and study aids were used.

————————— ————————— ——————————————

City   Date   Signature